1-1-1970

Polyethylene crystallized under the combined orientation and pressure effects in the Instron Capillary Rheometer.

John Hoyle Southern
University of Massachusetts Amherst

POLYETHYLENE CRYSTALLIZED UNDER THE COMBINED ORIENTATION AND PRESSURE EFFECTS IN THE INSTRON CAPILLARY RHEOMETER

A Dissertation Presented

By

John H. Southern

Approved as to style and content by:

R S Porter
(Chairman of Committee)

Charles E. Carson, Jr.
(Member)

Tracy D. Pace
(Member)

(Member)

POLYETHYLENE CRYSTALLIZED UNDER THE COMBINED ORIENTATION AND PRESSURE EFFECTS IN THE INSTRON CAPILLARY RHEOMETER

A dissertation Presented

By

John H. Southern

Submitted to the Graduate School of the
University of Massachusetts in
partial fulfillment of the requirements for the degree of

DOCTOR OF PHILOSOPHY

July 1970
Major Subject: Polymer Science and Engineering

ACKNOWLEDGEMENT

I would like to express my appreciation for the assistance rendered by my thesis advisor, Professor Roger S. Porter. Without his numerous constructive criticisms and suggestions during the research conducted over the previous twenty-two months, this thesis would not have been possible.

Professors Richard S. Stein and Fraser Price have both been "devil's advocates" concerning my interpretations of the microscopy and x-ray data. I am grateful for their continued help in this crucial matter. Drs. Seymore Newman and H. van Oene, both of Ford Motor Company, have also been of great assistance, particularly in the interpretation of the rheological data.

I would especially like to thank Dr. Richard G. Crystal of Xerox Corporation for providing the necessary microscopy studies, Dr. C. Richard Desper of U.S. Army Materials and Mechanics Research Center for providing the precise x-ray measurements noted in Chapter III, and Mr. Robert D. Ulrich of the University of Massachusetts for his advice and technical assistance. I gratefully acknowledge the numerous assists from friends whose patience with me was most certainly tested during this labor.

The financial support came from the National Science Foundation in grant GK-2065. I am indebted to the National Science Foundation and continue to hope that it will regain its former role in supporting graduate students and their research.

PREFACE

The thesis has been written in a chronological order with each chapter summarizing prevously obtained data. Hopefully, the repetition that this procedure entails does not belabor the significant results. Each chapter constitutes a separate manuscript and has either been revised and accepted for publication or is in the process of being critiqued. The project was initially intended to be a rheological study of partially crystalline melts. However, such intense interest was generated by the transparent, high density polyethylene samples crystallized in the Instron Capillary Rheometer that the primary studies were concerned with defining this crystal structure.

Chapter I contains an outline of the procedure for crystallization in the rheometer, together with orientation and melting point properties of translucent strands that were isolated in a preliminary study. The evidence is consistent with the presence of an extended chain component in the structure and is of such an unusual nature in comparison with conventional polyethylene bulk crystallized structure that additional studies were warranted. In Chapter II, the paramount importance of the crystallization temperature on the sample orientation, melting point, and degree of transparency is emphasized. Additional aspects of the crystallization procedure are pointed out in Chapter II as well as Chapter V.

Precise x-ray and birefringence measurements of the amorphous and crystalline orientation in the sample strands

constitute the main subject of Chapter III. The high degree of crystallite orientation and crystalline content is used to explain the significant light transmission of the samples. Chapter IV summarizes the data and the conclusions obtained from calorimetric and birefringence determinations of the melting point. A comparative melting behavior study is also presented with known polyethylene structures and with irradiated Instron samples.

The data in Chapters I-IV is consistent with an extended chain crystal structure; however, only the microscopy and electron diffraction studies of Chapter V provide definitive proof of the presence of such a structure. The morphology of the Instron sample is defined in this chapter. Chapter VI is merely a correlation of x-ray determinations of crystallite size with electron diffraction data and existing models for the crystal structure of polyethylene. The appendices are included in order to define certain oscillatory flow behavior that sometimes accompanied the Instron crystallization procedure, to further define the x-ray procedure, to present data concerning the crystallization of polypropylene, and to outline several areas of possible interest for future research.

TABLE OF CONTENTS

CHAPTER I

POLYETHYLENE CRYSTALLIZED UNDER THE ORIENTATION AND PRESSURE OF A PRESSURE CAPILLARY VISCOMETER

Crystallization of a polymer while it is subjected to orientation has recently become a subject of great interest.[1-11] This introductory study is concerned with inducing crystallization under the influence of pressure and orientation and also with the nature of the crystalline structure so formed from two commercial high density polyethylenes. The resins utilized are Phillips Marlex 6009 having a melt index of 0.9 and Dupont Alathon 7050 having a melt index of 2.1. As most of the experiments were conducted on the Dupont samples, the subject will be Alathon 7050 unless noted otherwise. The Marlex 6009, with its distinctly different melt index, was largely used to confirm the generality of the phenomena observed with the Alathon 7050. Crystallization is induced in a capillary of 0.0508 cm. diameter, 2.56 cm. length, and 90° entrance angle by means of an Instron Capillary Rheometer[12] operating at constant plunger velocity.

Pressure losses in the barrel, elastic energy effects, entrance corrections, and the Rabinowitsch-Mooney shear rate correction were found to be of negligible importance to the conclusions derived from the data obtained from the rheometer; consequently, these corrections were not made on the rheological data that is presented. For a given plunger speed in the rheometer, the usual pressure trace for polyethylene in the

melt state is characterized by a smooth curve that levels off to an equilibrium value of the pressure. Such an equilibrium value was attained for the Alathon 7050 at 140°C for plunger velocities less than or equal to 0.5 cm./min., corresponding to a maximum apparent shear rate of 461 $sec.^{-1}$. For a capillary of given dimensions, the shear stress can be computed directly from this equilibrium pressure value, and the shear rate is directly proportional to the plunger velocity. For shear rates as high as 461 $sec.^{-1}$, it was found that the shear stress and shear rate data obtained at 140°C could be superimposed on similar data taken at 160°C by means of an exponential shift factor[13]. The ability to superimpose flow curves obtained at different temperatures implies that the basic flow mechanisms for the polymer chains do not change from one temperature to another. Specifically, since the polyethylene is in the melt state at 160°C, one can assume that it is also fully melted at 140°C up to the shear rate of 461 $sec.^{-1}$. Since it can be assumed that the formation of a significant number of crystallites would lead to new flow mechanisms due to an increased number of stronger entanglement points, one can state that no crystallites form at shear rates up to 461 $sec.^{-1}$. This shear rate is accompanied by a shear stress of 1.81×10^6 $dynes/cm.^2$, corresponding to a pressure of 364 atmospheres.

At 140°C, the available plunger velocities greater than 0.5 cm./min. resulted in crystallization, as evidenced by the

data presented in Figure 1 which indicates the effect of crystallization on the pressure trace.* Literature values[2] for shear rates leading to crystallization in polyethylene are consistent with the shear rates computed directly from these plunger velocities (1.0 cm./min. and greater). One should note the irregular oscillations shown in Figure 1. For a particular polyethylene, the exact number and position of these oscillations within each pressure trace is a function of both the packing of the pellets into the barrel prior to extrusion and of the exact amount of polyethylene remaining in the barrel at a given time. Because of the packing problem, it is impossible to exactly duplicate the oscillations occurring in each trace. These pressure traces are distinctly different from the smooth trace terminating in an equilibrium pressure that is described above as the norm for polyethylene in the melt state. For the plunger velocity shown in Figure 1, the pressure was rising rapidly when the operational limit of the Instron was attained at the pressure of 1920 atmospheres. This final rapid rise in pressure was accompanied by the reduction of visible flow of the extrudate from the rheometer. From a phenomenalistic viewpoint, the upward trend evidenced by the pressure trace implies the formation of crystallites. As will be further explained, the crystallites are formed under a combination of pressure and orientation effects occurring at the entrance to the capillary. During the accompanying irregular oscillations, the extrudate was observed to exit from the capillary in a

* Refer to note on page 16.

series of pulses. For a well defined oscillation, a relatively unswollen, rough extrudate exited rapidly during the downslope of the pressure trace. As the pressure rose on the upslope of the oscillation, the extrudate became swollen and smooth in appearance, and its exit velocity from the capillary was greatly reduced. It is probable that the oscillations are due to the onset of crystallization in the entrance to the capillary where the pressure and orientation effects would be expected to be at a maximum. Of the various plunger velocities resulting in crystallization, the lowest pressure oscillations were observed in Figure 1 to occur at the 5.0 cm./min. plunger velocity in the vicinity of 900 atmospheres. A pressure of this magnitude raises the equilibrium melting point above the ambient temperature of 140°C, and it becomes feasible to define a degree of supercooling for the polyethylene, an amount by which the 140°C temperature is below the equilibrium melting temperature. An empirical equation has been developed for high density polyethylene that relates the degree of supercooling (ΔT) to a static pressure (P_c in atmospheres) and temperature of crystallization (T_c in °C) as indicated in Equation 1:[14]

$$\Delta T = T_M + \left(\frac{.02^{\circ}C}{atm.}\right) P_c - T_c \qquad (1)$$

T_M is designated as the equilibrium melting point of the perfect polyethylene crystal and is $142 \pm 1^{\circ}C$[15]. Using the P_c of 900 atmospheres observed for the first oscillations and a T_c of

140°C, the value of 20°C was obtained for the degree of supercooling of the perfect polyethylene crystal implying that the crystallites may very well be responsible for the oscillations. As entropy[3] effects resulting from orienting the melt prior to crystallization have been neglected in applying Equation 1 (developed for static conditions), it can be assumed that the actual degree of supercooling is somewhat greater than 20°C. It is possible that the formation of these crystallites in the capillary entrance region results in the swollen, sluggish extrudate that is accompanied by an increase in the pressure. An alternating stick-slip flow mechanism for the semi-crystalline mass in the capillary may have been responsible for the pressure oscillations. An alternate explanation in which the oscillations are attributed to the inclusion of elastically deformed polyethylene in the flow stream from the vortices of this material existing at the entrance to the capillary is discussed in Appendix I.

It must be emphasized that the exact pressure is known only at the plunger head; however, within the ± 2% reproducibility of the pressure traces for the polyethylene in the melt state at 0.5 cm./min. and 140°C, it was found that the barrel correction could be neglected. Hence, the pressure value at the capillary entrance can be assumed to be equivalent to that indicated by the pressure trace. The pressure in the capillary is known to be a non-linear function of the distance from the capillary entrance for a viscoelastic material such as polyethylene. In the series of experiments discussed in

this report, no attempt has been made to determine this pressure gradient directly. The pressure values noted herein are valid only down to the capillary entrance. It is also of interest to note that shear heating may be occurring within the capillary, though evidence of this effect was not observed with the rheometer temperature at 140°C and the rheometer thermocouple located adjacent to the capillary entrance. As the temperature of the polyethylene in the rheometer is a major variable in obtaining crystallization, additional experiments are suggested in order to determine the precise temperature of the flowing melt as it exits from the capillary, after undergoing the effects of shear over the entire length of the capillary.

Once crystallization had occurred at 140°C as a result of pressure and orientation, it became important to extract the strand from the capillary in order to examine the crystalline structure so produced. A procedure was developed to prevent a portion of this crystalline structure from being melted during its removal from the rheometer assembly. At 140°C, if the pressure were to be removed, the polyethylene that had frozen in the capillary would melt, destroying the original orientation. Equation 1 suggests that, if the pressure is maintained above 1650 atmospheres, the equilibrium melting point of the polyethylene at this pressure will be sufficiently high to prevent melting. Hence, the temperature of the rheometer assembly was decreased at the rate of 1°C/min. from 140°C while maintaining the pressure between 1650 and 1920 atmospheres.

At the temperature of 114°C, it was assumed that the crystalline structure of the polyethylene would not alter and consequently the pressure was removed. The strand extracted from the capillary and the plug removed from the barrel were both analyzed on the Perkin-Elmer Differential Scanning Calorimeter Model-1B (hereafter identified as the DSC)[16,17]. The plug was found to have an average heat of fusion of approximately 47 cal/g.and a melting point of 133.4°C at a heating rate of 5°C/min. As these values are normal for high density polyethylene, we can conclude that polyethylene which is simply crystallized as a function of pressures up to 1920 atmospheres followed by a cooling rate of 1°C/min. does not yield unusual crystal structures. The polyethylene in the rheometer is, of course, subject to an annealing effect during the cooling cycle down to 114°C. However, the low melting point of the plug implies that this effect is minimal.

The strand obtained from the capillary was sectioned in a plane perpendicular to the axis of flow and tested in the DSC. The results are presented in Table I. On the basis of the temperature of the peak in the fusion curve, commonly referred to as the melting point, one can delineate three regions in the strand. Considering the heats of fusion and the melting points, two of these regions apparently have distinctly different crystal structures than that of the plug taken from the barrel. It should be noted that Region 1, nearest the entrance to the capillary, was translucent to visible light.

In contrast, Region 3, which was closest to the exit of the capillary, was opaque as was the plug in the barrel. The intermediate Region 2 was not definable under an optical microscope; however, DSC results implied that this relatively small portion of the strand is a transition zone that contains some of the translucent region and some of the opaque region. Figure 2 shows the typical melting curves observed on the DSC for segments of the strand taken from various regions. The dual peaks of the transition region strongly suggest the existence of two different crystal formations. To reinforce this hypothesis, the breadth of the fusion curves obtained for Region 3, representing a measure of the magnitude of the distribution of crystallite perfection, are significantly greater than those obtained for the relatively high melting point structure composing Region 1.

It is now necessary to formulate an explanation incorporating the data presented. The cessation of extrudate flow that was observed in the vicinity of 1600 atmospheres at 140^{o}C implies that the material has massively crystallized in some portion of the rheometer. As a result of the large orientation effects occurring in the entrance to the capillary (more fully explained below), the polyethylene is assumed to "freeze" in the entrance and upper portions of the capillary. A pressure drop from near a maximum of 1920 atmospheres to approximately atmospheric pressure immediately develops down the length of this relatively solid material. Essentially, the polyethylene of Region 3 may have crystallized under the pressure and

orientation forces; however, this segment is at such a low pressure that its melting point is below 140°C. In Table I, this includes the portion of the strand from 0.60 to 2.50 cm. from the capillary entrance. Either this Region 3 material never crystallizes, simply remaining in the melt state, or a crystal structure forms under the orientation-pressure effects and subsequently melts as a result of the low pressure-high temperature combination. For either case, the segment would be in the melt state at 140°C and would crystallize during the cooling cycle down to 114°C. This conclusion was confirmed by the results of a separate experiment carried out in the following manner. The Instron barrel was packed at 140°C and the plunger velocity was set at 0.5 cm./min. After equilibrium was attained, plunger motion was halted and the pressure removed. The sample crystallized in the rheometer under atmospheric pressure on reducing the temperature from 140°C to 114°C at a rate of 1°C/min. At this juncture, the strand was removed from the rheometer and examined on the DSC. Except for the lack of pressure and orientation during crystallization, this strand received the same treatment as the one examined in Table I. A comparison of the two showed that Region 3 of the strand in Table I had a heat of fusion of 46.5 cal/g. which was similar to that of the strand produced without benefit of pressure and orientation. Furthermore, the melting points were approximately 133.5°C. One concludes that the basic crystal structure and the percent crystallinity were the same

in both cases. Essentially, Region 3 consists of material that is crystallized as a function only of thermal conditions. In addition to the evidence provided by the heats of fusion and the melting points, wide angle x-ray photographs of Region 3 showed concentric rings that define a crystal structure that is lacking in orientation. This lack of orientation supports the above explanation.

An explanation for the existence of the relatively high melting point material composing the zone adjacent to the capillary entrance is now in order. As has been previously asserted, these crystals with final melting points of more than 138°C are the result of orientation in the entrance to the capillary and of pressure exerted on the material. Using a plunger speed of 1.0 cm./min. to induce crystallization, extrudate flow was observed to cease in a range between 1500 to 1600 atmospheres. One could postulate that a critical degree of supercooling, as computed from Equation 1, resulted in crystallization. The region melting above 138°C did not result from pressure induced crystallization alone because the polyethylene in the barrel was subjected to similar pressure, yet it melted at 133.5°C. However, if to the effect of the pressure on the melting point, resulting in a driving force for crystallization, one adds the orientation effect that occurs at the capillary entrance, it is possible to explain the formation of the high melting point structure.

Orientation is believed to be mainly due to the velocity

gradients parallel to the axis of flow. As an example of the velocity gradient along the center axis of flow, the material must accelerate from a velocity of 5 cm./min. in the barrel to 1750 cm./min. in the capillary. A study of a number of strands formed under orientation and pressure shows that an increase in the plunger velocity results in greater penetration of Region 1 down the capillary, i.e., a greater amount of high melting point material in the strand. At 140°C, a plunger velocity of 1.0 cm./min. produced a Region 1 that extended approximately 0.35 cm. down the capillary away from the entrance, whereas a Region 1 of a 0.85 cm. length was produced at a 5.0 cm./min. plunger velocity. It should be noted that a greater plunger velocity produced a greater velocity gradient along the axis of flow. This parallel gradient is largest in the conical entrance region of the capillary[18] and is believed to be the principal reason for the drawing of the polymer chains into an oriented crystal structure. As a confirmation of the importance of the parallel velocity gradient, a distribution of crystal perfection was found to exist along the strand axis. As in Table I, it was consistently found that the melting points of the translucent material rose to a maximum in the transition region. Furthermore, wide angle x-ray photographs indicated increased orientation along the axis of flow on traveling down the translucent portion of the strand away from the capillary entrance. The increase in the degree of orientation determined from x-ray data is believed to be linked with the observed

increase in the melting point. A typical x-ray photograph indicating the orientation in Region 1 is shown in Figure 3.

Orientation phenomena in capillary viscometers are usually attributed to the shearing conditions resulting from velocity gradients perpendicular to the axis of flow. If such is the case for the crystallization procedure described above, one would expect to get a radial distribution of shear rate and/or shear stress. With the possible exception of the coexisting structures in Region 2, this was not observed in the DSC studies of strands such as the one shown in Table I. Essentially, a dual peak would be expected for the fusion curves of segments from Region 1 if a radial distribution occurred, and such is not the case. Thus the velocity gradient perpendicular to the axis of flow does not seem to be the significant factor in producing the oriented crystal structure.

As indicated previously, the polyethylene in the rheometer is subject to annealing after crystallization has occurred (during the thermal cooling cycle). It is possible that annealing results in an elimination of a radial distribution of crystallite perfection and in the resulting narrow fusion curve shown in Figure 2-a for a Region 1 segment. However, the assertion that the important velocity gradient is parallel to the axis of flow and in the capillary entrance region is consistent with results noted in the literature. Specifically, crystallization in polypropylene is initiated in the capillary entrance region[19], where the greatest velocity gradient is

parallel to the flow axis[18]. In polypropylene studies, it was also found that the first crystallites are formed in the center of the cylindrical extrudate[20], a position where a condition of zero radial velocity gradient exists in conjunction with a maximum longitudinal velocity gradient (parallel to the axis of flow in the capillary). Thus the evidence leads to the conclusion that the Instron procedure does not result in crystallization induced from the shearing action provided by the radial velocity gradient within the capillary. Crystallization is the direct result of the longitudinal velocity gradient in the entrance region in combination with the applied pressure.

For the Dupont polyethylene, we have seen that the segment encompassing Region 1 of the strand was both highly oriented and had a melting point in the vicinity of 138.5°C. For high density polyethylenes, experiments to produce melting points of this magnitude from lamellar chain folded crystals have required growth time measured in hours and very low values of the degree of supercooling. However, conditions existent in the capillary during the crystallization due to orientation and pressure permit, at most, a few minutes for the crystallization to occur under relatively enormous degrees of supercooling. In conjunction with these factors, observations on the electron microscope and the DSC lead to the proposition that the fundamental component of the oriented crystal structure consists of polymer chains in an extended conformation[21].

Electron micrographs utilizing a Japan Electron Optics scanning microscope, Model JSM-1, were obtained on fracture surfaces of the strands broken under liquid nitrogen. Region 1 was found to have a very fibrillar substructure with probable orientation of the fibers along the axis of flow. A photograph of a fracture surface in the transition region of a Marlex 6009 sample showed a columnar structure with the columns definitely oriented along the flow axis as can be seen in Figure 4. In contrast to this photograph, Figure 5 showed a fracture surface in Region 3 of the same Marlex strand. Note the complete lack of oriented structure in this material that is thermally crystallized and is assumed to be entirely chain folded. When tested on the DSC, the segment shown in Figure 5 had a single melting peak at 133.4°C, whereas the transition region segment shown in Figure 4 resulted in dual melting peaks of 133.1°C and 136.3°C. The transition region may, in fact, be composed of extended chain crystallites oriented along the axis of flow in conjunction with chain-folded lamellae. Such a proposed structure would be consistent with the columnar structure shown in Figure 4, as well as the observed dual melting peaks. Higher magnifications of Region 3 segments showed surfaces that exhibited signs of microdrawing, a result of the fracture process; however, in none of the Region 3 material was there any evidence of a fibrillar substructure such as was consistently found for Regions 1 and 2. The essential factor is that the polyethylene in Regions 1 and 2, crystallized

under both orientation and pressure, has a definite fibrillar structure as exemplified in Figure 4.

It has been shown that polyethylene extended chain crystals can be superheated much more readily than can folded chain crystals[22-24]. If the high melting point portion of the strand produced in the capillary of the Instron Rheometer is indeed composed of an extended chain structure, then this portion should be clearly more prone to superheating than a lamellar chain folded structure formed from the same polyethylene. In order to test the proposition concerning the existence of an extended chain crystal structure in those portions of the strands showing orientation, Region 1 of strands formed from the Dupont resin at 140°C and a 5.0 cm./min. plunger speed was sectioned into two segments, identified as being either nearest the entrance or nearest the exit of the capillary. At a selected series of six scan rates, these segments were run from 69°C to 162°C. Each segment was held at 162°C to insure melting, and then recrystallized by returning the temperature to 69°C at 10°C/min. A second scan was immediately run at the pre-selected scan rate on the sample which is assumed to have recrystallized into a lamellar chain folded structure. The first scan is on oriented material, and the second scan is assumed to be on unoriented material. An examination of Figure 6 showed that the curve corresponding to the first scan had an average slope (a measure of the degree of superheating) that was more than twice that obtained for the second scan.

This observation agrees with the assumption that extended chains constitute the fundamental component of Region 1.

The data presented constitutes supporting evidence for the formation of an extended chain crystal structure in the Instron Capillary Rheometer. However, more intensive x-ray, thermal, and electron microscopy studies will be provided in succeeding chapters to determine the exact nature of the structure. It should be noted that other researchers have postulated structures formed under the influence of orientation that lacked an extended chain component[9-11]. The unusual melting behavior of the crystal structure found in Region 1 of the strand is not sufficient to prove the presence of extended chains.

* Crystallization of the polyethylene in the Instron Rheometer was also evidenced by an observed increase in the density of the material in the rheometer barrel. The density increase accompanying the above-mentioned pressure rise was measured at 140° C for Alathon 7050. The density of the polyethylene in the melt state was 0.80 g/cm^3 under a plunger velocity of 0.5 cm/min.; however, a plunger velocity of 1.0 cm/min., leading to a rapid pressure rise, resulted in a density increase to 0.94 g/cm^3 (as calculated from weight extruded, volume displaced, and volume remaining).

REFERENCES

1. C. L. Sieglaff and K. J. O'Leary, ACS Polymer Preprints, 10, 57 (1969).
2. A. K. van der Vegt and P. P. A. Smit, Advances in Polymer Science, Society of Chemical Industry, London, Monograph 26, 313 (1967).
3. Keinosuke Kobayashi and Toshio Nagasawa, Internat. Conf. Rheol., Kyoto, Japan (1968).
4. A. J. Pennings, Proc. Int. Conf. on Crystal Growth, Boston (Oxford: Pergamon Press), 389 (1966).
5. R. B. Williamson and R. C. Novak, J. Polymer Sci., Pt. B, 5, 147 (1967).
6. R. B. Williamson and W. F. Busse, J. Appl. Phys., 38, 4187 (1967).
7. A. Keller and M. J. Machin, J. Macromol. Sci. (Phys.), B1 (1), 41 (1967).
8. A. Keller, Reports on Progress in Phys., Pt. 2, 31, 623 (1968).
9. Toru Kawai et al., Kolloid-Z. u. Z. Polymere, 221, 28 (1967).
10. Toru Kawai et al., Kolloid-Z. u. Z. Polymere, 222,1(1968).
11. Toru Kawai et al., Kolloid-Z. u. Z. Polymere, 229, 168 (1969).
12. R. L. Ballman and J. J. Brown, Bulletin SA-2, Instron Engineering Corp., Canton, Mass.

13. R. Mendelson, Trans. Soc. Rheol., 9, 53 (1965).

14. B. Wunderlich, J. Polymer Sci., Pt. A, 2, 3697 (1964).

15. J. D. Hoffman, SPE Trans., 4, 315 (1964).

16. E. S. Watson et al., Anal. Chem., 36, 1233 (1964).

17. M. J. O'Neil, Anal. Chem., 36, 1238 (1964).

18. P. Schummer, Rheol. Acta, 6, 192 (1967).

19. C. L. Sieglaff and K. J. O'Leary, Trans. Soc. Rheol., to be published.

20. G. V. Vinogradov and Prosorovskaya, Rheol. Acta, 3, 156 (1964).

21. F. R. Anderson, J. Appl. Phys., 35, 64 (1964).

22. E. Hellmuth and B. Wunderlich, J. Appl. Phys., 36, 3039 (1965).

23. B. Wunderlich et al., J. Macromol. Sci. (Phys.), B1(1), 93 (1967).

24. A. G. Wikjord and R. St. John Manley, J. Macromol. Sci. (Phys.), B2(3), 501 (1968).

TABLE I

Results of DSC Study of Strand Formed Under a Plunger Speed of 1 cm/min. at 140°C.

	Length from Capillary Entrance (Centimeters)		Temperature of Peak in Fusion Curve (± 0.4°C)	Heat of Fusion (± 4% in Calories/gram)
Region 1.	0 - .15		138.1	56.8
	.15 - .32		138.7	59.4
Region 2.	.32 - .49		138.9, 133.6	58.5
	.49 - .60		137.6, 134.5	66.5
Region 3.	.60 - .75		133.9	45.8
	.75 - .85		134.3	43.8
	.85 -1.00		134.1	46.9
	1.00 -2.50	End of Strand	133.9	46.7*

* The segment from 1.00 to 2.50 cm. is accurate to ± 2% due to the x 8 scale on the DSC. The smaller segments required the use of the x 2 scale which resulted in less accurate measurements for the heat of fusion.

LEGEND FOR ATTACHED FIGURES

Instron Pressure Traces During Crystallization at 140 °C, Using a Capillary of Diameter 0.0508 cm. and of Length 2.56 cm.

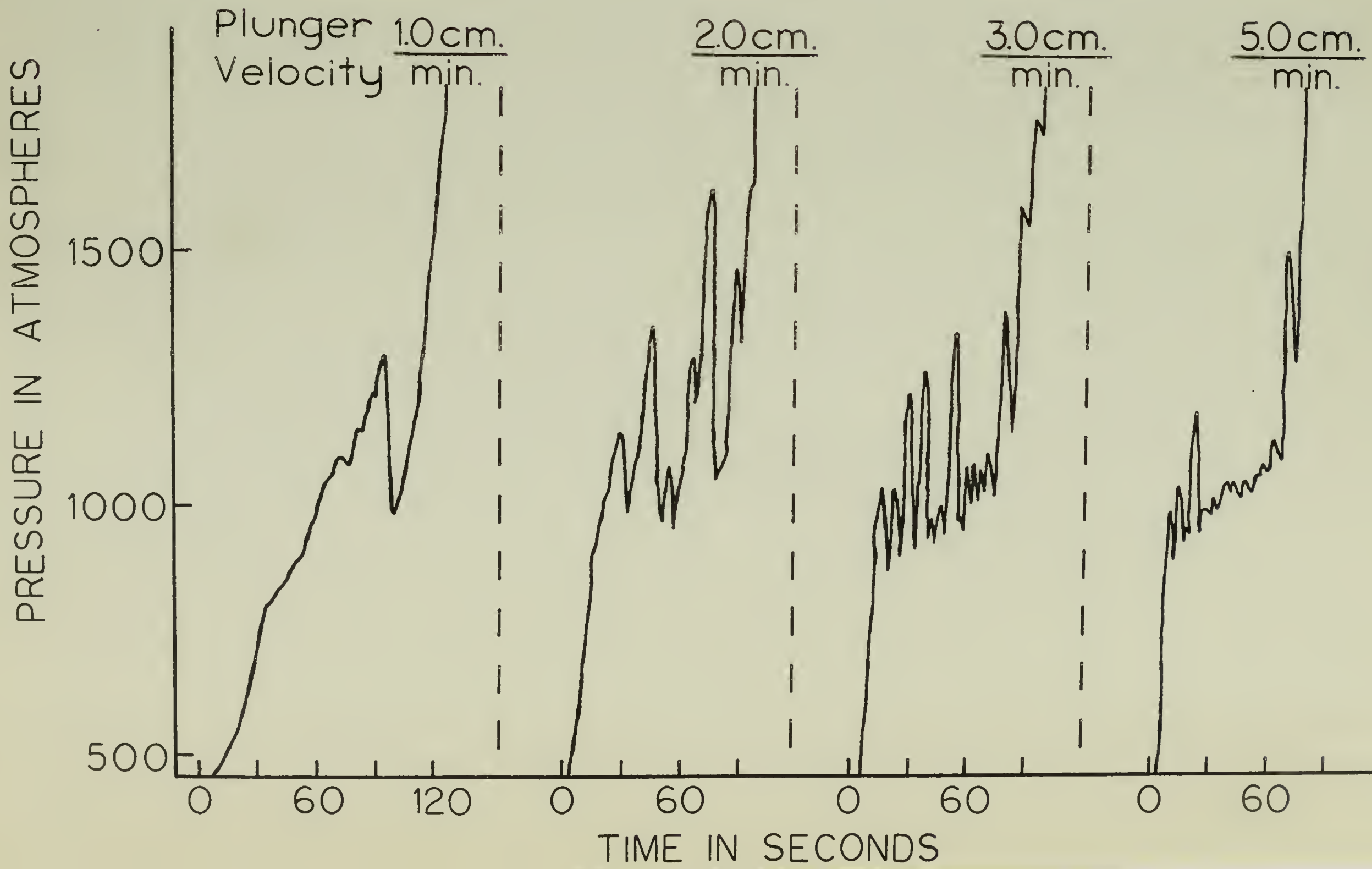

DIFFERENTIAL SCANNING CALORIMETRY OF STRAND FORMED AT 5.0 CM./MIN. AND 140 °C

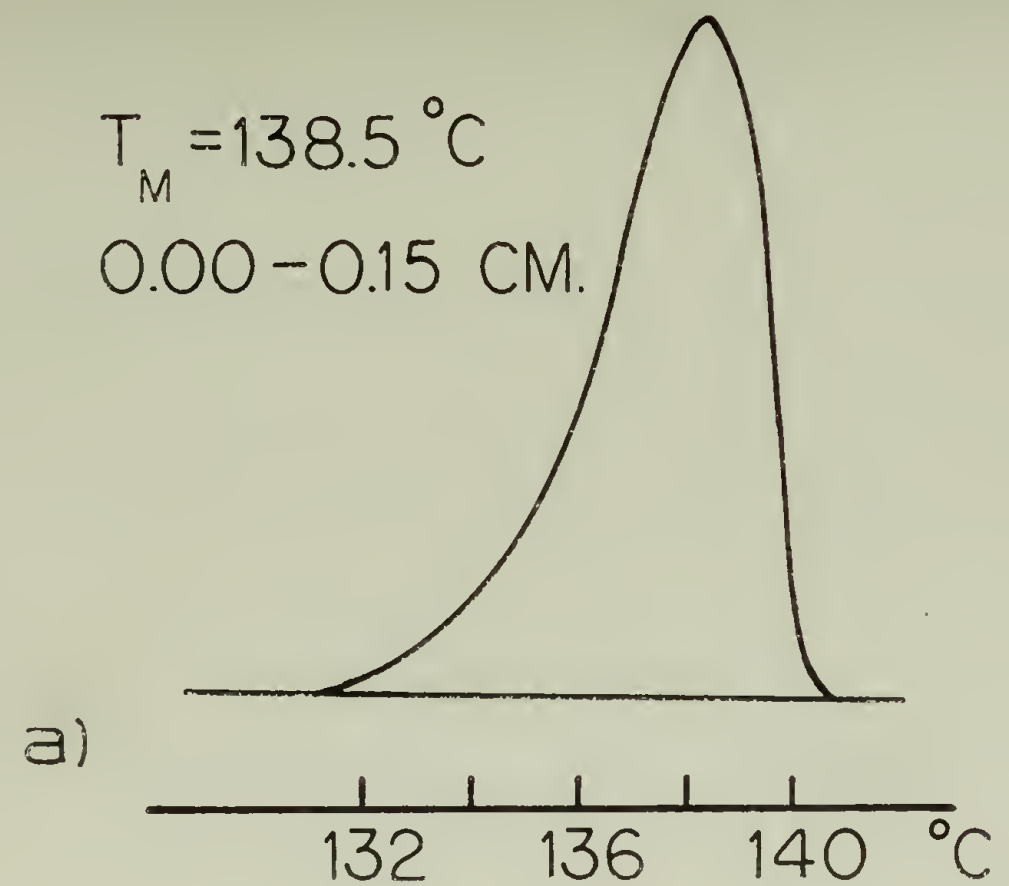

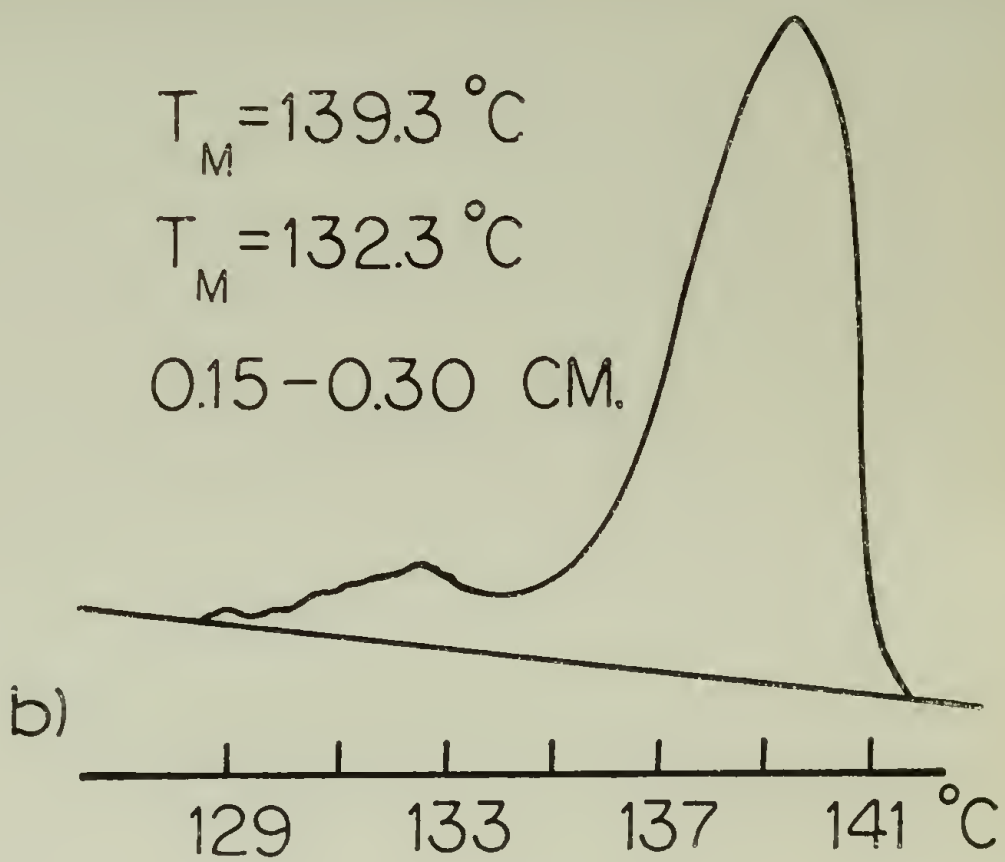

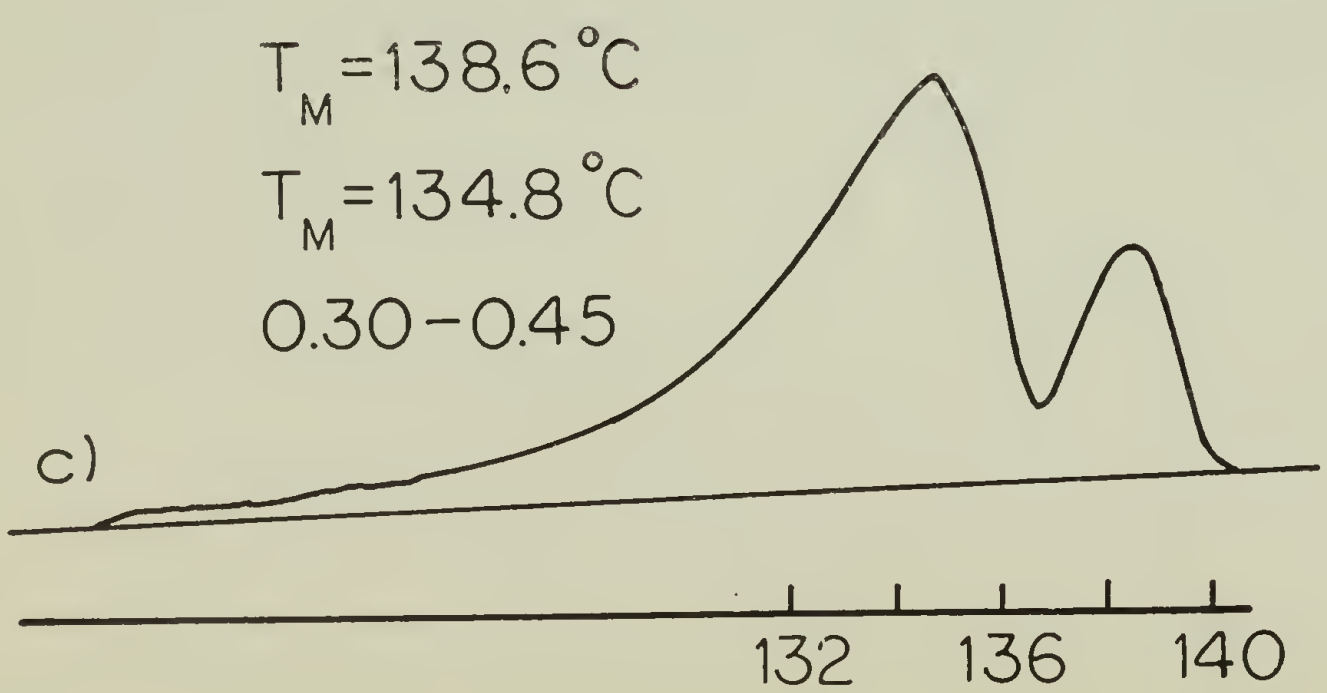

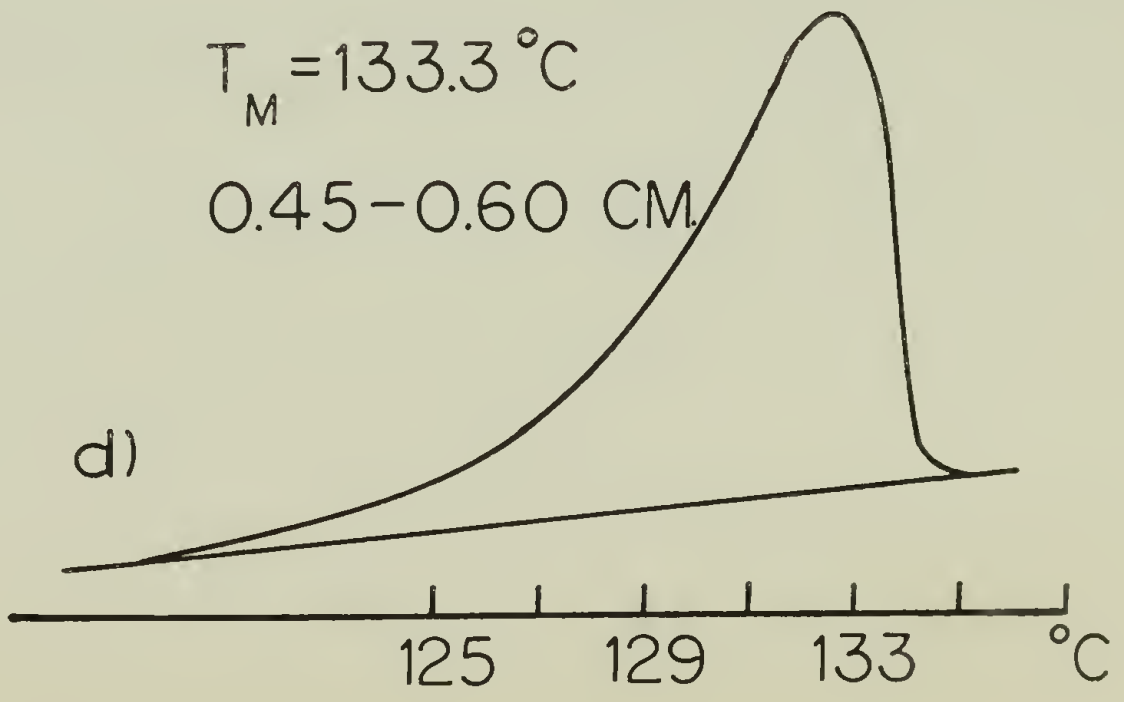

Effect of Scan Rate of Differential Scanning Calorimeter on Melting Point of Translucent Portion of Strands Formed at 5 cm./min. and 140 °C

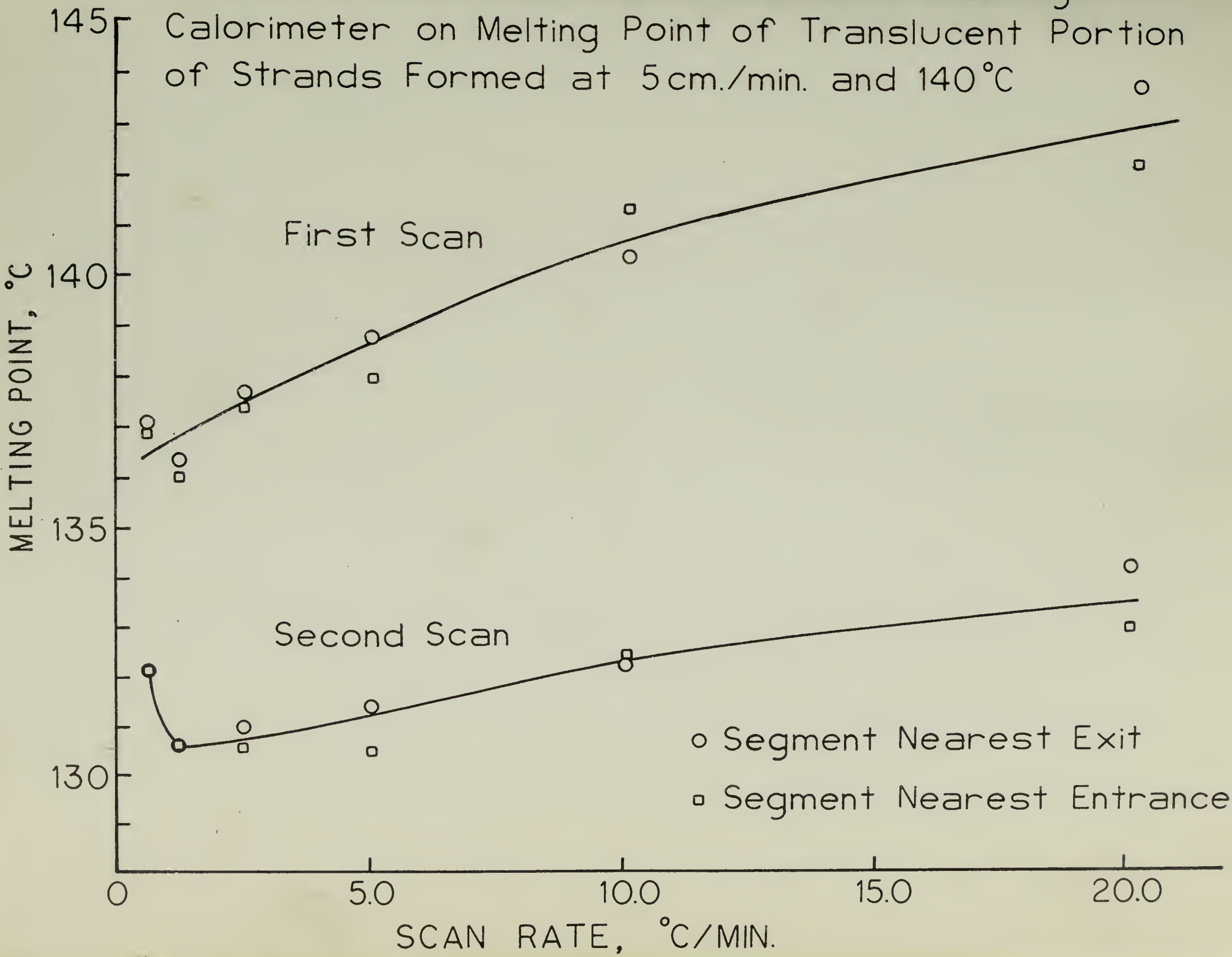

CHAPTER II

THE PROPERTIES OF POLYETHYLENE CRYSTALLIZED UNDER ORIENTATION AND PRESSURE EFFECTS OF A PRESSURE CAPILLARY VISCOMETER

This is a study of crystallinity induced in a high density polyethylene under the influence of orientation and pressure effects in an Instron Capillary Rheometer.[25-27] The crystal structures so produced are found to be unusual in terms of melting point, orientation, modulus, and transparency. The instrumentation used in analyzing the crystal structures included a Perkin-Elmer Differential Scanning Calorimeter Model 1-B (DSC), wide angle x-ray equipment, and the $\overline{To}$ $\overline{Yo}$ Vibron instrument for dynamic tensile modulus measurements.

Crystallization Procedure

All tests were performed on a single polyethylene, Dupont Alathon 7050, unless noted otherwise. It has a density of 0.978 g/cm^3 and a melt index of 2.1. Gel permeation chromotography and light scattering provided number and weight average molecular weights for this polymer of 18,400 and 52,500, respectively.

In the procedure used for inducing crystallization, the Instron Capillary Rheometer was operated at a series of constant plunger velocities. The effect of certain plunger speeds in combination with test temperatures of 130°C to 145°C was such that the recorded Instron pressure trace failed to attain a steady state or even an average value over long times. The

pressure required to move the plunger at a constant velocity was observed to increase to the maximum value attainable in the rheometer (1900 atm.), with accompanying reduction of extrudate flow. This is contrary to the usual observations concerning the extrusion of high density polyethylenes and was suggestive of crystallization in the rheometer.

The specimen of interest consisted of the strand that crystallized in the rheometer capillary. After reduction of flow, the pressure was maintained in the vicinity of 1900 atm. in order to prevent the structure from returning to the melt state. This is accomplished under such a pressure since the equilibrium melting point of the polyethylene will be approximately 180°C,[28] a value that is much higher than the ambient rheometer temperatures (130-145°C). It can be assumed that no melting occurs in the crystallized material once it has formed in the high pressure segment of the capillary length adjacent to the capillary entrance. A pressure drop exists over the length of the capillary, and the polyethylene in the capillary adjacent to the exit is subject to reorganization due to the lower pressure value.

The rheometer was cooled after reduction of flow at a rate of 1°C/min., while maintaining the 1900 atmospheres of pressure. On cooling to 110°C, it was assumed that no additional changes would occur in the crystal structure at atmospheric pressure; hence, the pressure was released and the capillary removed from the rheometer. The polyethylene strand in the capillary

was sufficiently cohesive to retain its cylindrical shape on being forced from the capillary. The capillary used to form the strands was of the following dimensions: 0.0508 cm diameter, 2.56 cm length, and 90° entrance angle. It is to be emphasized that only the segment that is adjacent to the capillary entrance retains the crystal structure formed under pressure and orientation. The crystallinity in the segment adjacent to the capillary exit is formed during the cooling cycle. This report is primarily concerned with the properties of the transparent segments near the entrance of the capillary that are under sufficient pressure to prevent reorganization during the cooling cycle. Note that the transparent segments were crystallized at lower temperatures than the 140°C Rheometer temperature used in Chapter I which resulted in translucent segments.

Effect of Plunger Velocity and Rheometer Temperature

As has been explained in greater detail in Chapter I, the crystallization process initially occurs in the entrance region of the capillary as the consequence of both pressure and orientation. For a given plunger velocity, it is reasonable that the influence of both pressure and orientation on the flowing melt is a function of the rheometer temperature. An example of this temperature effect is presented in Figure 7 in which a 0.5 cm/min. plunger velocity was utilized. At 139°C, the pressure trace is observed to attain an equilibrium value of 373 atm.

The general shape of this pressure trace is typical of those obtained for a fully melted polyethylene.

Figure 7 also contains a pressure trace at a 138°C rheometer temperature. Never leveling off as in the 139°C example, the pressure during extrusion at 138°C increases to the 1900 atm. limit with accompanying reduction of extrudate flow. Thus a temperature drop of about 1°C was sufficient to result in massive crystallization in the rheometer. Due to temperature gradients existing in the barrel and capillary, the accuracy of the temperature in the rheometer was limited to $\pm$ 0.5°C (neglecting the possibility of shear heating). It should also be noted that the pressure traces presented in this report represent uncorrected data. Such factors as pressure losses in the barrel, elastic energy effects, and entrance corrections are of negligible importance to the conclusions derived here.

Rheometer temperature is critical not only in obtaining crystallization in the capillary but also in determining crystal structure within the strand. For a constant plunger velocity of 5.0 cm/min., Table II shows the melting points from peak maxima of DSC fusion curves for the four millimeter strand segments adjacent to the capillary entrance crystallized at various rheometer temperatures. These melting points, ranging from 137.6°C to 140.1°C, are indicative of an extended chain crystal structure and/or a chain folded structure with a relatively long fold period. The brief time for crystallization under the combined influence of pressure and orientation

is consistent with the formation of a crystal structure containing an extended chain component, since lengthy annealing times are usually required to form long fold periods. However, low angle x-ray studies are necessary for more definitive crystal structure determinations. It is interesting to note that the maximum melting point in Table II has the relatively high value of 140.1 $\pm$ 0.4°C. For crystallization temperatures below 136°C and also for those above 139°C, the melting points are notably lower. The implications of these results to the crystal morphology will be discussed in conjunction with the orientation data obtained from wide angle x-ray equipment. It is also of interest to point out, for comparative purposes, that the initial melting points of the Alathon 7050 (prior to processing in the Instron) were on the order of 132 - 133°C.

A wide angle x-ray photograph of the high melting point portion of a strand produced at 136°C is shown in Figure 8. The presence of arcs, rather than concentric circles, in the reflections is evidence for crystal orientation in this segment. A quantitative measure of the orientation was obtained by performing an azimuthal scan to determine the average angle between each axis of the crystallite unit cell and the direction of flow in the capillary.[29-31] The orientation functions presented in Table III as a function of crystallization temperature were obtained from the average angle values (ϵ) using the following equation:

$$f_x = \frac{3 \langle \cos^2 \epsilon \rangle - 1}{2} \qquad (2)$$

where x refers to either the a-, b-, or c-axis of the unit cell. An orientation function value of -1/2 corresponds to a particular axis of the unit cell being perpendicular to the flow direction, and a value of + 1 indicates that the axis is aligned parallel to the flow direction. In all cases presented in Table III, the x-ray beam was targeted on the strands at a point approximately 4 mm. from the capillary entrance. The c-axis of the unit cell is the axis down the length of the polymer chain. The c-axis orientation function is approximately + 0.9 for crystallization temperatures of 132 - 138°C. This is conclusive evidence that the polymer chains are significantly aligned in the crystal structure in the direction parallel to the flow axis.

It was also observed that c-axis crystal orientation decreased with increasing crystallization temperatures above 138°C; see Table III. Sieglaff and O'Leary[26] have provided a qualitative confirmation of this effect using a technique for the crystallization of polypropylene that is similar to the one described in this report. For polypropylene crystallized over the range of 170 to 195°C, they reported that crystal orientation generally decreased with increasing rheometer temperature. For polyethylene, the data presented in Table III shows that c-axis orientation decreases above 138°C; however, below this temperature down to 132°C, the orientation does not change significantly as a function of crystallization temperature.

The drop in orientation in the structure crystallized at 140°C relative to that crystallized at 138°C is also accompanied by a decrease in the melting point. Specifically, the data in Tables II and III show that, as the melting point dropped from 140.0°C to 138.8°C, the orientation function also dropped from + 0.9 to + 0.7 on going from the 138°C to the 140°C crystallization temperature. This comparison constitutes supporting evidence for a correlation of increasing crystallite perfection, as measured by increasing melting point, with increasing c-axis orientation. Such a correlation could be explained by an increase in the number of extended chain crystallites relative to the lower melting point, chain folded lamellae; an enhanced importance of extended chains in the crystal structure would result in the observed melting point increasing with increasing c-axis orientation.

An entirely different effect was observed in comparing the strands crystallized at 132°C and 134°C. As shown in Table II and III, crystal orientation did not change significantly for the two strands, but the melting point increased from 137.6°C to 139.6°C on going from a crystallization temperature of 132°C to 134°C. A possible explanation for this observation is an annealing of the internal defects in the crystal structure that is more easily accomplished at higher temperatures. Such an annealing process does not, in general, have a significant effect on the orientation function, hence the approximately constant orientation data for crystallization temperatures

from 132 - 138°C.[32,33]

Perhaps the most remarkable property of the strands crystallized at temperatures from 132 - 138°C is their transparency to visible light. They are extremely clear, as can be seen in the transmission photograph, shown in Figure 9, which contains a transparent segment crystallized at 136°C. It is possible to look through the 0.05 cm diameter segment and observe the scale markings on a clear ruler that has been placed beneath the strand. The strand in this photograph has been immersed in an oil of similar refractive index in order to reduce the lens effect due to its cylindrical shape. The opaque segment seen adjacent to the transparent one was crystallized during the cooling cycle. As a point of comparison to show the distinct differences in the crystal structure, the melting point of the transparent segment (adjacent to the capillary entrance) is 140°, while that of the opaque segment (adjacent to the capillary exit) is 134°C.

It must be emphasized that light is being transmitted through segments that are highly crystalline. Using a value of 69.2 cal/g. as the heat of fusion of the perfect extended chain crystal,[34] the experimental DSC heats of fusion of 57.2 cal/g. (± 2%) for the transparent segment shown in Figure 3 indicate 83% crystallinity. A density measurement for percent crystallinity gave a value of 86%, using 1.001 $cm^3/g.$ as the specific volume of the perfect crystal and 1.173 $cm^3/g.$ as that of the completely amorphous unit.[34] It is not expected that

density and specific heat measurements should give an identical value for the crystalline content; they are based on different calibrations for crystallinity determination.

It was found that the temperature in the Instron Rheometer is a critical factor in obtaining transparent segments. This is emphasized by the observation that a plunger velocity of 5.0 cm/min. resulted in a translucent segment for crystallization at 139°C, whereas a transparent segment was obtained at 138°C. As indicated in Figure 10, the pressure traces for 138°C and 139°C, that accompanied the formation of these segments, were distinctly different. As noted in Chapter I, a possible explanation for the irregular pressure oscillations at the higher temperature could involve an alternating formation and destruction of a crystalline network in the flowing polyethylene, resulting in a stick-slip flow mechanism. Evidence obtained from extrudate weight and plunger volume displacement gave effective density data which implied that a density increase was occurring in the material remaining in the rheometer barrel during these oscillations. The observed density increase is evidence for the existence of a critical density requirement at a given temperature that must be met in order to induce stable crystallites from the flowing melt. It is of interest that transparent segments, formed at rheometer temperatures below 139°C, were accompanied by pressure traces during crystallization that were similar in form to the 138°C trace shown in Figure 10.

The physical change from transparent to translucent as a function of increasing crystallization temperature has been observed previously on an industrial type of extrusion apparatus.[35] Similar in principle to the Instron Capillary Rheometer, the apparatus produced a transparent polyethylene tube at temperatures near the atmospheric melting point of the polyethylene. A temperature gradient, maintained down the barrel, is necessary in order to produce a continuous extrudate. The gradient prevents the solidification of the material in any region other than that at the die exit.

It is of interest to note that, for a given rheometer temperature, the plunger velocity has little effect on the clarity of the strand. An increase in the plunger speed from the 5 cm/min. value that resulted in the pressure traces in Figure 4 to a value of 10 cm/min. at the 139°C temperature still resulted in the formation of a translucent strand accompanied by pressure oscillations. This reinforces the earlier assertion that the temperature is the critical factor in producing transparency. Additional evidence supporting this conclusion was obtained from the crystallization of Marlex 6009. For Alathon 7050 and Marlex 6009, the melt indices of 2.1 and 0.9, respectively, are indicative of differences in the molecular weight distributions of the two polymers. The strands produced from both polymers exhibited the previously described change from transparency to translucency at 139°C. The lack of influence of plunger velocity and molecular weight on the

transparent to translucent change may indicate that 138°C is a maximum temperature for the formation of transparent polyethylene by means of pressure and orientation techniques available in an Instron Rheometer. The translucent quality observed in strands crystallized at temperatures greater than 139°C may be the result of a partial melting of the structure, an effect that can be attributed to the pressure drop which occurs in the capillary.

Superheating of the Transparent Segments

Other studies[36] have shown that extended chain crystals are more superheatable than chain folded crystals. With this superheating effect in mind, a series of DSC scans at different heating rates were obtained on transparent segments produced at 136°C and on translucent segments produced at 140°C.[25] These results are compared in Figure 11. Note that the apparent melting points (from maxima in fusion curves) for the transparent segments rise from 137.5°C to 146.7°C at scan rates of 0.625°C/min. and 20°C/min., respectively. This constitutes a 9.2°C rise in the apparent melting point due to superheating. Over identical scan rates, the translucent strands exhibited only a 6.5°C melting point increase. The conclusion is that the transparent segments are significantly more superheatable than the translucent segments, and hence it is probable that extended chains form a more important element in the overall crystal structure of the transparent segments.

In Figure 11, the shapes of the two curves at scan rates

below 2.5°C/min. are of some importance. The curve for the translucent segments goes through a minimum which is lacking in the curve for the transparent segments. A minimum value suggests that the material is reorganizing into a more perfect crystal structure at sufficiently low heating rates. Such observations are the norm for chain folded structures that increase their fold period as well as anneal out the irregularities in the crystal structure.[36] A model of a chain folded structure in combination with an extended chain structure is one possible crystal scheme that could account for the observed superheating and annealing of the translucent segments. The validity of such a proposed model will be established in electron diffraction studies reported in a later chapter.

Effect of Time at 136°C on Transparent Segment Length

If the cooling cycle were not immediately initiated on cessation of extrudate flow, it was found that the length of the transparent segment could be increased as a function of time at the constant crystallization temperature. Figure 12 shows the transparent segment length as a function of time at 136°C. The transparent segment formed after 30 minutes at 136°C prior to initiating the cooling cycle was found to extend 16 mm into the capillary from the entrance, as compared with the 10 mm long segment formed in zero minutes before cooling (maintaining approximately 1900 atmospheres until the cooling cycle is finished).

It was found that extrusion continued very slowly after

crystallization had occurred. From Figure 12, this extrusion rate was computed to be approximately 0.2 mm/minute. · As there was no detectable effect of time on either the crystal perfection or crystal orientation (the entire transparent segment length had a c-axis orientation function of + 0.9 and a melting point of 140°C), the advancing crystal structure can be assumed to be moving down the capillary as a solid plug. The implication of these observations is that only a very slow flow rate at the 1900 atm. of pressure is required to produce the oriented, transparent crystal structure. Hence,the orientation produced in the structure may not be due to the magnitude of the flow rate, but only to the magnitude of the change in the flow rate occurring in the conical capillary entrance region. This longitudinal change in velocity per unit distance through the entrance region is, in all probability, the critical factor in producing the oriented, transparent structure. In suggested experiments using glass capillaries, it is hoped that it will be feasible to conclusively define the exact manner in which the final crystal structure is formed.

Elastic Modulus of a Transparent Segment

The strand annealed for 80 minutes at 136°C before cooling was transparent throughout its 25 mm length (see Figure 12). This strand was tested on the Vibron at 30°C and the results compared with those of an unoriented strand of similar length that was formed by simply cooling polyethylene in the melt state at 1°C/min. The data is presented in Table IV together

with Takayanagi's data obtained on a drawn polyethylene, Marlex 50, having an orientation function +0.98, and 86% crystallinity, and a melting point of 137°C.[37] The tensile storage modulus attained the largest value for the strand crystallized under the pressure and orientation conditions existing in the Instron Rheometer. This modulus value of 6.6×10^{10} dynes/cm^2 is more than four times that of the unoriented, thermally-crystallized strand. This high modulus is due to both the high crystalline content and to the orientation of these crystals.

Conclusions

Evidence has been presented to show that strands can be formed in the Instron Rheometer that have a relatively high melting point, modulus, and oriented crystal content, combined with the property of being transparent. The distinctive engineering possibilities of these transparent strands indicate the need for additional research in this field. Our own work continues with the goals of developing a process for the rapid production of a continuous strand with such properties as well as determining more about the crystal structure. The remainder of this thesis will be primarily devoted to detailing the structure and the thermal properties of the strands crystallized with the Instron procedure.

REFERENCES

25. J. H. Southern and R. S. Porter (Chapter I), accepted for publication in J. Macromol. Sci. (Phys.) (1970).

26. C. L. Sieglaff and K. J. O'Leary, ACS Preprints, Div. of Poly. Chem., 10, 57 (1969).

27. A. K. van der Vegt and P. P. A. Smit, Advances in Polymer Science, Society of Chemical Industry, London, Monograph 26, 313 (1967).

28. B. Wunderlich, J. Polymer Sci., Pt. A, 2, 3697 (1964).

29. J. T. Judge and R. S. Stein, J. of Appl. Phys., 32, 2357 (1961).

30. C. R. Desper and R. S. Stein, ONR Tech. Report No. 80, Project NR 056-378, Contract Nonr 3357 (01), Univ. of Massachusetts, Oct. 1, 1965.

31. Z. W. Wilchinsky, J. Polymer Sci., Pt. A-2, 6, 281 (1968).

32. D. V. Rees and D. C. Bassett, Nature, 219, 368 (1968).

33. W. Statton and P. Geil, J. Appl. Polymer Sci., 3, 357 (1960).

34. B. Wunderlich and C. Cormier, J. Polymer Sci., Pt. A-2, 5, 987 (1967).

35. M. Bowman, U.S. Patent 3382220, May 7 (1968).

36. E. Hellmuth and B. Wunderlich, J. Appl. Phys., 36, 3039 (1965).

37. M. Takayanagi et al., J. Polymer Sci., Pt. C, No. 15, 263 (1966).

TABLE II

MELTING POINT AS A FUNCTION OF RHEOMETER CRYSTALLIZATION TEMPERATURE BY DIFFERENTIAL SCANNING CALORIMETRY* (SCAN RATE 5°C/MIN.)

Rheometer Crystallization Temperature (°C)	Melting Point (±0.4°C)
132	137.6
134	139.6
136	140.1
137	140.0
138	140.0
139	140.0
140	138.8
142	139.0
144	138.8

*The samples were the 4 mm. segments adjacent to the capillary entrance crystallized at a plunger speed of 5.0 cm/min.

TABLE III

X-RAY ORIENTATION DATA AS A FUNCTION OF CRYSTALLIZATION TEMPERATURE

Temperature (^{o}C):	132	134	136	138	140	142
Orientation Functions (±0.05)						
a - Axis	-0.4	-0.4	-0.4	-0.4	-0.3	-0.3
b - Axis	-0.5	-0.5	-0.5	-0.5	-0.4	-0.3
c - Axis	+0.9	+0.9	+0.9	+0.9	+0.7	+0.6

TABLE IV

MODULI OF POLYETHYLENE CRYSTALLIZED UNDER VARIOUS CONDITIONS MEASURED ON THE VIBRON (30°C, 110 cps)

Sample Description:	Instron At 136°C	Unoriented, Thermally Formed	Drawn Marlex 50 (Takayanagi)
Tensile Storage * Modulus (dynes/cm.^{2})	6.6×10^{10}	1.5×10^{10}	4.0×10^{10}
Tensile Loss Modulus (dynes/cm.^{2})	6.6×10^{8}	3.7×10^{8}	2.8×10^{8}

* Note that the theoretical elastic modulus for polyethylene is $260\text{-}320 \times 10^{10}$ dynes/cm.^{2} [A. Peterlin, Polymer Engin. and Sci., 9, 172 (1969)].

LEGEND FOR ATTACHED FIGURES

INSTRON PRESSURE TRACES

USING A CAPILLARY OF DIAMETER 0.0508 CM
AND LENGTH 2.56 CM

A PLUNGER VELOCITY OF 0.5 CM/MIN.

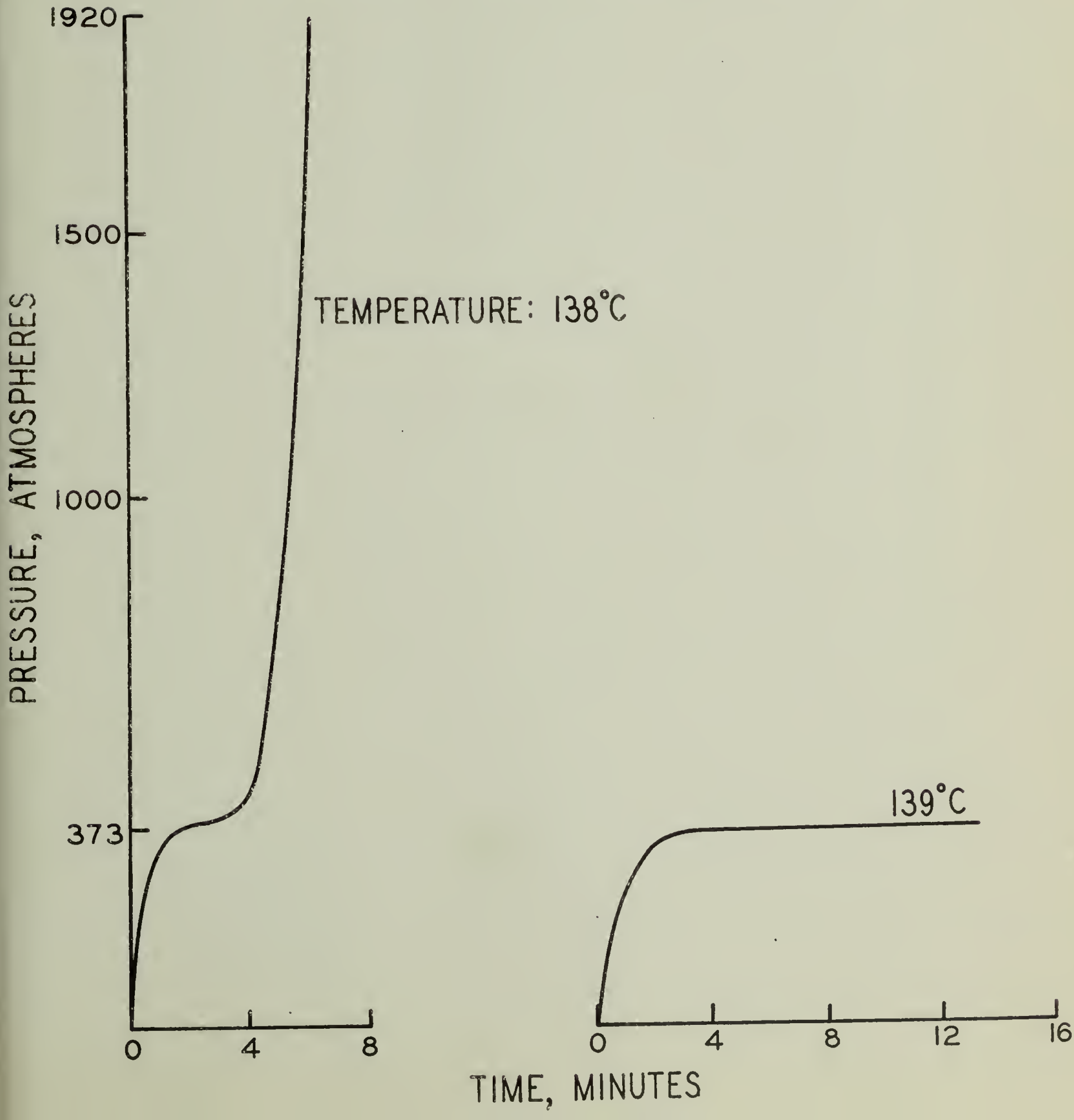

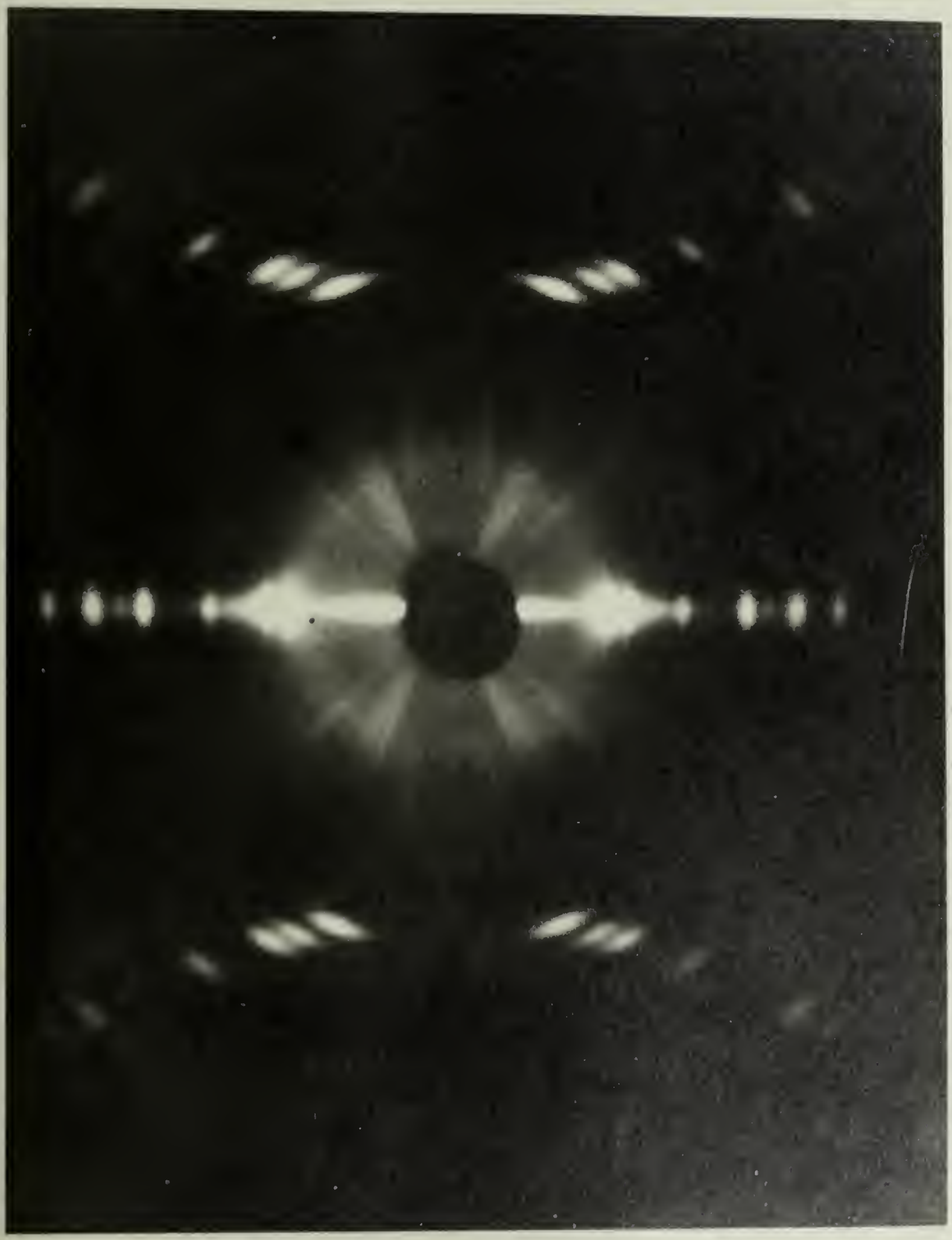

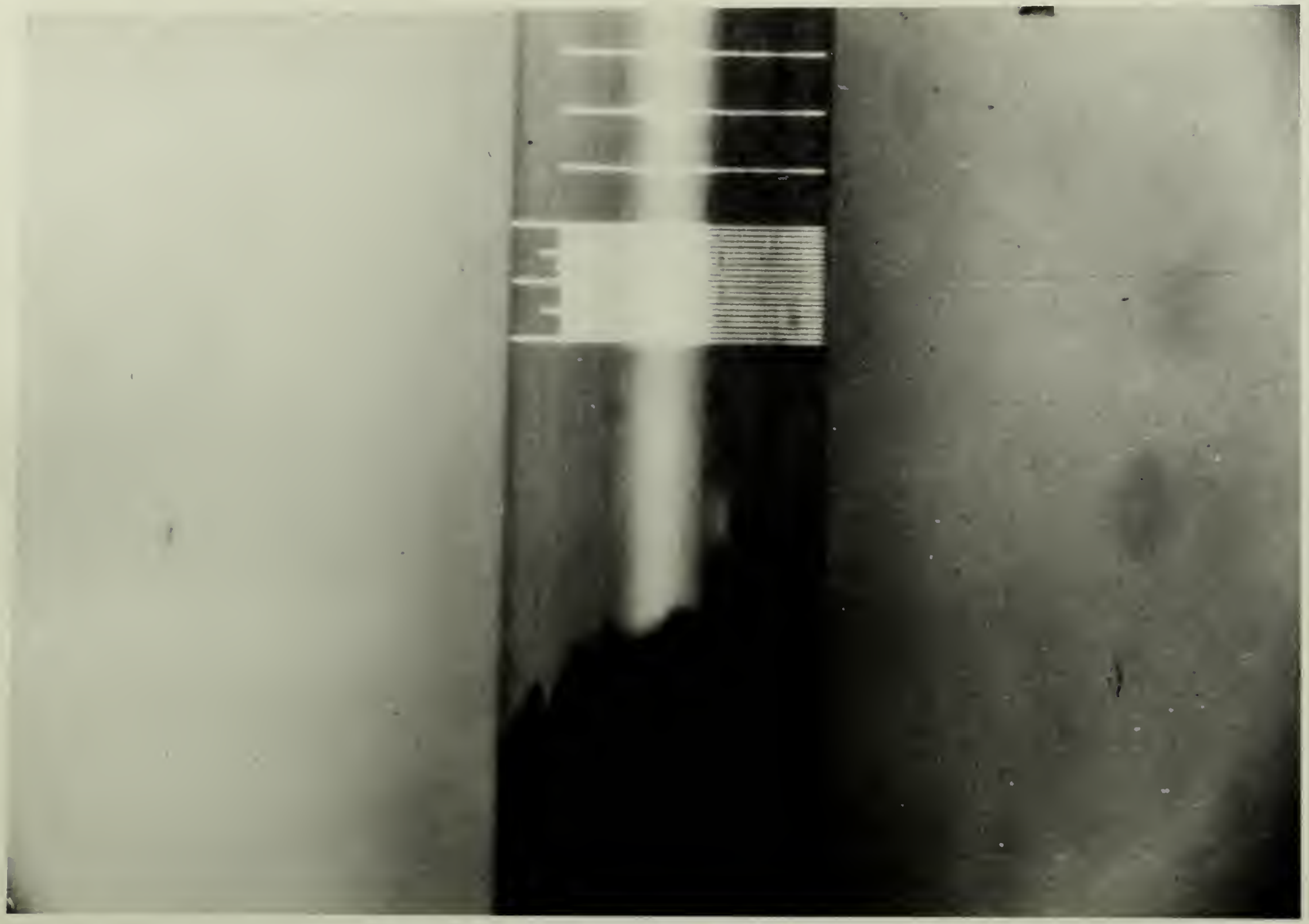

INSTRON PRESSURE TRACES DURING CRYSTALLIZATION

USING A CAPILLARY OF DIAMETER 0.0508 CM
AND LENGTH 2.56 CM

A PLUNGER VELOCITY OF 5.0 CM/MIN.

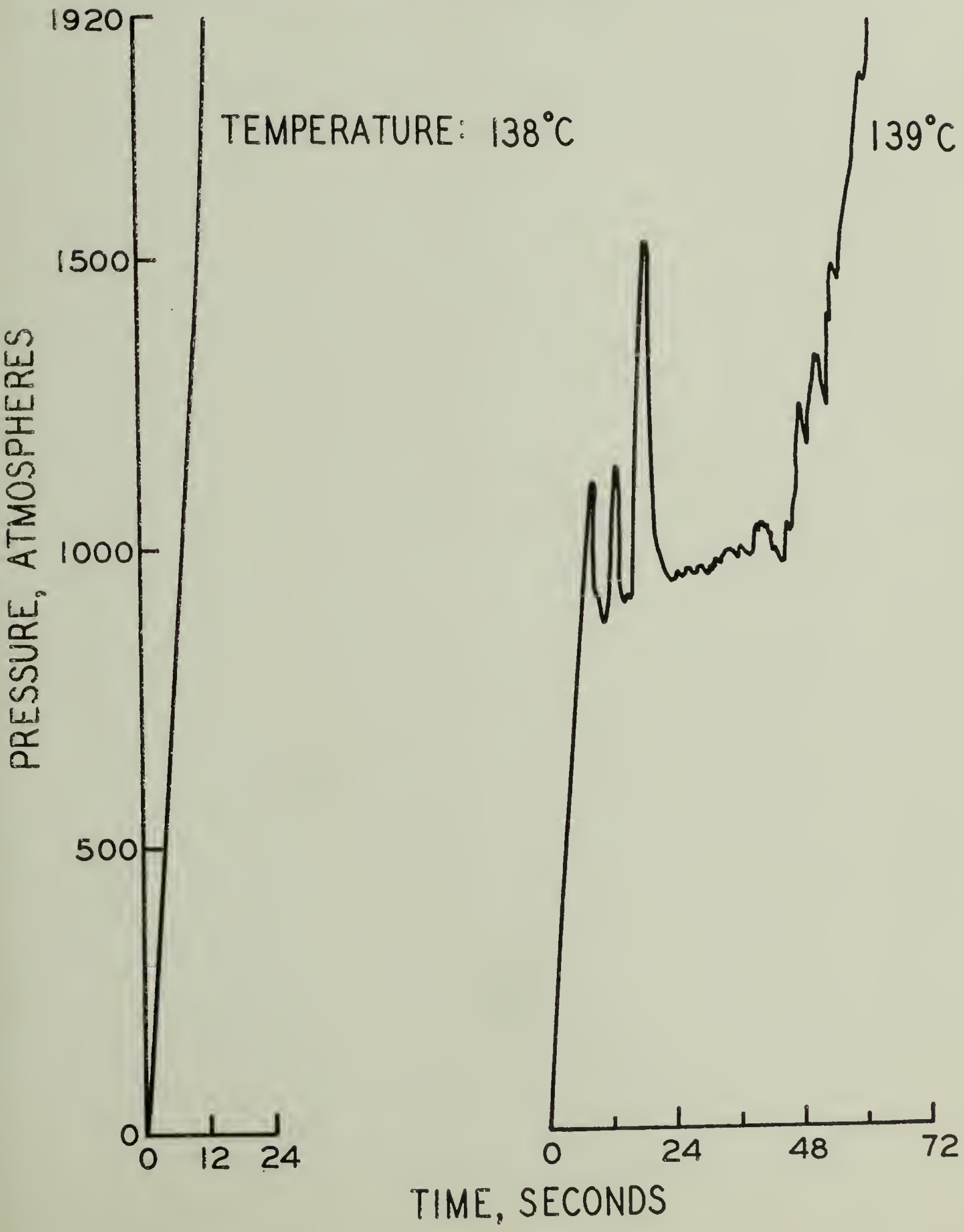

COMPARISON OF SUPERHEATING FOR STRANDS FORMED AT 136°C AND 140°C

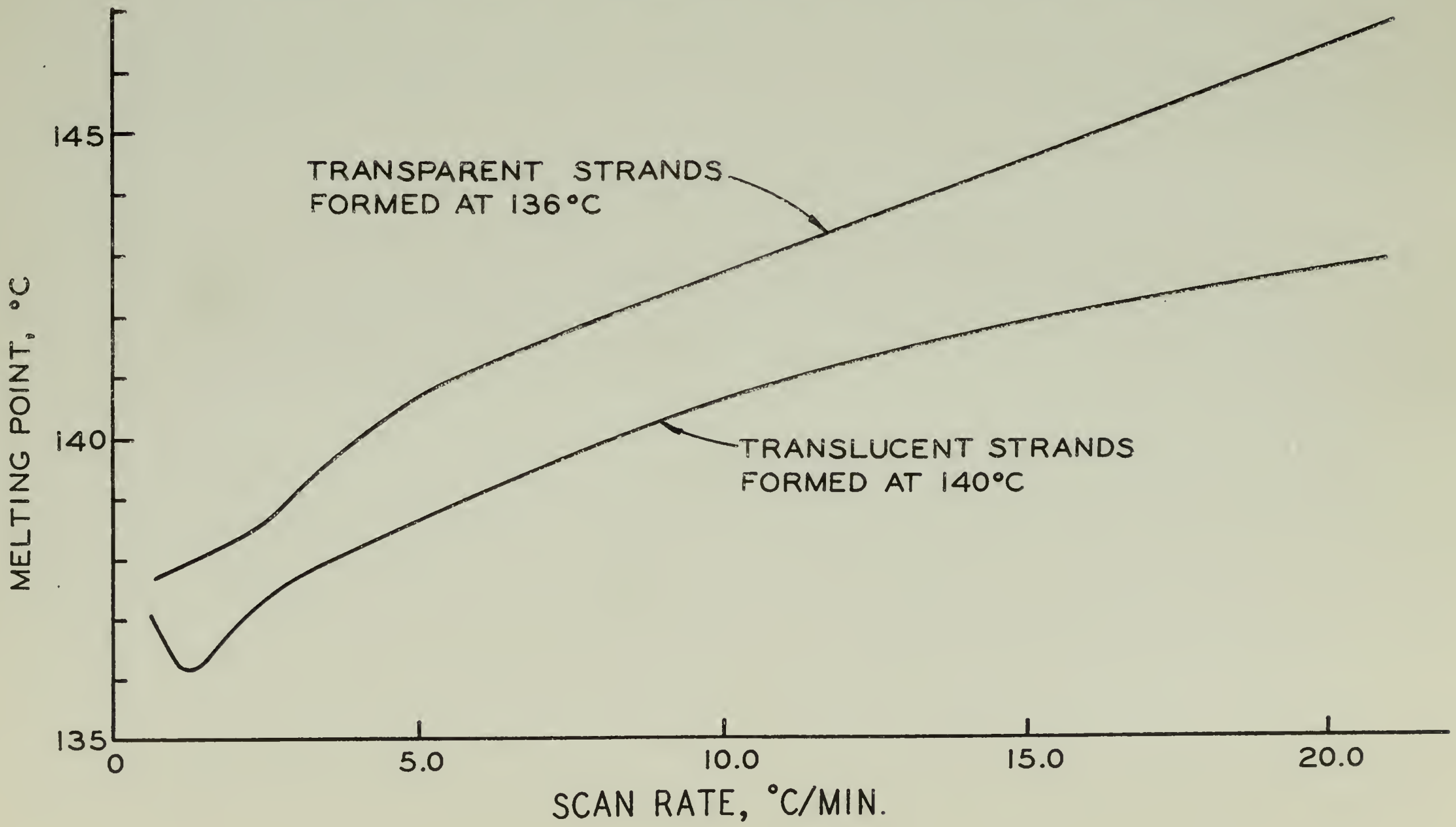

TRANSPARENT SEGMENT LENGTH AS A FUNCTION OF TIME AT 136°C UNDER A MAXIMUM PRESSURE OF 1900 ATMOSPHERES

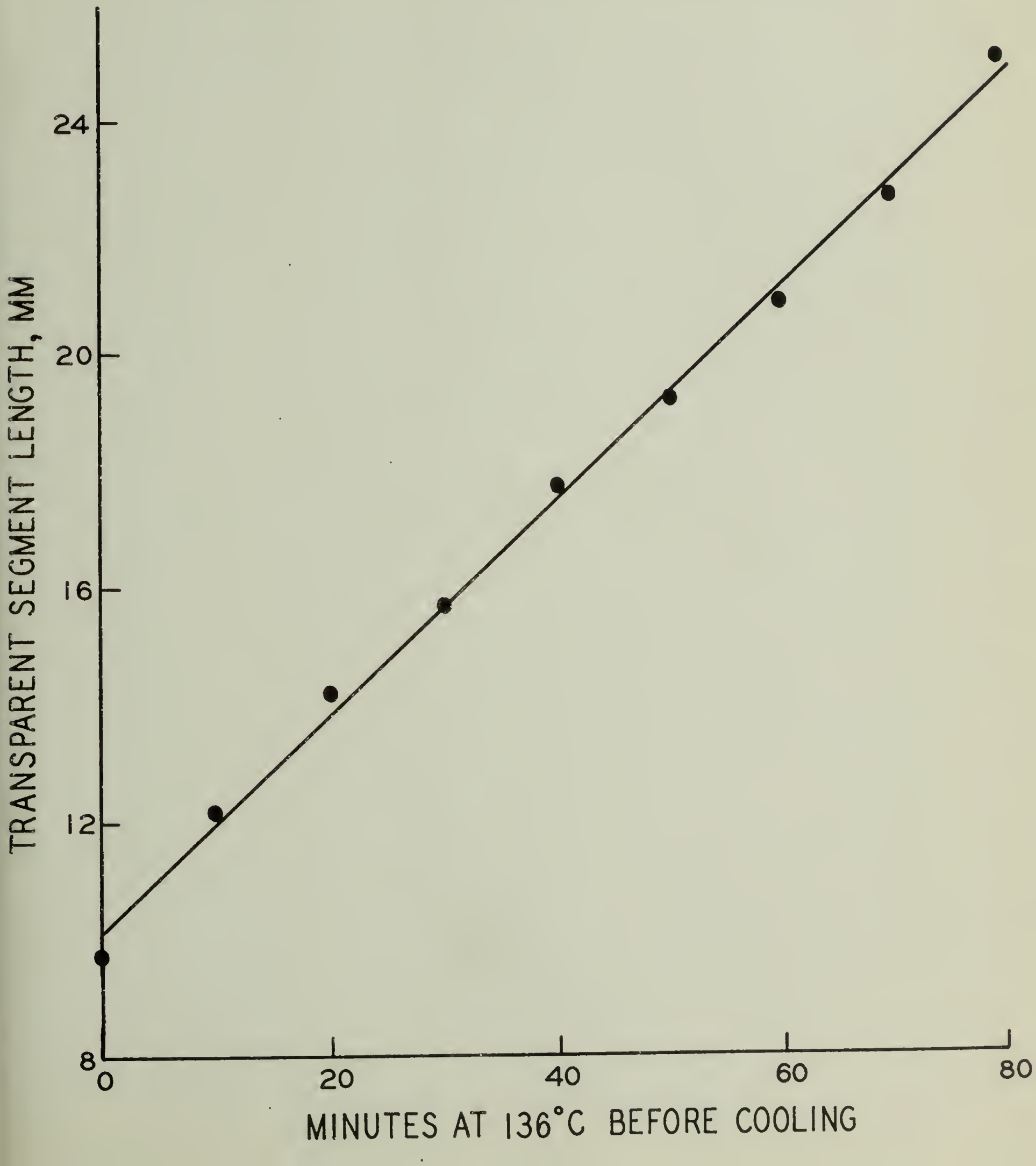

CHAPTER III

THE ORIENTATION AND STRUCTURE OF POLYETHYLENE CRYSTALLIZED UNDER THE ORIENTATION AND PRESSURE EFFECTS OF A PRESSURE CAPILLARY VISCOMETER

Introduction

High density polyethylene has been crystallized under combined orientation and pressure effects in the Instron Capillary Rheometer.[38-40] The crystal structure so formed has both a high degree of crystal perfection and a high degree of crystal orientation. The structure is distinctly different from that which is commonly observed in high density polyethylene, since it is highly crystalline (83% by weight) as well as transparent. The measurement of the specific orientation functions for both the crystalline and the amorphous polyethylene chains constitute the main subject of this study. It is important to note that the unusual transparency of the structure permits the determination of the amorphous orientation in conjunction with the crystalline orientation.

The single polymer used in this study is a high density polyethylene, Dupont Alathon 7050, with number and weight average molecular weights of 18,400 and 52,500 respectively. A procedure has been developed to crystallize the polyethylene in the capillary of the rheometer.[38,39] By selecting a rheometer temperature, in the vicinity of the atmospheric melting point of polyethylene, it is possible to increase the plunger velocity to such a value that a critical combination

of pressure and orientation in the flowing melt is exceeded. At this critical condition, rapid crystallization occurs, and the resulting strand is extracted from the capillary. The birefringence and x-ray measurements described in this study were carried out on strands crystallized at 136°C in a capillary of 0.0508 cm. diameter, 2.56 cm. length, and 90° entrance angle and under a plunger velocity of 5.0 cm./min. Based on the plunger volume displacement and the capillary dimensions, a nominal shear rate at the wall of the capillary is calculated to be 4614 $sec.^{-1}$ under these conditions. An examination of the structure produced in the Instron, see Table V, reveals an unusual combination of properties that can be compared to samples of cold-drawn, cold-drawn and annealed, and thermally crystallized polyethylene.

Crystal Orientation

A wide angle x-ray photograph of the polyethylene segment crystallized in the Instron is shown in Figure 13. The diffraction spots have been indexed according to the usual orthorhombic unit cell, although a faint line at d = 4.56Å may arise from a small amount of monoclinic material.[41,42] The weakness of this line and the absence of other monoclinic lines indicate that the fraction of monoclinic material is negligible.

The orientation function for a crystal diffraction plane in a uniaxially oriented specimen is defined as:[43]

$$f_{hk\ell} = \frac{3}{2} \langle \cos^2 \varepsilon \rangle - \frac{1}{2} \qquad (3)$$

where ε is the angle between the fiber axis and the (hkℓ) plane normal. By convention, x-ray diffractometer angles are defined such that an angle χ, which is the complement of ε, is used as the independent variable. Using this convention, the orientation function is calculated from the following equation:

$$f_{hk\ell} = \frac{\int_o^{\pi/2} I_{hk\ell}(\chi) P_2(\sin\chi) \cos\chi d\chi}{\int_o^{\pi/2} I_{hk\ell}(\chi) \cos\chi d\chi} \qquad (4)$$

where

$$P_2(\sin\chi) = \frac{3}{2}\sin^2\chi - \frac{1}{2} \qquad (5)$$

is the Legendre polynomial of degree two.

The initial orientation measurements reported in Chapter II were determined by azimuthally (as a function of χ) measuring the intensity distribution of the (110) and (200) reflections. A value of $f_c = +0.9$ was calculated for the c-axis orientation, using the Wilchinsky formula[44] to analyze the observed intensity distribution for Instron strands identical to those used in this study. The orientation function f_c corresponds to the c-axis of the orthorhombic unit cell (equivalent to $f_{00\ell}$ in the above nomenclature) and measures the average deviation between the capillary axis of flow and the polymer chain backbones, which are parallel to the c-axis in the polyethylene crystalline lattice. As defined in Eqn. (3), a c-axis orientation function of -0.5 indicates that the polymer

chains are aligned perpendicular to the capillary axis of flow; a value of 0.0 indicates a random orientation; and a value of + 1.0 indicates perfect parallel alignment with the capillary axis of flow. It has since been noted that the Soller slits on the x-ray apparatus used for this determination of f_c and others reported previously[39] had a resolution of approximately 4^o in the χ direction (2^o for each of two slits). This resolution is adequate for samples that are not as highly oriented; however, the sample in question was found to have such a high degree of orientation that higher resolution equipment and techniques are required for precise measurement of the orientation.

An x-ray apparatus of sufficient resolution was available at the Army Materials and Mechanics Research Center. Preliminary diffractometer scans made at low resolution (see Figure 14) revealed that the (002) peak of the transparent strands crystallized in the Instron is unusually intense, attaining approximately one-half the intensity of the (110) reflection. The primary reason for this lies in the high degree of orientation. In a uniaxially oriented specimen, the effect of orientation is to enhance the intensity of meridional reflections [such as (002)] relative to that of equatorial reflections [such as (110)]. This point will be more fully developed and demonstrated quantitatively. The important point is that the appearance of a strong (002) reflection permits the direct determination of the c-axis orientation function without using the conventional,

indirect procedure requiring azimuthal scans of the (110) and (200) reflections and subsequent interpretation from the Wilchinsky formula.[44]

Figure 15-a shows the direct measurements of the c-axis orientation distribution that was obtained from an azimuthal scan (χ) of the (002) reflection. The receiving slit was stopped down in the vertical direction to obtain a χ resolution of 0.5^{o} (see Appendix II for details). A value $f_c = + 0.996 \pm 0.002$ was calculated from the data using Eqn. (4). From Eqn. (3), it can be verified that $f_c = + 0.996$ corresponds to an value of $2^{o}58'$; i.e., the polymer chains in the crystalline regions are oriented at an average angle of less than 3^{o} relative to the capillary flow axis. It is believed that such a high degree of orientation for polyethylene has not been reported in previous literature.

The orientation distributions of the (110) and (200) planes are given in Figures 15-b and 15-c. From the measurements, experimental values for f_{110} and f_{200} were calculated and are reported in Table VI. The Wilchinsky formula was then applied to this data, yielding a value of + 0.995 for f_c, in close agreement with the directly measured value of + 0.996.

In order to compare intensities of different (hkℓ) reflections on a common basis, it is necessary to average out the effect of orientation by spherical integration:

$$\bar{I}_{hk\ell} = \frac{\int_{o}^{\pi/2} I_{hk}\ (\chi)\ \cos\chi d\chi}{\int_{o}^{\pi/2} \cos\chi\ d\chi} \qquad (6)$$

The quantity $\bar{I}_{hk\ell}$ is the randomized intensity of the ($hk\ell$) peak, or the intensity one would observe if there were no preferred orientation.

When preferred orientation is present, the intensity will have some maximum value I_{max} greater than the randomized intensity. Thus, we may say that the effect of preferred orientation is to amplify the intensity at some particular orientation above the randomized intensity level. The degree of amplification depends upon the orientation of the diffraction plane in question. The experimental results (Table VI) show that the (002) maximum was nearly 1000 times the randomized level. In contrast, the (110), (200), and (020) intensities showed maximum intensities that were approximately 20 times their respective randomized values.

The reason for this lies in Eqn. (6). The factor $\cos \chi$, which is part of the differential solid angle, approaches zero as the meridian point ($\chi = 90^{o}$) is approached. This is exactly where the (002) peak has its maximum intensity. With such a small weighting factor operating on the (002) intensity, the intensity is amplified by a significant amount in order to achieve a given randomized intensity. At the equatorial position, $\cos \chi$ is 1.00 and much less amplification occurs for the (hk0) reflections.

The most highly oriented crystals previously reported have been obtained by conventional cold drawing procedures rather than by an extrusion-type procedure, such as occurs in the

Instron Rheometer. C-axis orientation functions that approach the +0.996 value reported in this study have been observed for samples that were cold drawn at large extension ratios. As noted in Chapter II, Takayanagi[45] has reported a c-axis orientation function of + 0.976 for a sample of high density polyethylene (Marlex 50) drawn five fold in length at a temperature of 38°C. It is important to note that the sample formed in the Instron Rheometer was essentially different from a purely cold drawn sample in that it has a distinctly higher melting point and a structure that is transparent. If polyethylene is cold-drawn and then carefully annealed for extensive time periods, it is possible to obtain a structure such as the comparative sample (listed as cold-drawn, annealed) found in Table V, which does have a large content of high melting point crystallites. However, the polyethylene crystallized under the combined pressure and orientation effects induced in the Instron has two distinct advantages relative to the cold-drawn, annealed polyethylene that make it particularly attractive from a commercial viewpoint: (1) a structure that is transparent to visible light and (2) a formation time measured in seconds or less.

Of particular significance in this study is the precise x-ray determination of the unusually high c-axis orientation. Through careful cold-drawing procedures, it is theoretically feasible to obtain values as great as $f_{c\text{-axis}} = + 0.996$, the value for the polyethylene crystallized directly from the

oriented melt in the Instron Rheometer. However, such a high orientation function has probably not been reported in the literature because of the inability to measure such values with conventional x-ray techniques; i.e., precise instrumentation and maximum care must be utilized to prevent smearing due to the vertical divergence values commonly used with x-ray diffractometers. With the conventional procedure, the x-ray beam diverges out of the plane of diffraction, both at the primary beam and the receiving slit position, a practice which has little effect on the 2θ resolution but limits the ability of the instrument to resolve χ. As stated above and detailed in Appendix II, it is necessary to stop down the height of the receiving slit on the instrument in order to resolve χ sufficiently to define the high degree of orientation present in the strands crystallized in the Instron at $136^{\circ}C$.

Amorphous Orientation

With the orientation of the polymer chains in the crystalline portion of the polyethylene strands well defined from x-ray techniques, it is of importance to determine the orientation of the polymer chains in the amorphous regions. Birefringence data has been used in conjunction with the x-ray results in order to define the amorphous orientation. Essentially, the experimentally measured birefringence of a sample is determined by crystalline, amorphous, and form contributions. The x-ray data is used to define the crystalline component to

the birefringence; thus it is possible to determine an amorphous orientation function (f_{amorph}) if the form birefringence contribution is negligible, as is usually the case.

The transparent segment of the strand crystallized under orientation and pressure in the Instron was placed between crossed polarizers. A calcite plate was then added in order to compensate for the retardation resulting from the oriented polyethylene in the strand. The total birefringence (Δ_T) is computed from Eqn. (7):

$$\Delta_T = R\ \lambda/t \qquad (7)$$

where R is the retardation in wavelengths (dimensionless), λ is the wavelength of the incident light, and t is the strand thickness. Stein[43,46] has expressed the total birefringence Δ_T as the sum of crystalline, amorphous, and form birefringence terms:

$$\Delta_T = \Delta_{cryst} + \Delta_{amorph} + \Delta_F \qquad (8)$$

or

$$\Delta_T = X_{cryst}\, f_c\, \Delta^o_{cryst} + (1 - X_c) f_{amorph}\, \Delta^o_{amorph} + \Delta_F \qquad (9)$$

where X_{cryst} is the crystalline fraction by volume and Δ^o_{amorph} and Δ^o_{cryst} are the intrinsic amorphous and crystalline birefringence terms, respectively. A value of 0.2 for Δ^o_{amorph} is calculated from the Denbigh values for bond polarizabilities,[47] and Δ^o_{cryst} is calculated from Equation (10) (subscripts a, b,

and c refer to axes of the orthorhombic unit cell):

$$\Delta^{o}_{cryst} = n_c - \frac{1}{2}(n_a + n_b) \qquad (10)$$

using the Bunn and Daubeny values[48] for the indices of refraction (n_x) of paraffin crystals. Equation (10) is valid when there is little difference between the a-and b-axis orientation function, as in the present instance (see Table VI).

The observed and calculated parameters used to determine f_{amorph} from Eqn. (9) are summarized in Table VII. f_{amorph} is + 0.17 for the transparent strands, implying only a slight bias of the amorphous chains to align parallel to the capillary axis in the final structure. It is of interest to point out that the amorphous chains, just after crystallization had occurred, were also probably in a highly constrained state, aligned parallel to the capillary flow axis. However, after crystallization, the strand was permitted to anneal for several minutes prior to and during the thermal cooling cycle required in order to extract the sample.[38,39] Though a pressure of 1900 atmospheres was maintained after crystallization, relaxation may have occurred in the amorphous regions, and this could be responsible for the observed lack of a significant orientation of the amorphous chains. On the basis of present theory, the value of + 0.17 for the amorphous orientation function represents a maximum, since the form birefringence value was neglected in the calculations. Form birefringence increases with increasing orientation of either the crystalline or amorphous components,[46]

and the form component, if significant, would result in a decrease in the computed orientation function of the amorphous chains, that is, a zero value (or perhaps even slightly negative) for the Instron strand being analyzed here. Also, the value for the intrinsic amorphous birefringence of polyethylene is presently in question due to conflicting theories.[47-49] Because of these two factors that cannot be resolved at this time, it is only feasible to assert that the amorphous chains in the transparent segment after extraction from the rheometer contribute very little to the total birefringence and can be assumed, for all practical purposes, to have a random orientation. This conclusion will be incorporated into the development of a structural model in Chapter VI.

Transparency

The unusual transparency of the polyethylene crystallized under combined orientation and pressure effects can be understood now that certain details of the structure have been elucidated. The turbidity of ordinary polyethylene results from scattering of light by the structural elements of the polymer. Stein and others[50-51] have shown that this scattering process arises from two terms: the correlation of density fluctuations and the correlation of orientation fluctuations within the polymer. In polyethylene, the latter term usually predominates and gives rise to most of the scattering.

The present sample shows a high degree of c-axes orientation, meaning that the crystallite c-axes (parallel to the

polyethylene backbone) are highly correlated with the macroscopic capillary axis. It follows that the c-axes are highly correlated in orientation with each other, and we might well expect that the characteristic distance for orientation correlation is quite large, in fact, larger than the wavelength of visible light. The scattering process is most effective, however, when the scattering entity is comparable in size with the wavelength of light. Therefore, the orientation fluctuations do not yield a significant scattered intensity. Also, the high degree of crystallinity (X_c = 0.83) would tend to minimize the amount of density fluctuations which would also reduce the intensity of light scattering. These two effects are, in all probability, responsible for the high degree of transparency in this material.

Conclusions

This study has been conducted in order to define the major orientation parameters of the unique structure produced in the Instron Rheometer. It was found that the conventional x-ray measurements were inadequate for making a precise determination of the orientation of the polyethylene chains in the crystalline component. Appendix II details the improved method used to obtain the c-axis orientation function of + 0.996 for the transparent strands. The amorphous orientation function was obtained in the prescribed manner; however, it should be emphasized that only the unusual transparent quality of the high density polyethylene strands permitted a determination

of the amorphous orientation. Additional x-ray measurements will be presented in Chapter VI in order to define the crystallite dimensions. Crystallite dimensions (from both x-ray and electron diffraction) in conjunction with the orientation functions will result in a definite model for the structure of the strands crystallized in the Instron Rheometer.

REFERENCES

38. J. H. Southern and R. S. Porter (Chapter I), accepted for publication in J. Macromol. Sci. (Phys.) (1970).

39. J. H. Southern and R. S. Porter (Chapter II), accepted for publication in J. Appl. Polymer Sci. (1970).

40. A. K. van der Vegt and P. P. A. Smit, Advances in Polymer Science, Society of Chemical Industry, London, Monograph 26, 313 (1967).

41. P. W. Teare and D. R. Holmes, J. Polymer Sci., 24, 496 (1957).

42. C. Gieniewski, private correspondence (1970).

43. R. S. Stein, J. Polymer Sci., 31, 327 (1958).

44. Z. W. Wilchinsky, J. Polymer Sci., Pt.A-2, 6, 281 (1969).

45. M. Takayanagi, et al., J. Polymer Sci., Pt. C, No. 15, 263 (1966).

46. S. Hoshino, J. Powers, D. G. LeGrand, H. Kawai, and R. S. Stein, J. Polymer Sci., 58, 185 (1962).

47. K. G. Denbigh, Trans. Faraday Soc., 36, 936 (1940).

48. C. W. Bunn and R. Daubeny, Trans. Faraday Soc., 50, 1173 (1954).

49. R. L. Rowell and R. S. Stein, J. Chem. Phys., 47, 2985 (1967).

50. R. S. Stein and P. R. Wilson, J. Appl. Phys., 33, 1914 (1962).

51. A. E. M. Keijsers, J. J. Van Aartsen, and W. Prins, J. Appl. Phys., 36, 2874 (1965).

TABLE V

COMPARISONS AMONG POLYETHYLENE SAMPLES CRYSTALLIZED BY DIFFERENT METHODS

	Instron at 136°C	Cold-drawn, annealed(45)	Cold-drawn(45)	Unoriented, thermally formed
% Crystallinity (by weight)	83	86	72	69
Melting Point (°C)	140	137	130	133.5
Low Angle X-Ray Spacing(Å)	230Å	408	169	-----
In-phase Modulus ($\times 10^{-10}$ dynes/cm.^{2})	6.6	4.0	6.6	1.5
Light transmission	transparent	opaque	opaque	opaque

TABLE VI

RESULTS OF SPHERICAL INTEGRATIONS

Diffraction Plane	I^{*}_{max}	$\bar{I}^{*}_{hk\ell}$	$I_{max}/\bar{I}_{hk\ell}$	$f_{hk\ell}$
(110)	121.4	5.635	21.6	-0.4974
(200)	28.8	1.319	21.8	-0.4977
(020)	3.09	0.142	21.7	-0.4951
(002)	179.9	0.186	966	+0.9960

c-axis orientation function

direct measurement, (002) plane: $f_c = 0.996$
indirect measurement, (110) and (200) planes: $f_c = 0.995$

*Corrected intensities in counts/second. Baseline and polarization corrections applied.

TABLE VII

BIREFRINGENCE CALCULATIONS

X_c	0.82
Δ^o_{cryst}	0.0585
Δ^o_{amorph}	0.2
f_c	0.996
Δ_T	0.054
Δ_{cryst}	0.048
$\Delta_T - \Delta_{cryst}$	0.006
f_{amorph}*	0.17

*Calculated by neglecting form birefringence.

LEGEND FOR FIGURES

UNCORRECTED X-RAY INTENSITY DISTRIBUTION VERSUS RADIAL ANGLE (2θ)

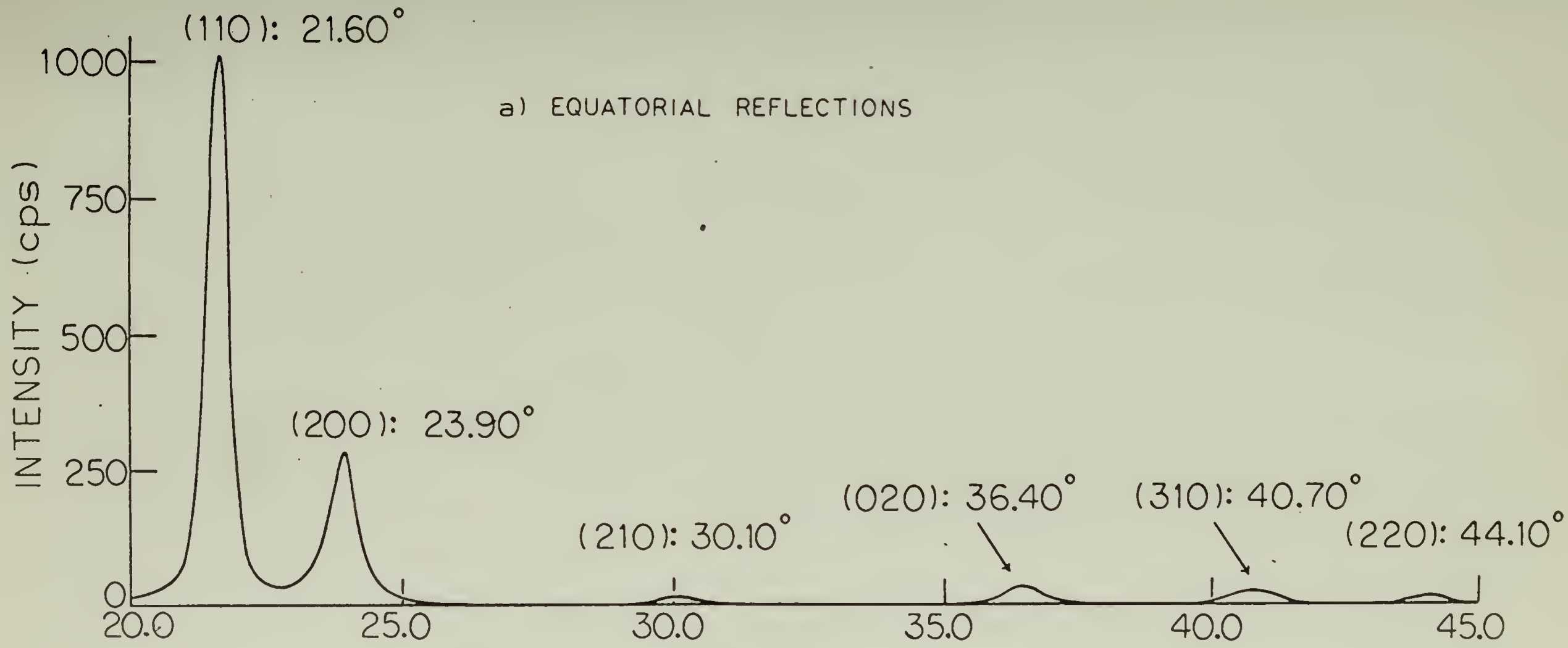

a) EQUATORIAL REFLECTIONS

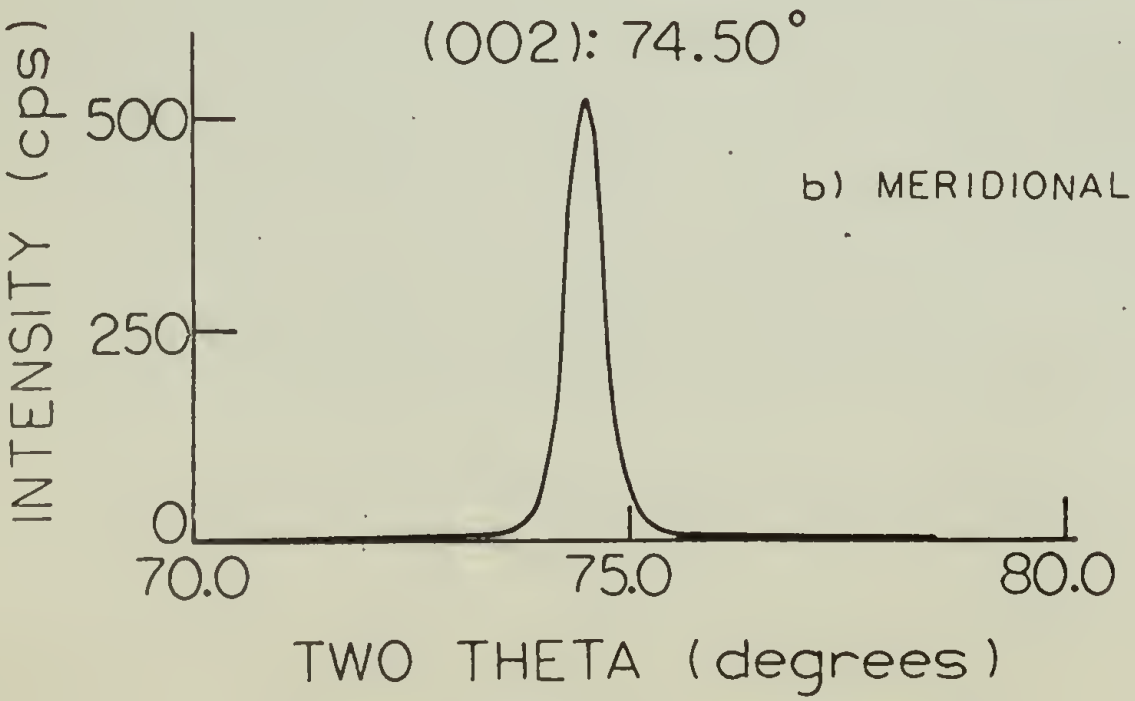

b) MERIDIONAL REFLECTION

NOTE: SAME PINHOLES AND SLITS IN BOTH a) AND b).

Azimuthal scans of (002), (110), and (200) planes. Baseline and polarization corrections applied.

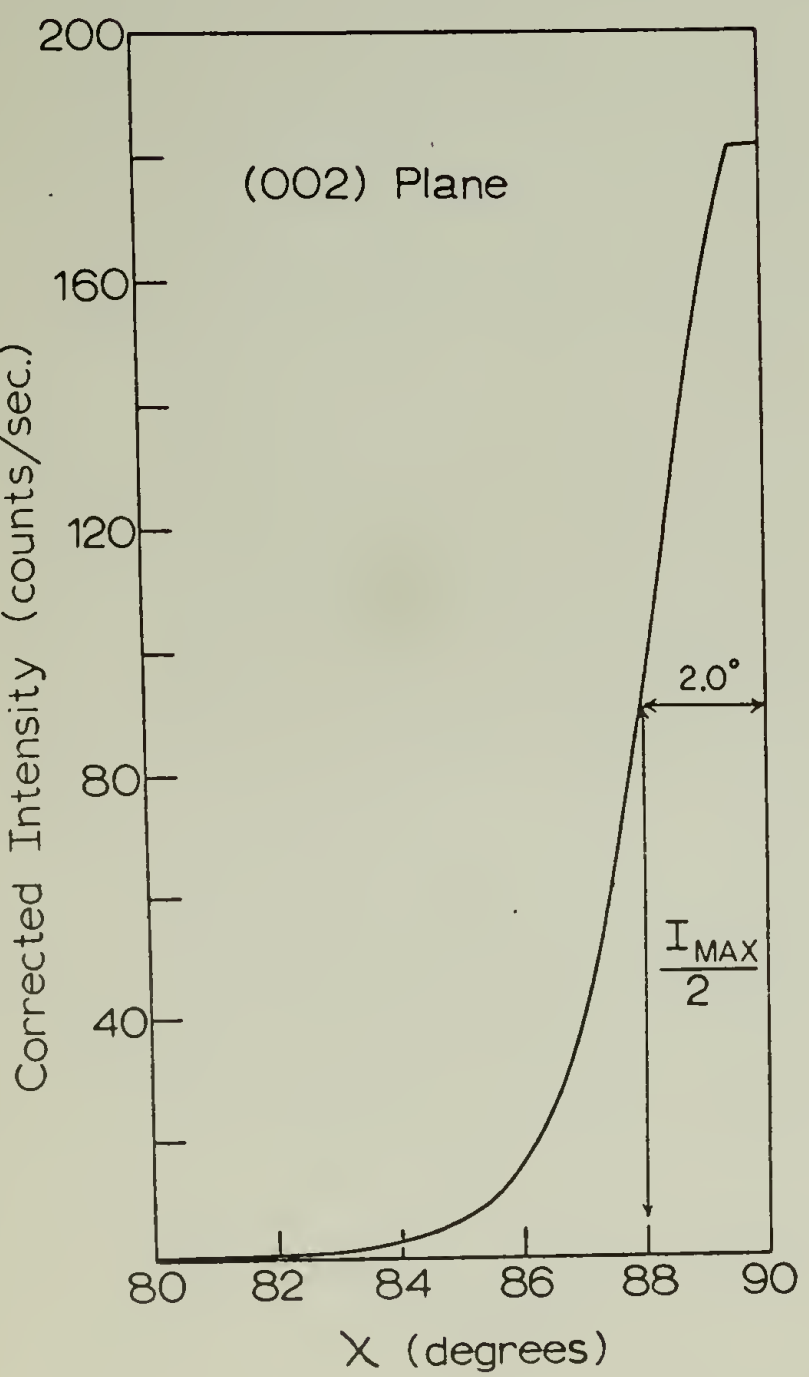

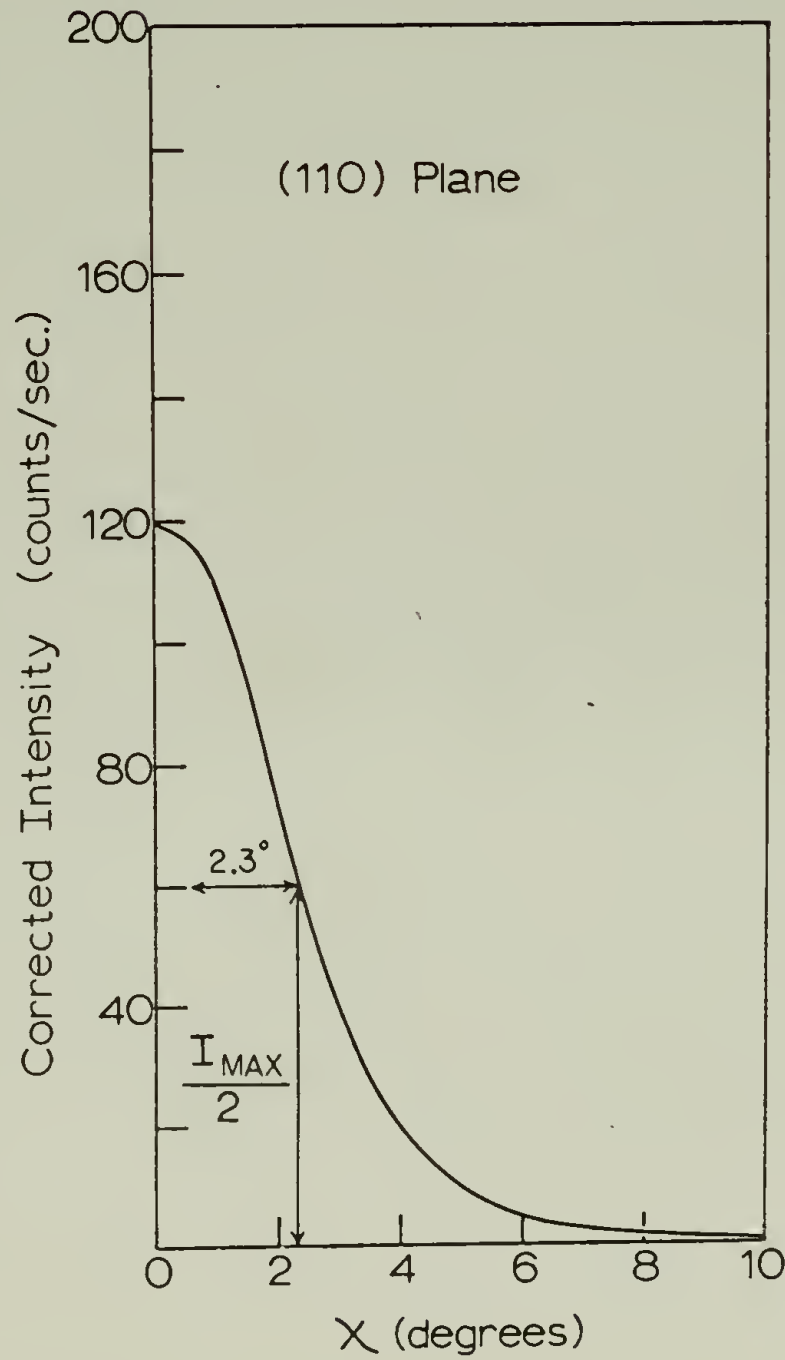

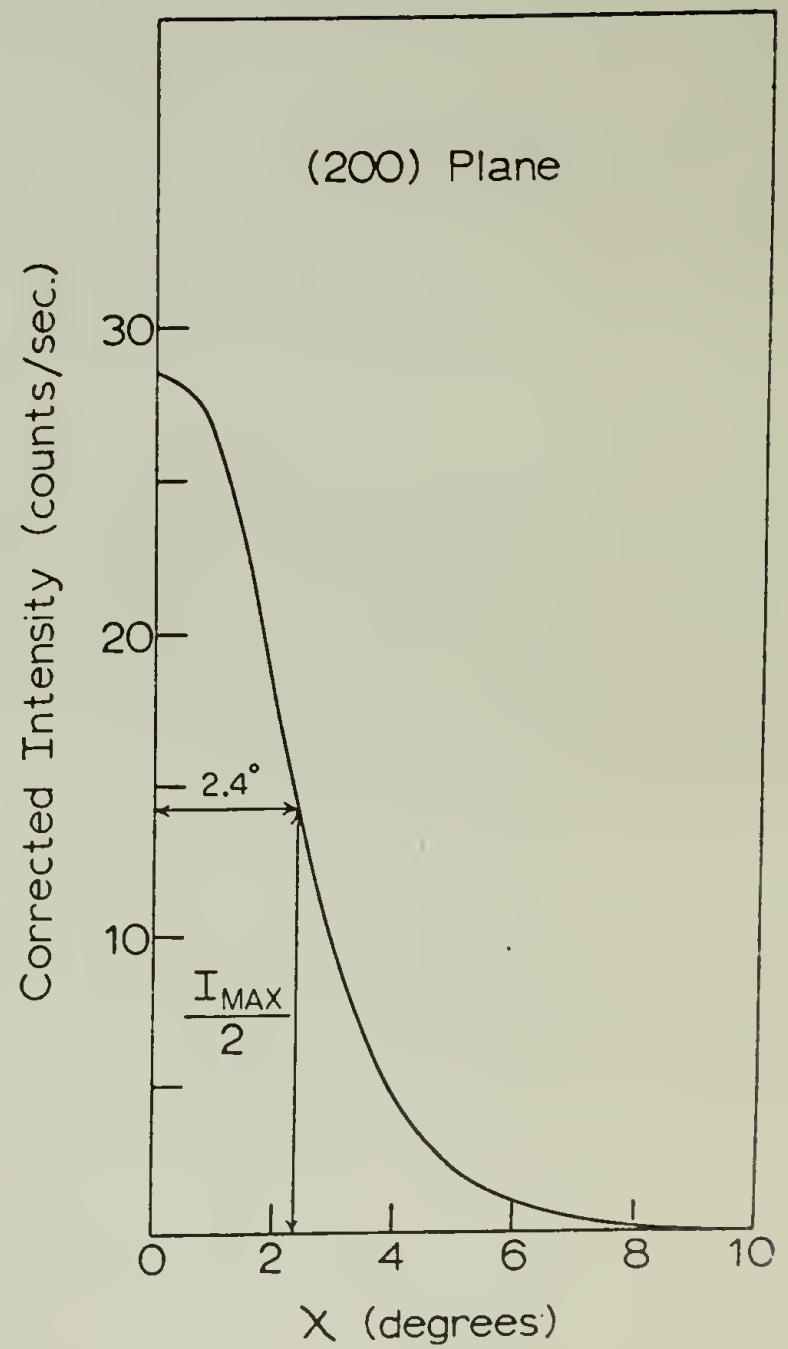

CHAPTER IV

THE MELTING BEHAVIOR OF POLYETHYLENE CRYSTALLIZED IN A PRESSURE CAPILLARY VISCOMETER

The subject of this study is the analysis of the thermal data obtained on the transparent Instron strands from the Perkin-Elmer Differential Scanning Calorimeter Model 1-B(DSC). The polyethylene used to form the strands was, in all cases, Dupont Alathon 7050 having a weight and number average molecular weight of 52,500 and 18,400, respectively. The data includes the magnitude of the melting points as well as the melting point values as a function of the heating rate. These melting points are compared with literature values obtained on specimens of pressure-crystallized extended chain crystallites[52,53] and stirrer-crystallized "shishkabob" structures.[54-56] The evidence is consistent with the presence of an extended chain component in the Instron strands. In addition, birefringence determinations are made of the final melting of the most perfect crystallites of the strands, using a Mettler Hot Stage mounted on a polarized light microscope. DSC results of irradiated strands are also presented in order to show the similarity of their melting behavior to the shishkabob structure crystallized under shear from dilute solution.

A series of fusion curves at different heating rates has been obtained on the DSC, adequately illustrating the high melting point values of the Inston strands as well as the tendency of these samples to superheat (see Figure 16 for thermal data

and Table VIII for sample formation conditions). This latter effect is indicated by the increase in the peak value of the fusion curve as the heating rate was raised. Note that all DSC values presented herein have been corrected for instrumental thermal lag.[57] The samples produced at the temperature of 136°C[58] had the highest melting points so far observed for the structure resulting from the Instron procedure. The high melting point of the Instron prepared samples as well as their tendency to superheat are properties that have been previously attributed in other laboratories to the presence of extended chains in a polyethylene crystal structure.[59]

The following section compares the data in Figure 16 with that obtained with the DSC on well-defined polyethylene structures. The melting point values shown in Figure 16 are distinctly higher than those predicted by a chain-folded model, as indicated by the following comparison of these Instron samples with a known chain-folded structure. Bair was able to grow single crystal mats having a 278Å ± 30Å low angle x-ray spacing by crystallizing at 90°C from a dilute solution of polyethylene in xylene, followed by annealing for a period of 570 hours at 128 ± 1°C.[60] This x-ray spacing is comparable to the average spacing of 230Å[61] obtained for the Instron strands. Bair's crystal structure has a melting point of 136.9°C, as determined from the peak value of the fusion curve measured with the DSC at a heating rate of 10°C/min., whereas the Instron sample had a melting point of 142.8 ± 0.4°C

at the same heating rate, as can be seen by the appropriate point in Figure 16. It should be noted that the Bair sample, crystallized by means of thermal treatments alone, has a greater crystalline content (94% versus 83% for the Instron sample), a higher weight average molecular weight (153,000 versus 52,500), and was crystallized directly from dilute solution, rather than from the melt. All of these factors would result in a higher melting point for the Bair sample[60,62,63] relative to the strands crystallized in the Instron Rheometer, assuming that the measured low-angle spacings can be considered as an indication of similar crystal fold periods. Thus it is necessary to explain the 142.8°C melting point observed for the Instron sample in terms of a crystal structure that is different from the conventional chain-folded model that definitely holds for Bair's single crystal samples. The 5.9°C increment of the Instron strand relative to a purely chain-folded structure having approximately the same low angle spacing is a primary reason for the assertion of an extended chain crystalline component in the Instron strands.

Also in the literature[52] is a DSC trace of a pressure-crystallized extended chain structure, having a peak melting point of 138°C at a heating rate of 8°C/min., and it is of interest to compare this with the melting point for the structure crystallized in the Instron. The latter value can be interpolated from Figure 16 to be 142.4°C at the same heating rate. Hence, the magnitude of the melting point for the Instron

sample is some 4°C greater than a known extended chain structure. This increment is largely attributed to the inability of the DSC to maintain the sample at the programmed temperature due to the difficulty of conducting heat into the cylindrical sample at the relatively rapid heating rates. Presumedly an extended chain crystal structure can also be formed by crystallizing the polyethylene by shearing a dilute solution.[55,64] A shishkabob structure is formed that is believed to contain an extended chain crystallite backbone that has nucleated epitaxial chain-folded lamellae. A DSC trace of such a polyethylene structure yielded a peak melting point of approximately 128°C with a high melting tail that returns to the base line at 135°C at a heating rate of 5.0°C/min.[54] The high melting tail is believed to represent the melting of the extended chain crystallites. Other researchers have observed high melting point tails for the shishkabob structures at temperatures as high as 147°C on the DSC at a heating rate of 5°/min.[56] This melting behavior can be compared with the single relatively sharp fusion curve that peaks at 140.8°C obtained from the Instron strand melting at the same heating rate. The lack of a high melting point tail for the DSC fusion curves of the Instron strands may be significant; however, no explanation will be proposed at this time. It is of interest that final melting occurred for the shishkabob structure at 134.1°C under equilibrium conditions (zero entropy production).[56] Similar conditions providing a sufficient amount of time to remove

the superheating effect can also be obtained on the Mettler Hot Stage, where final melting has been observed, for an Instron strand such as that melted in Figure 17 (see Table VIII for conditions of sample formation), at a temperature of 134.5°C. The low melting point under equilibrium conditions for a presumedly extended chain crystal structure has been attributed to imperfections within the structure.[56] Thus the comparative studies of melting point values of the Instron strands with those of purely chain folded samples, pressure crystallized extended chain structures, and the shear crystallized shishka-bobs (supposedly containing both extended chain and chain-folded crystallites) have consistently implied that a model having an extended chain crystal component provides a likely explanation for the melting behavior of the Instron samples.

In further defining the melting behavior of the Instron strands, it is relevant to show the DSC fusion curve. A typical example is shown in Figure 17. The lowest DSC heating rate of 0.625°C/min. is chosen in order to minimize superheating. The fusion curve initially departs from the base line at 131.6°C and returns at 136.4°C. This melting range of less than 5°C indicates an unusually narrow distribution of crystallite perfection for a polyethylene crystal structure. Furthermore, it is believed that the electronics of the DSC are so arranged and the calibration is so performed that the melting point defined from the peak value of the fusion curve for a structure having a graded degree of crystal perfection, such as occurs in

all polymers, more nearly approximates the temperature at which the majority of the crystallites melt rather than the temperature at which the final crystallites melt. In support of this hypothesis, the temperature scale of the Mettler Hot Stage was calibrated with the same standard samples (Fisher thermetric standard adipic and benzoic acid) used to calibrate the DSC trace obtained in Figure 17. The temperature at which birefingence due to the crystal structures of the standards disappeared was equated with the peak value of the DSC trace obtained on the same standards. With such a correlation, it is possible to place the melting point determined from birefringence (T_{FINAL}) on the same scale as the DSC fusion curve. This has indeed been done in Figure 17 using a duplicate sample of that melted in obtaining the fusion curve. T_{FINAL} is 137.0°C, significantly higher than the melting point of 135.4° defined from the DSC fusion curve. The important point is that the Instron strands have a small amount of relatively perfect crystallites that have not melted by the 135.4°C peak value of the fusion curve nor even at the 136.4°C temperature at which the curve returns to the baseline. It is of interest to note that electron diffraction studies will be presented in Chapter V which indicate the existence of an extremely perfect crystal structure existing only in the inner core of the Instron strands. It is probable that this structure constitutes the high melting point material detected only with the birefringence measurement of the melting process.

Previous researchers have found that irradiation of polyethylene results in crosslinks that effectively prevent the reorganization of the crystal structure during melting. For example, the multi-peak fusion curve often obtained for single crystal samples is reduced to a single peak on irradiating the samples; furthermore, this single peak is usually in the vicinity of the initial peak of the unirradiated specimen.[60] The melting behavior of the Instron strands can be compared in Figure 18 for samples that have been exposed to 0,50,and 80 MRADS. In contrast to the results obtained with single crystals, the fusion curves of the Instron strands were resolved from a single peak into at least two peaks. Such a phenomenon has also been observed for the melting of irradiated samples of the shishkabob structure and definitely indicates a discontinuity in the structure produced in the Instron Rheometer. The lower melting peak of the irradiated strands may result from a less oriented crystalline component which is more subject to irradiation-induced crosslinks that may act as sites for melting than is a more oriented component.[65] Alternatively, the appearance of the two peaks may be the direct result of different degrees of order in the crystal structure, the existence of which has been indicated by electron diffraction data (see Chapter V). It is relevant to note that the similarity of the melting of the irradiated strands and the irradiated shishkabobs is consistent with the presence of both chain folded and extended chain components in the crystal structure of the Instron strands.

Also note that the dual peak of the fusion curves of the irradiated strands is a function of the crystal structure existing prior to irradiation and is not due to the destruction of crystallites. This is borne out by the approximately equal heats of fusion for the unirradiated sample and those irradiated at the doses as high as 50 MRADS (see Figure 18 for confirmation). The lack of temperature drop in the high melting peak of the irradiated relative to the unirradiated samples is also consistent with this observation. There may be some crystallite destruction at the higher irradiation levels, as evidenced by the slight drop in the heat of fusion of the samples irradiated at 80 MRADS.

An additional study of the melting behavior of irradiated strands will be presented in Chapter V in conjunction with electron microscopy and electron diffraction data. The thermal data in this chapter have been collected in order to emphasize the unusual melting behavior of the Instron strands; that is, the relatively high, sharp melting points, the apparent superheatability, and the multi-peak fusion curves on irradiation. The comparison of these properties with those of known structures in the literature is of definite use in developing a structural model for the Instron strands.

REFERENCES

52. D. V. Reas and D. C. Bassett, J. Polymer Sci., Pt. B, 7, 273 (1969).

53. B. Wunderlich and F. Arakawa, J. Polymer Sci., Pt. A, 2, 369 (1964).

54. F. Kawai, K. Ebara, and H. Maeda, Kolloid-Z. u. Z. Polymere, 229, 168 (1969).

55. A. J. Pennings, Proc. Int. Conf. on Crystal Growth, Boston (Oxford: Pergamon Press), 389 (1966).

56. B. Wunderlich, R. M. Cormier, A. Keller, and M. J. Mackin, J. Macromol. Sci. (Phys.), B1, 93 (1967).

57. Perkin-Elmer Corporation, Thermal Analysis Newsletter, 5, Norwalk, Connecticut.

58. J. H. Southern and R. S. Porter (Chapter II), accepted for publication in J. Appl. Polymer Sci. (1970).

59. E. Hellmuth and B. Wunderlich, J. Appl. Phys., 36, 3039 (1965).

60. H. E. Bair, F. W. Huseby, and R. Salovey, Analytical Calorimetry, R. S. Porter and J. F. Johnson, eds. (New York: Plenum Press), 31 (1968).

61. C. Desper, private communication (1970).

62. T. W. Huseby and H. E. Bair, J. Polymer Sci., Pt. B, 5, 265 (1967).

63. H. E. Bair and R. Salovey, J. Macromol. Sci. (Phys.), B3, 3 (1969).

64. R. B. Williamson and R. C. Novak, J. Polymer Sci., Pt. B, 5, 147 (1967).

65. R. Kitamaru and L. Mandelkern, J. Polymer Sci., Pt. B, 2, 1019 (1964).

TABLE VIII

CONDITIONS FOR THE FORMATION OF THE INSTRON STRANDS* USED IN EACH FIGURE

Samples Used in Figure:	Temperature (°C)	Plunger Velocity (cm/min.)	Capillary Dimensions		
			Diameter (cm.)	Length (cm.)	Entrance Angle
16	136	5.0	0.0508	2.55	90°
17 and 18	132	0.5	0.0762	2.34	90°

* See Chapters I, II, and V for additional details of the crystallization procedure and the resulting structure, using Alathon 7050 polyethylene.

LEGEND FOR FIGURES

EFFECT OF HEATING RATE ON PEAK MELTING POINT OF TRANSPARENT PORTION OF STRANDS FORMED AT 5CM/MIN. AND 136 °C

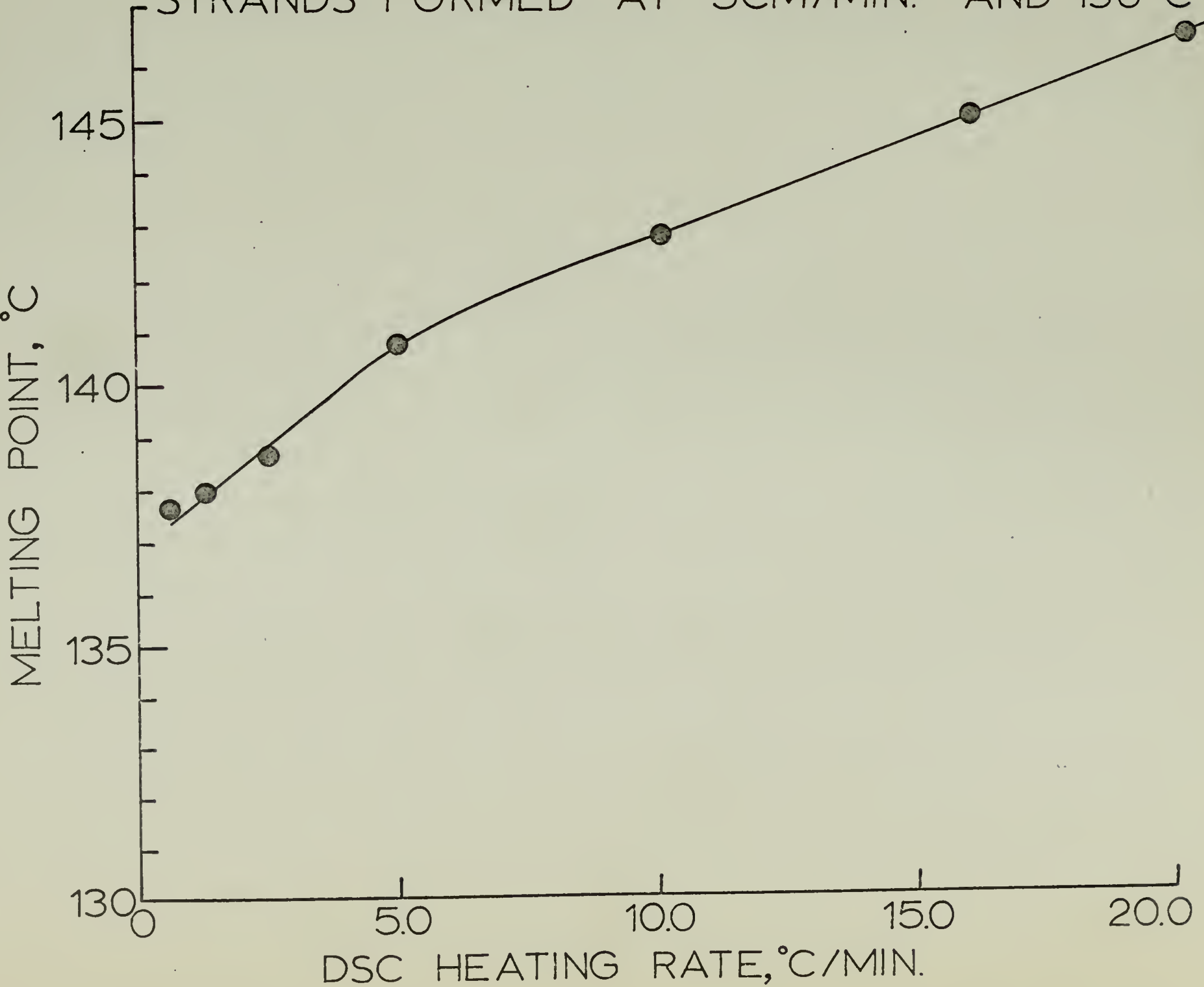

FUSION CURVE OF TRANSPARENT SEGMENT OBTAINED ON DIFFERENTIAL SCANNING CALORIMETER CALIBRATED BY OPTICAL PROCEDURE

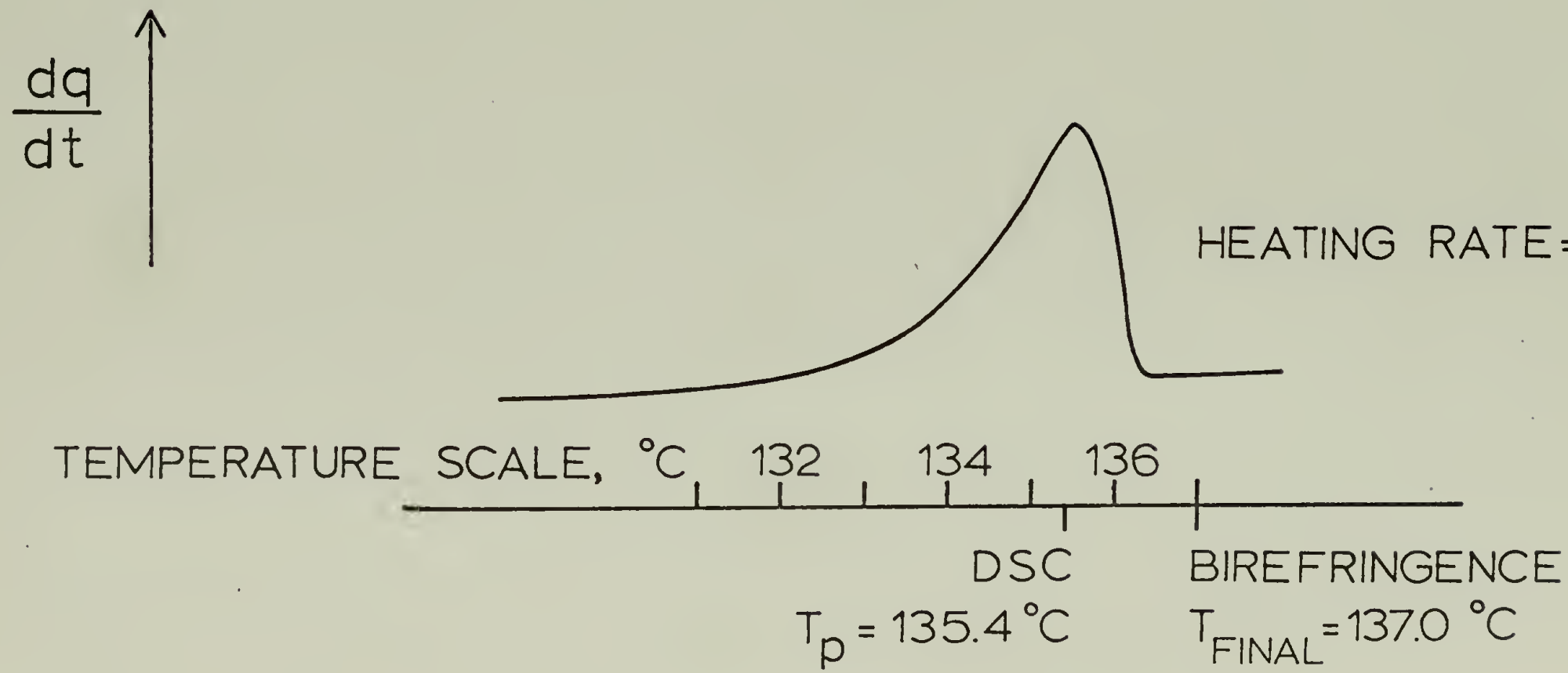

EFFECT OF RADIATION ON FUSION CURVES OF TRANSPARENT SEGMENTS PRODUCED IN INSTRON

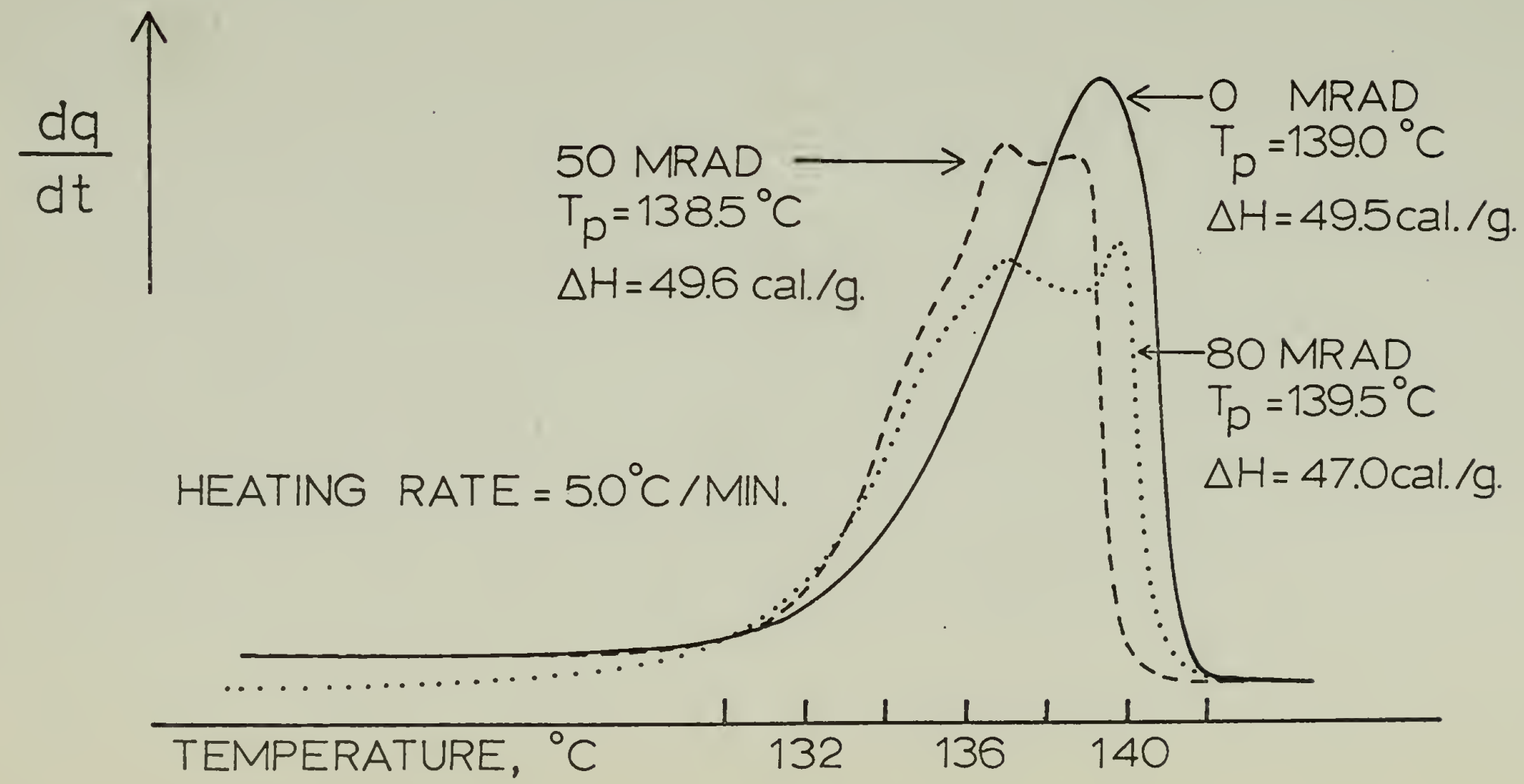

CHAPTER V

THE MORPHOLOGY OF POLYETHYLENE CRYSTALLIZED UNDER THE SIMULTANEOUS PRESSURE AND ORIENTATION EFFECTS OF A PRESSURE CAPILLARY VISCOMETER

Introduction

The morphologies of linear polyethylene crystallized from the melt under high pressure and crystallized under shear from both the melt and dilute solution have been reported previously. Wunderlich and others[66-71] have described the extended chain structure crystallized under static pressures of at least 3000 atm. The morphology so produced is characterized by striated, extended chain crystals in which the molecular axis is oriented parallel to the striations. Pennings and others[72-74] have demonstrated that a fibrous morphology is generated when, for example, a dilute solution of polyethylene (1% in xylene) is stirred during crystallization. Electron microscopy studies have shown that the individual fibers crystallized under these shearing conditions contain chain-folded lamellae attached to an extended chain central backbone, resulting in a "shishkabob" arrangement. Furthermore, Keller and Hill[75-76] have shown that an analogous, fibrous crystalline structure can be generated when a lightly crosslinked polyethylene is cooled under stress from the melt. They reported extensive evidence that the resulting morphology is based on extended chain backbones acting as sites for nucleation of chain folded growth in directions perpendicular to the extended chain crystal structure.

This paper describes the crystalline morphology induced in linear polyethylene when crystallized under the simultaneous influence of flow orientation and high pressure realized in the Instron Capillary Rheometer. Essentially, the pressure and orientation effects resulted in a uniquely transparent high density polyethylene having a significant content (approximately 85%) of oriented crystallites.[77-79] The resulting highly ordered, fibrous texture was seen to have many similarities to morphologies generated in shear crystallized, high pressure crystallized, and cold drawn polyethylene.

Experimental

The polymer used in this study was commercially available high density polyethylene Dupont Alathon 7050, having number and weight average molecular weights of 18,400 and 52,500 respectively. Samples were prepared with the Instron Rheometer operated at a constant plunger velocity using a 0.0508 cm. diameter by 1.55 cm. long capillary with a 90° entrance angle. Specifically, the crystal structure was induced under the combined orientation and pressure effects produced at a 0.5 cm/min. plunger velocity and a rheometer temperature of 136°C.

After initiating the 0.5 cm/min. plunger velocity at 136°C, a sustained pressure rise was observed (see Figure 19), together with abnormal extrudate swelling. Both factors were evidence of crystallite formation. Crystallite nucleation and growth were expected since the equation of state developed by Wunderlich[66] for high density polyethylene indicated that the

melt was definitely in a supercooled state under the existing pressure and temperature conditions. An observed decrease in the linear extrusion velocity, attributed to crystallization, was accompanied by a rapid increase in the pressure to the 1920 atm. upper limit available in the Instron Rheometer. The pressure trace (Figure 19) showed a distinct curvature change at 575 atm. which occurred after crystallization had been initiated. This inflection point implied that crystallization had resulted in a significant contraction of the polyethylene in the reservoir. Plunger motion was halted at 1920 atm., and extrusion continued at 0.02 cm/min.[78] The distinctive sample morphology discussed herein resulted from the intense orientation effects that occurred as the crystallizing polyethylene was forced under 1920 atm. from the 0.9530 cm. diameter cylindrical reservoir into the 0.0508 cm. diameter capillary. The partially crystalline mass was subjected to high shear as well as pressure, leading to crystal reorganization as well as additional crystallization. The augmented crystalline content was confirmed by the increased heat of fusion of the transparent strands obtained from the capillary relative to that of the polyethylene obtained from the reservoir.[77] The specimens were removed from the rheometer after cooling to 114°C under 1920 atm. This cooling cycle circumvented the melting that would have occurred at 136°C at atmospheric pressure.

Microscope Examination

Specimens were examined by scanning electron microscopy

(SEM) as well as by direct transmission and replication electron microscopy (TEM). SEM specimens were prepared by fracturing the transparent strands longitudinally, vacuum coating with 50Å gold film, and then observing with a Cambridge Ultrascan instrument. TEM specimens were prepared using such techniques as one and two step replication methods, ultramicrotomy with Br_2 staining, and selected area electron diffraction. A Phillips EM 200 electron microscope equipped with a tilting stage and a Jeolco T7 electron microscope were used to observe the TEM specimens. Where necessary, preparation and observational procedures will be further discussed in conjunction with specific micrographs.

Results

Sample Appearance

The transparent strands were formed by a procedure that was similar to a drawing operation. Peterlin has noted that extensive drawing causes melting during deformation[80]; hence it was not unexpected that the restructured Instron strands bore little relationship to the polyethylene obtained from the reservoir. Furthermore, the transparent strands were not simply the result of crystallization directly from the flowing melt in the capillary. Indeed, transparent strands were also formed at 60°C by simply applying 1920 atm. to a solid plug of polyethylene in the reservoir, forcing it into the capillary to form the unusual structure of the strand. However, the lower temperature procedure often resulted in microcracks located

mainly in the central core of the strands (see Figure 20). These cracks were evidence of crystallite destruction due to excessive drawing. The fusion curve for the sample shown in Figure 20 was both lower and broader in melting temperatures than those crystallized at 136°C.[78] The existence of microcracks running both perpendicular to and at 45° to the strand length, together with the observed lower melting point, were consistent with the disruption of the crystallite structure due to excessive stress. The central core structure failed under tensile stress, as indicated by the cracks in the region perpendicular to the strand length; the structure failed in shear near the outer radius, as indicated by cracks oriented at 45° to the tensile force (the maximum shear plane). This was consistent with a previous observation that the maximum longitudinal velocity gradient, responsible for drawing, occurs along the central axis of the strand; while the maximum radial velocity gradient, a shearing effect, occurs near the outer radius. Morphological observations described in this paper indicate basic structural differences between the inner core and the outer sheath of the strand. In all probability, these differences arose from the different orientation effects attributed to the different velocity gradients existing in the central core and the outer sheath regions during the crystallization process.

Scanning Electron Microscopy

In spite of the 200Å resolution limit of the SEM, its

large depth of field proved to be an invaluable tool in defining the structure. Two distinct fibrous textures were observed. One of these, shown in Figure 21, was found only in the outer sheath of the strand. 3000 Å diameter fibers, oriented parallel to the flow direction, formed the dominant structure for radius values 0.008-0.025 cm. delineating the outer sheath (see Figure 20 for schematic). A cross texture running perpendicular to the 3000 Å diameter fiber axes was observed upon close inspection of Figure 21. This cross texture appeared to be spaced more or less periodically along the main fibers at 500 Å intervals and often spanned several adjacent fibers. The cross texture appeared to be basically lamellar; however, the SEM resolution limit was approached in attempting to further define the texture. In many cases, this lamellar cross texture was observed to twist around the central fiber thread in a helical fashion. Both the size and orientation of the fibers were consistent with the previously published observations[77] concerning the scanning electron micrograph of a sample fractured by bending at liquid nitrogen temperatures.

The strand inner core consisted of a fine ribbon-like morphology, rather than the 3000 Å diameter fibers comprising the outer sheath. When freshly cleaved samples were first introduced into the SEM, the ribbons appeared to be flat and aligned parallel to one another as well as to the capillary axis (Figure 22a). After approximately thirty minutes, these ribbons began to move apart and coil up into a twisted array.

This effect is illustrated by comparing the structures (note arrows) in Figures 22a and 22b, two photomicrographs taken at ten minute intervals. The higher magnification photomicrograph in Figure 23 shows the separate ribbons curling away from larger ribbon bundles (note arrow). Regular cross striations were also observed on the inner core ribbons; however, this particular cross texture appeared to resemble a crystallographic pleating rather than a lamellar overgrowth. The individual ribbons varied in approximate width between 1,000-5,000 Å and were estimated to be approximately 200-400 Å thick. The ribbon substructure will be described in the transmission electron microscopy section since the thickness measurements approach the SEM resolution limit.

It should be mentioned that the ribbon coiling implies two important features of this particular morphology. First, inter-ribbon bonding is significantly lower than that of the outer sheath. The cross texture observed with the latter structure apparently imparts a three dimensional cohesiveness to the fibers, suggesting the presence of inter-fibrillar linkages. Indeed, no fiber coiling or separation was observed after extensive time periods in the SEM. Second, the ribbons in the bulk crystallized state undoubtedly contained a significant residual strain which is apparently relieved by the coiling mechanism. Such residual strain may have had inherent crystallographic as well as shear-induced origins similar to those causing periodic twisting in polyethylene spherulites.[81]

Transmission Electron Microscopy

Specimens were examined in the conventional electron microscope using both fracture replication and direct transmission techniques. Fracture surface replication proved somewhat difficult because of surface roughness. However, good quality replicas were obtained by shadowing the surface directly with Pt-C, evaporating a thin carbon layer, and finally stripping the layers with acetone-swollen acetate strips. The acetate was then removed by dissolving in amyl acetate, leaving a negative Pt-C shadowed carbon replica. Selected area electron diffraction was performed on several polyethylene fiber fragments which fortunately adhered to such replicas.

The inner core ribbon-like fibrous texture seen in the SEM photomicrographs was also observed in the shadowed carbon replicas. Electron micrographs showed that the ribbons extended for tens of microns and contained fine fiber bundles (see arrow in Figure 24) oriented parallel to the strand long axis. Individual fiber bundles were examined by staining with Br_2 vapor which preferentially attacks the less ordered regions between the component fibers. Specimens were mounted in an epoxy embedding material (Cargille NYSEM) and sectioned on a Sorval Porter Blum MT-2 ultramicrotome using a Dupont 43^{o} diamond knife. Sectioning across a strand proved impractical since the fiber bundles readily splayed apart due to the apparently weak bonding between the fiber bundles. Sectioning parallel to the strand axis proved to be more feasible,

but stringy rather than smooth sections were obtained with this procedure. Figure 25 is a transmission electron micrograph of microtomed Br_2 stained fibers from the strand inner core. The fibrous, stringy texture was quite visible; however, fiber splaying due to the action of the knife was also obvious. The ultimate subunit of the ribbon structure was found to be a 200-250 Å diameter fiber (see arrow in Figure 25). Since individual fibers adhered to several of their neighbors after splaying apart, some type of inter-fiber bonding may have existed within a fiber bundle. A nodular structure that was superimposed on the ultimate fibers was also observed; however, this was probably an artifact of the Br_2 vapor staining process.

Electron Diffraction

Unstained sectioned fibers and in a few cases unshadowed fibers adhering to the carbon replicas were examined by electron diffraction using electron microscope stage tilting techniques. Exceptionally well-developed spot patterns were obtained from the strand inner core where the ribbon-like structure was observed. Proper stage rotation revealed a highly ordered and oriented crystal structure within the ultimate fibers. Figures 26 and 27 contain reciprocal lattice diagrams corresponding to the observed electron diffraction patterns from the inner core material. Note that the shorter exposure time of Figure 26 permitted observation of

lower order reflections, whereas the longer exposure time of Figure 27 provided the higher order reflections. In both cases, (o,k, ℓ) plane diffractions were observed, while (h,o,ℓ) reflections were undetectable with further stage rotation. No explanation was found for the failure to detect the (h,o,ℓ) reflections.

The polyethylene crystal structure is based on an orthorhombic unit cell, requiring the reciprocal and true lattice parameters to be identical. Furthermore, polyethylene belongs to the P_{nma} space group. Such symmetry conditions require that permissible (o,k, ℓ) reflections satisfy the equation: $k + \ell = 2n$. Each of the twenty-six distinct reflections, observable in Figures 26 and 27, comply with this restriction. The electron diffraction data show that an unusually high degree of crystalline order (for polyethylene) exists in the strand inner core. The crystallographic c-axis, the axis parallel to the polyethylene chain backbone, was found to be oriented parallel to the strand long axis (within $\pm 5^{o}$). This high degree of chain orientation is consistent with the c-axis orientation function of +0.996 determined previously with wide angle x-ray measurements. In contrast, electron diffraction studies of the outer sheath 3000 Å diameter fiber morphology produced only typical oriented fiber patterns, similar to those obtained by Keller[75,76] from stress crystallized polyethylene. The resulting diffuse arcs may have been produced by the polycrystalline lamellar cross texture observed on the 3000 Å diameter fibers.

Discussion and Conclusions

Two distinct morphological units are produced in the Instron strands; i.e., the highly crystalline ribbons in the inner core and the less ordered 3000 Å diameter fibers of the outer sheath. Similarly described units have been observed by Pennings and Kiel[72] for the fibrous structures crystallized under the influence of shear in a dilute solution. They too described the morphological entities as being either ribbons or fibers having a lamellar overgrowth. The 3000 Å diameter fibers may well be the melt crystallized analog of the dilute solution grown fibers observed by Pennings and Kiel. Fibrous morphologies are not uncommon in crystalline polymers, especially if the polymer chain backbone is too stiff to accommodate chain folding. O'Leary and Geil[82] have described the fibrous textures in crystalline polytetrafluoroethylene in a manner similar to that used to define the polyethylene structure of this report. Crystal[83] has also described a fibrous morphology for crystalline poly-N-vinylcarbozole, an apparently stiff molecule containing bulky pendant groups which inhibit free rotation about the polymer backbone. Because chain folding cannot be accommodated in poly-N-vinylcarbozole, this polymer apparently crystallizes into a fibrous structure containing weak inter-fiber bonds. While c-axis orientations were noted in these references, sharp spot electron diffraction patterns were not reported.

Additional evidence for the existence of two distinct

morphological units in the Instron strands was found in the fusion curves obtained from the melting of the strands in the Perkin-Elmer Differential Scanning Calorimeter model 1-B (DSC). The DSC traces for two strands crystallized with the Instron procedure at 132°C are shown in Figure 28. Note that these strands appeared basically similar in structure to those examined in the above micrographs (crystallized at 136°C). One of the strands was exposed to 25 MRADS of irradiation in order to suppress reorganization during melting.[84,85] Both strands were found to have relatively high peak value melting points, consistent with the presence of extended chain crystals.[69] Furthermore, the irradiated strand showed a multi-peak fusion curve indicative of discontinuities in the crystal structure. A possible explanation for such behavior would be that the more perfect inner core ribbon structure melted at the higher peak temperature, and the less ordered outer sheath structure, containing chain folded lamellae, melted at the lower peak temperature. The primary effect of the radiation has been to resolve the single fusion curve, corresponding to the unirradiated sample, into low and high melting peaks for the irradiated sample. These observations are consistent with the hypothesis that the structure in the inner core of the strand appears to be dominated by an extended chain crystalline structure, while that of the outer sheath is dominated by epitaxial chain folded lamellae.

The inner core ribbon structure was the most perfect of

the two crystalline units defined in this study. Well developed single crystal electron diffraction patterns obtained from ribbons indicate that they are made up of extended chain crystals. The eighth order reflection along the c-axis has been detected (see Figure 27), using a 5000 Å aperture. In order to obtain such an electron diffraction pattern, the crystalline order must have been retained over this distance. Note that a lamellar structure connected by tie molecules, such as the model proposed by Peterlin for drawn polyethylene[80], would not result in sharp diffraction spots for the (o,k,ℓ) planes over a 5000 Å length of the fiber. In the Peterlin model, the lamellae that stack together to form a fibril would be free to rotate around the c-axis, thereby prohibiting the formation of coherent sets of diffraction planes for all except the (o,o,ℓ) planes. Figures 26 and 27 show the presence of other sets of diffraction planes. Only a well developed extended chain crystal model which maintains a high degree of order over at least 5000 Å can account for the observed diffraction spots from the inner core fibers.

The formation of an extended chain structure by crystallizing from the bulk polyethylene is particularly significant from an improved mechanical properties aspect. In addition to the transparent quality of the strands, the modulus values of the central core containing the extended chain crystal structure may well be extremely high in the direction parallel to the strand length. If defect-free, extended chain ribbons can be produced with a commercial process analogous to the Instron procedure, significant increases in mechanical properties

would indeed be realized.

REFERENCES

66. B. Wunderlich and T. Arakawa, J. Polymer Sci., Pt. A, 2, 3697 (1964).

67. E. Hellmuth and B. Wunderlich, J. Appl. Phys., 36, 3039 (1965).

68. B. Wunderlich and C. Cormier, J. Polymer Sci., Pt. A-2, 5, 987 (1967).

69. D. Rees and D. Bassett, J. Polymer Sci., Pt. B, 7, 273 (1969).

70. L. Mandelkern, M. Gopalan, and J. Jackson, J. Polymer Sci., Pt. B, 5, 1 (1967).

71. B. Wunderlich, J. Polymer Sci., Pt. B, 5, 7 (1967).

72. A. Pennings and A. Kiel, Kolloid-Z. u. Z. Polymere, 205, 160 (1965).

73. T. Kawai, T. Matsumoto, M. Kato, and H. Maeda, Kolloid-Z. u. Z. Polymere, 222, 1 (1969).

74. R. Williamson and R. Novak, J. Polymer Sci., Pt. B, 5, 147 (1967).

75. M. Hill and A. Keller, J. Macromol. Sci. (Phys.), B3, 153 (1969).

76. A. Keller, Reports on Progress in Phys., 31, 623 (1968).

77. J. H. Southern and R. S. Porter, accepted for publication in J. Macromol. Sci. (Phys.) (1970).

78. J. H. Southern and R. S. Porter, accepted for publication in J. Appl. Polymer Sci. (1970).

79. C. R. Desper, J. H. Southern, R. D. Ulrich, and R. S. Porter,

submitted to J. Appl. Phys (1970).

80. A. Peterlin, Polymer Engin. and Sci., 9, 172 (1969).

81. J. R. Burns, J. Polymer Sci., Pt. A-2, 7, 593 (1969).

82. K. O'Leary and P. H. Geil, J. Appl. Phys., 38, 4169 (1967).

83. R. G. Crystal, accepted for publication in J. Appl. Phys. (1970).

84, H. E. Bair and R. Salovey, J. Macromol. Sci. (Phys.), Be, 3 (1969).

85. T. W. Huseby and H. E. Bair, J. Polymer Sci., Pt. B, 5, 265 (1967).

LEGEND FOR ATTACHED FIGURES

INSTRON PRESSURE TRACE AT 136°C UNDER A PLUNGER VELOCITY OF 0.5 CM./MIN. WITH A CAPILLARY OF 0.0508 CM. DIAMETER, 1.55 CM. LENGTH, AND 90° ENTRANCE ANGLE

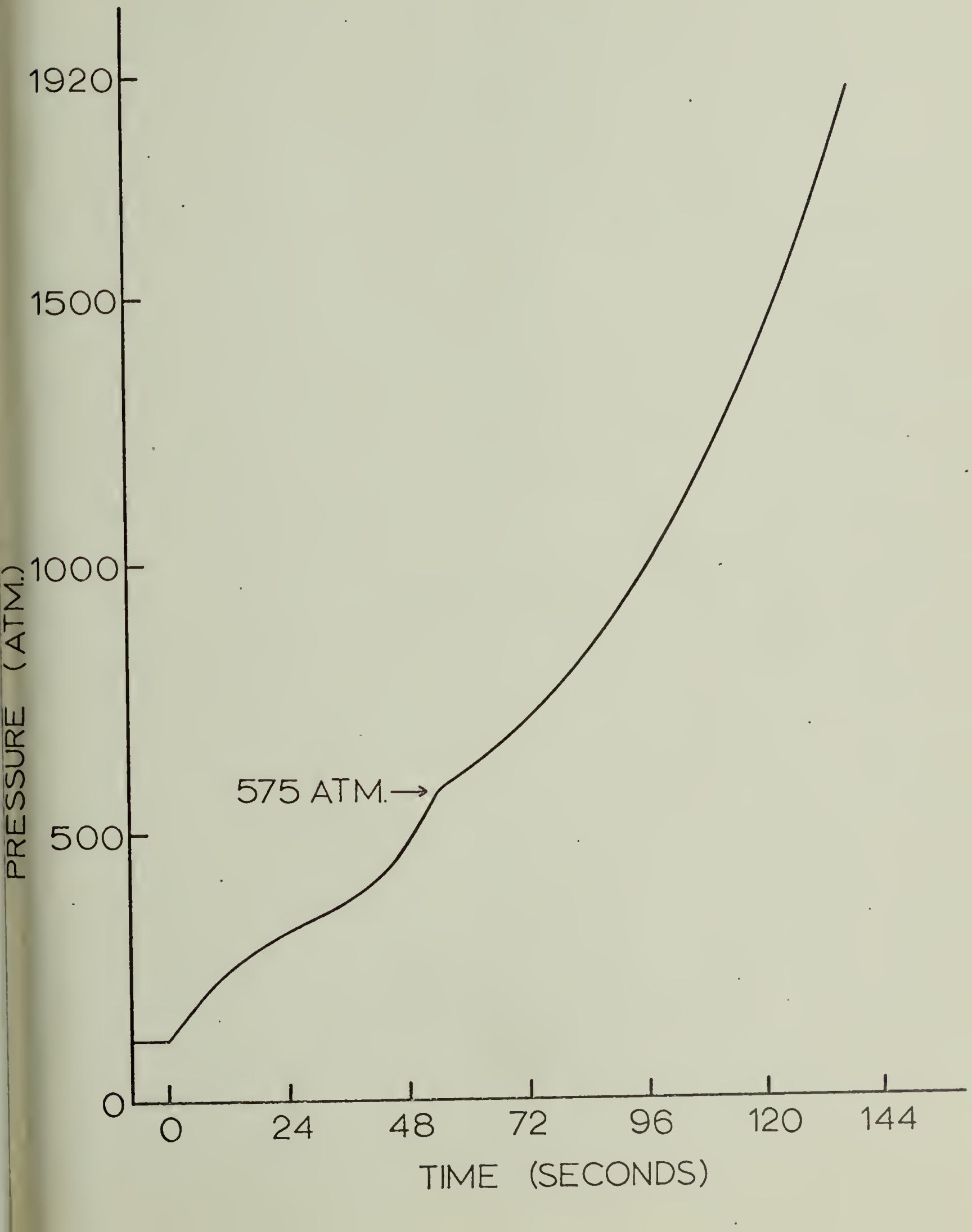

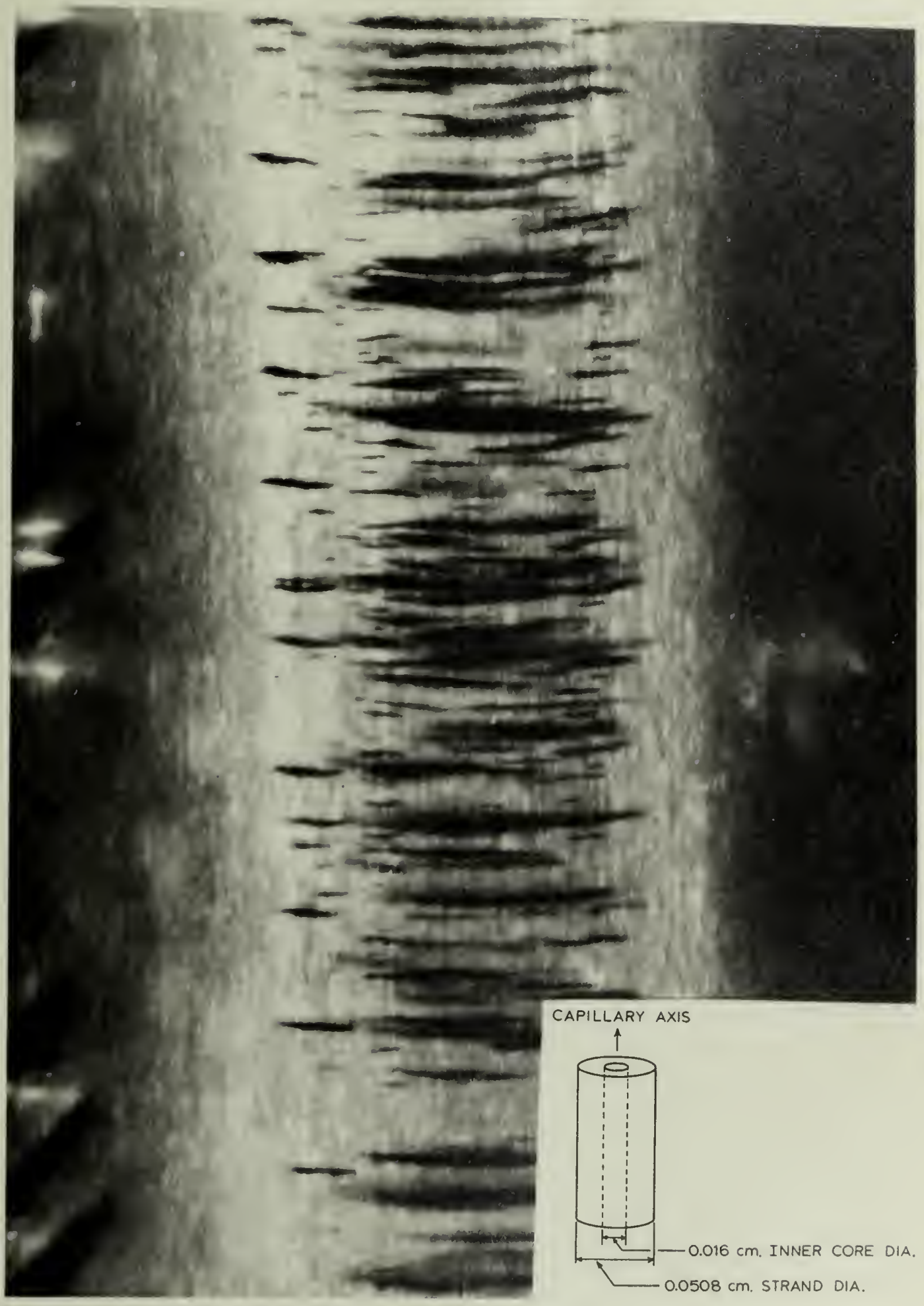
CAPILLARY AXIS
0.016 cm. INNER CORE DIA.
0.0508 cm. STRAND DIA.

FIGURE 21

FIGURE 22-a

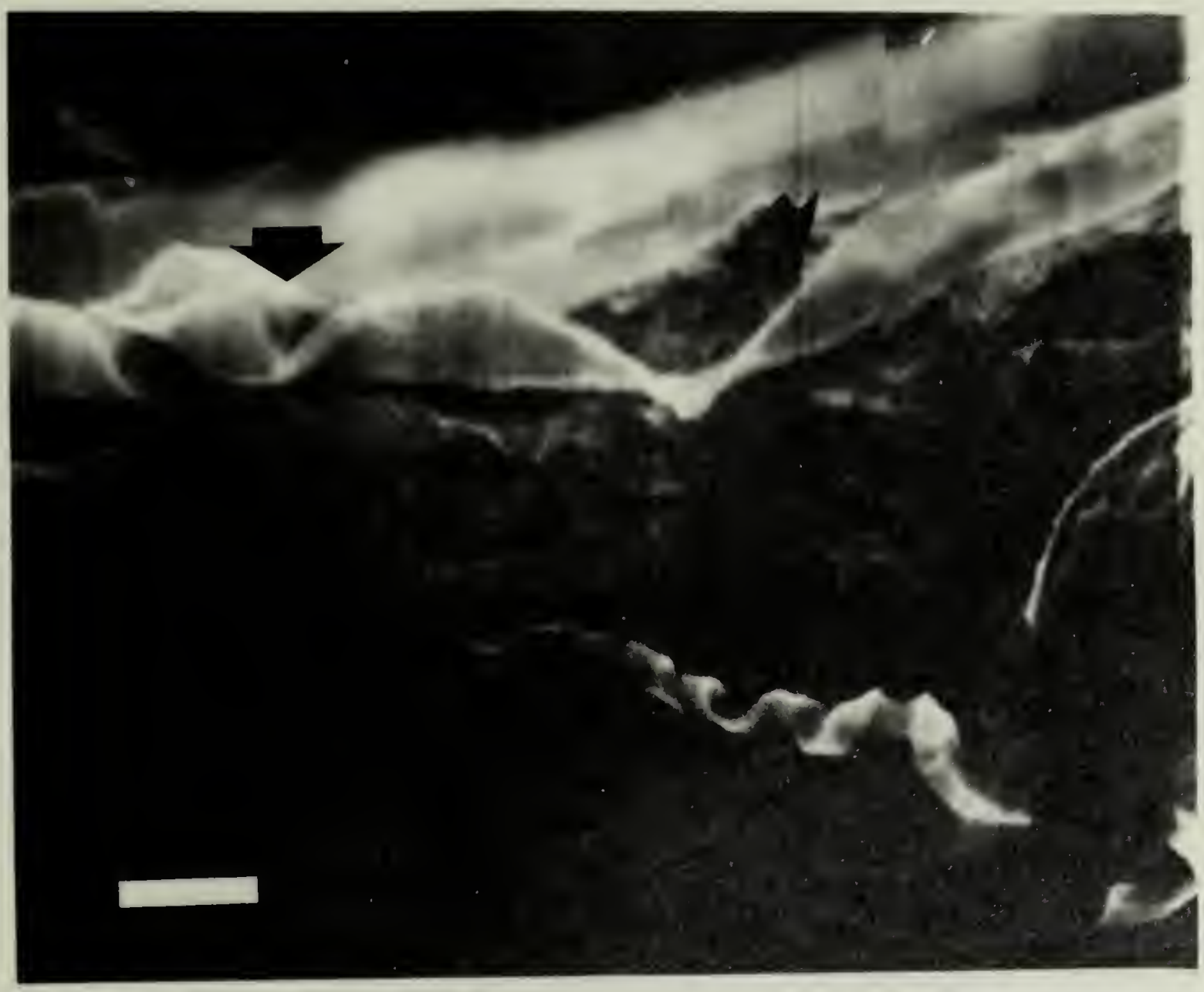

FIGURE 22-b

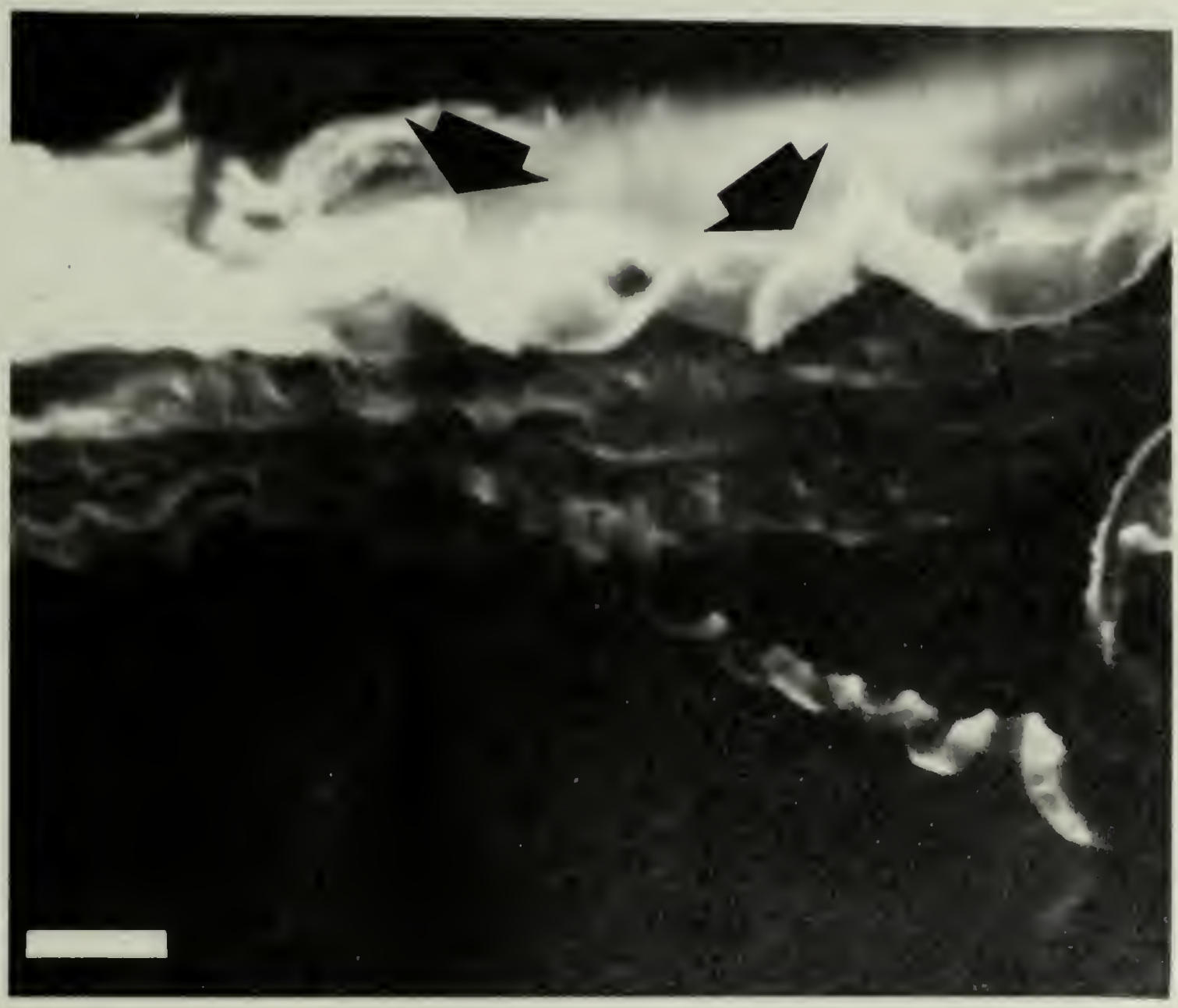

FIGURE 23

FIGURE 24

FIGURE 25

FIGURE 26

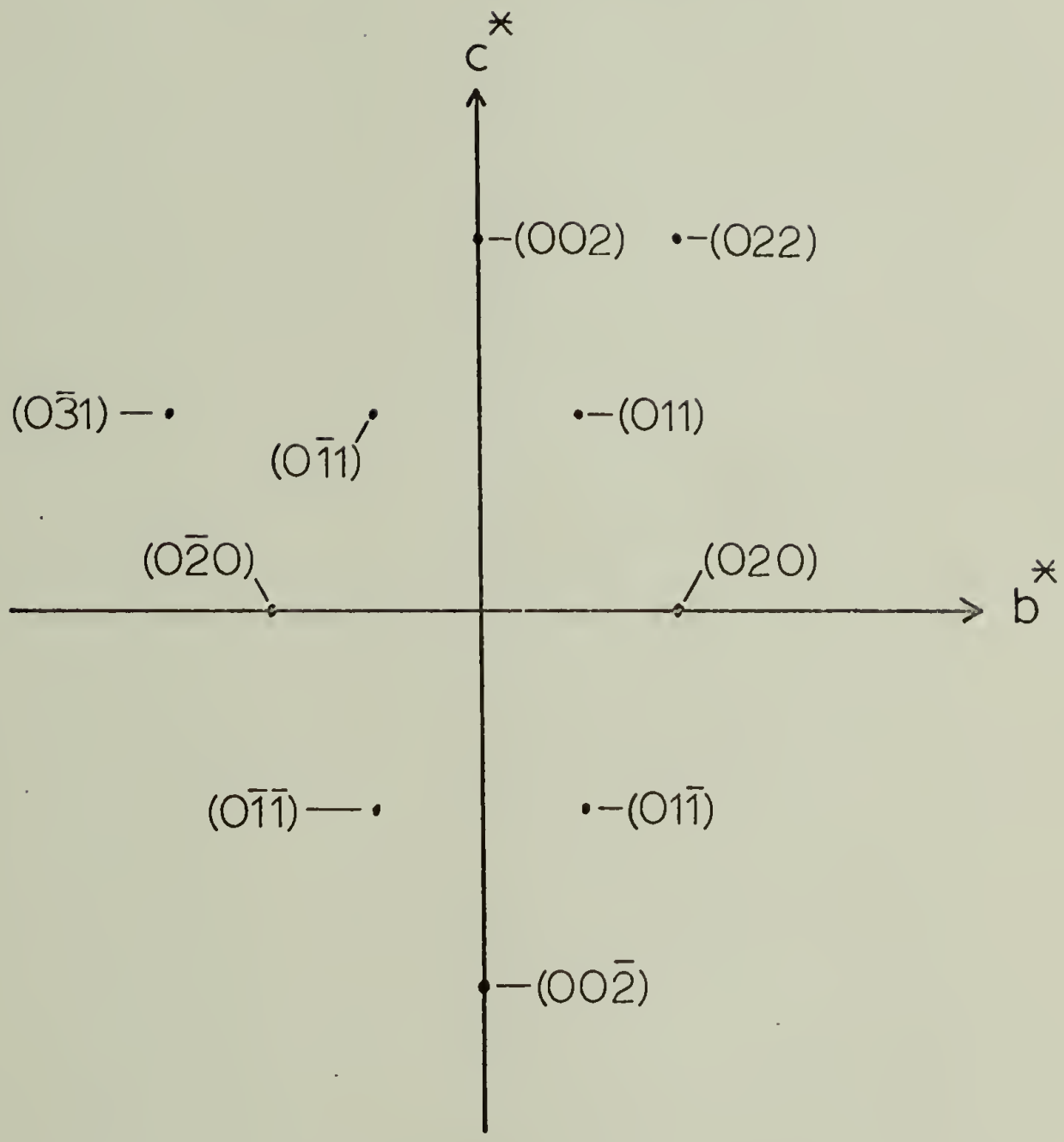

FIGURE 27

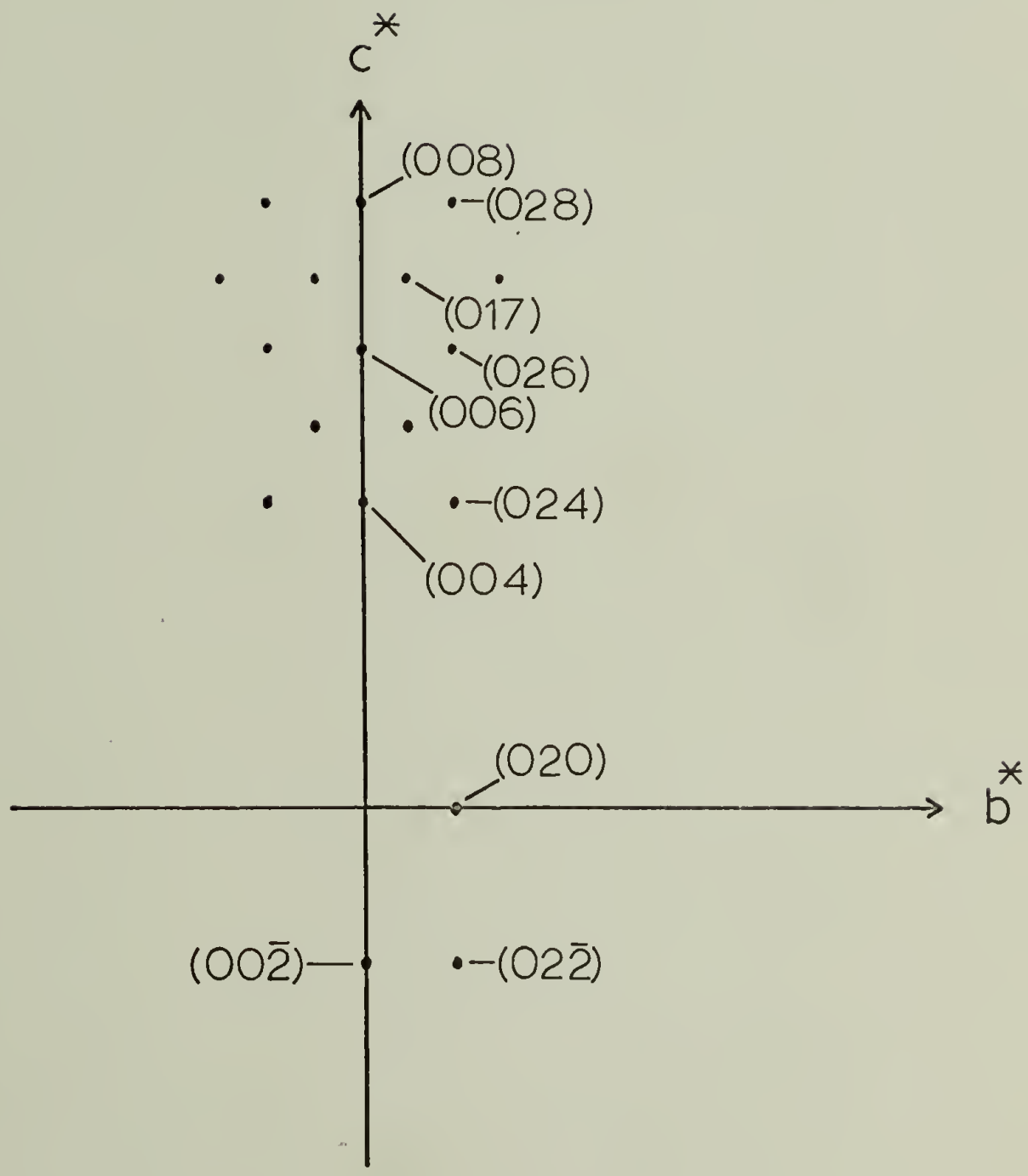

EFFECT OF RADIATION ON MELTING BEHAVIOR OF A TRANSPARENT SEGMENT PRODUCED IN INSTRON AT 132°C IN A CAPILLARY OF 0.0762 CM. DIAMETER UNDER A PLUNGER VELOCITY OF 1.0 CM./MIN.

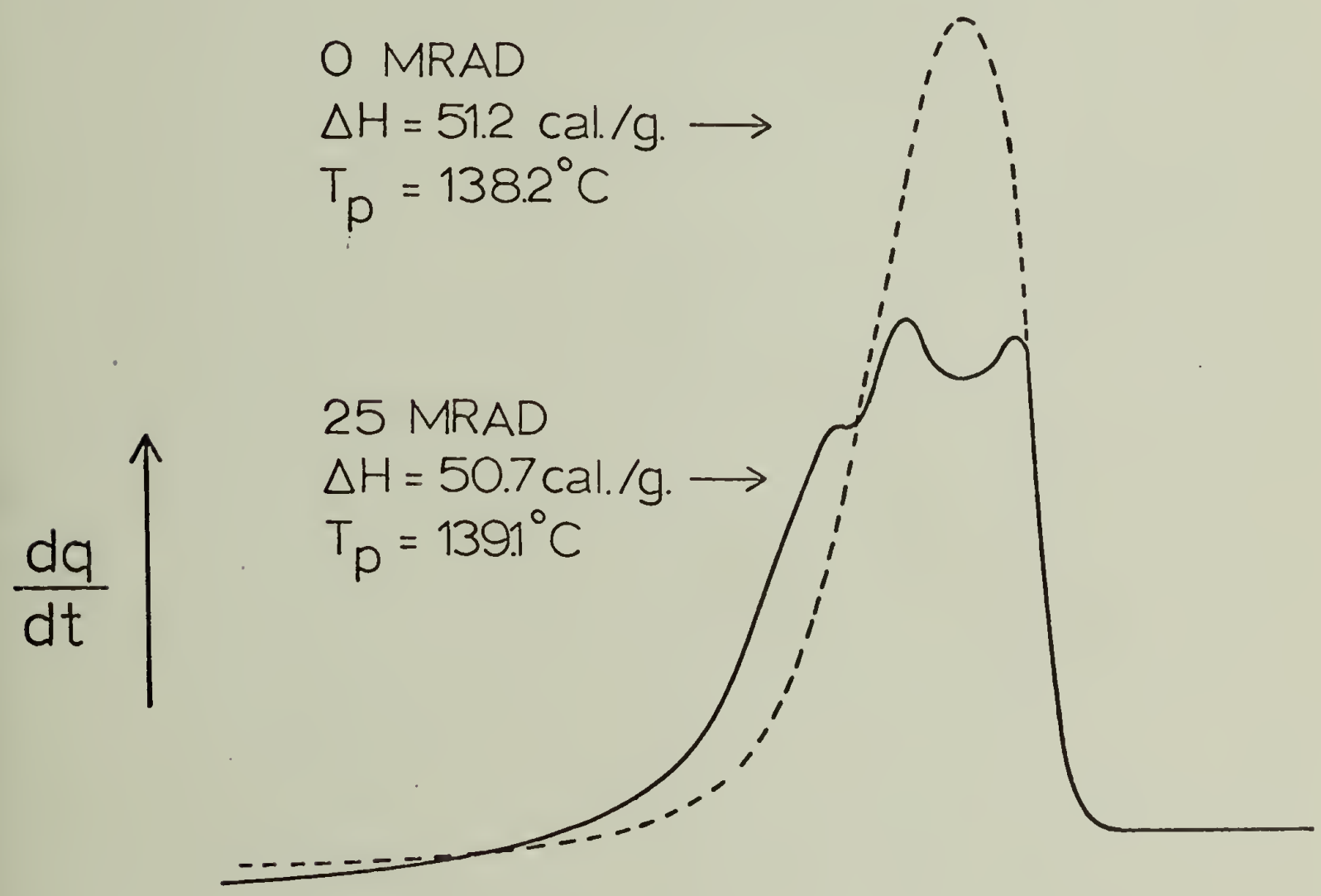

CHAPTER VI

THE CRYSTAL STRUCTURE OF POLYETHYLENE CRYSTALLIZED UNDER BOTH ORIENTATION AND PRESSURE EFFECTS

Introduction

High density polyethylene has been crystallized in the Instron Capillary Rheometer under the combined effects of pressure and orientation. The data that has been amassed in previous research on the resulting transparent polyethylene strands[86-90] is correlated in this report with specific models for the crystalline structure. Electron microscopy and electron diffraction have revealed the existence of an inner core of highly ordered crystallites as well as a distinctly less perfect crystal structure composing the outer sheath of the strand.[90] The applicability of specific models based on the concepts of extended chain, chain folded, and combinations of extended chain and chain folded crystallites is evaluated for both the structure of the inner core and that of the outer sheath. Recently obtained electron diffraction and wide angle x-ray estimations of the crystallite size are discussed in some detail. In addition, a low angle x-ray spacing is presented. The values from electron and x-ray diffraction are related to the selected structural models.

Sample Preparation

The samples discussed herein were crystallized from Dupont Alathon 7050 which has a number and a weight average molecular weight of 18,400 and 52,500, respectively. This polymer is a

relatively narrow distribution, high density polyethylene. In the crystallization procedure, transparent strands were formed in capillaries of 0.0508 cm. diameter and 90° entrance angle at a rheometer temperature of 136°C. The capillary length varied from 1.55-2.56 cm. and the plunger velocity from 0.5-5.0 cm/min. Neither the capillary length nor the plunger velocity have been observed to alter the final structure.

In order to induce crystallization in the polyethylene in the rheometer, the plunger velocity was increased in fixed increments at a temperature near the atmospheric melt transition. The pressure also rose in order to maintain the incremented flow rate resulting from the increased plunger velocity applied to a presumedly incompressible melt. Due to the pressure, the melt became supercooled. At some particular plunger velocity (depending on the geometry conditions of the capillary, the viscosity of the sample, and the rheometer temperature), the pressure produced a critical degree of supercooling and crystallization occurred. This was evidenced by abnormal extrudate swelling and a sustained rise in the pressure. Though as yet unproven, the velocity gradient parallel to the axis of flow and existing in the capillary entrance region may have produced a significant orientation of the melt that reduced its entropy. The result would have been to augment the degree of supercooling relative to that calculated solely from static pressure conditions. Because the transparent

strands have also been produced with a knife edge capillary, consisting only of a 90° cone, the primary crystallization process apparently occurred in the rheometer barrel and capillary entrance region, followed by plug flow of the crystallized strand down the capillary. The final structure was formed by the deformational stresses applied to the randomly oriented lamellae as they were forced into the capillary entrance region under approximately 1900 atm. of pressure. The structure was effectively melted under the stress,[92] and the oriented melt then recrystallized as it moved into the capillary. After cooling the rheometer system while maintaining the pressure, the strand was extracted from the capillary and examined with various techniques. It was found to have the relatively high melting point of 140.0 ±.5°C,[87,89] as determined from the peak value of fusion curves measured on the Perkin-Elmer Differential Scanning Calorimeter Model 1-B. From the same fusion curves, the crystalline content of the transparent structure was measured at 83 ±2%. The strand was found to have the highest degree of uniaxial orientation thus far recorded for polyethylene. The c-axis orientation function was calculated from azimuthal x-ray scans to be +0.996±.002 relative to the strand axis, implying that the average polyethylene chain in the crystal lattice was aligned at an angle of less than 2° 58' to the strand axis.[88] Scanning and transmission electron microscopy have revealed that the strand was composed of two morphological units: a ribbon-like structure in its inner core and a 3000 Å diameter fiber structure in its outer

sheath.[90] The inner core included radius values from the strand axis out to approximately 0.008 cm., while the outer sheath included the remainder of the strand. A cross texture that resembled a lamellar structure was found only on the 3000 Å diameter fibers. The ribbons of the inner core were composed of 200-250 Å diameter fibers that extended for microns in a direction parallel to the strand axis.

Results

Crystallite Size from x-ray Measurements

In order to evaluate the structure of the transparent strands, measurements of the crystallite size were successfully obtained from wide angle x-ray measurements. It is well known that a small crystallite size will lead to broadening of the high-angle (radial) x-ray diffraction lines. This has been expressed in the familiar Scherrer equation:[93-95]

$$L_{hk\ell} = \frac{K\lambda}{\beta \cos\theta}$$

where $L_{hk\ell}$ is the dimension of the crystallites perpendicular to the ($hk\ell$) planes, β is the breadth at half-maximum (expressed in radians), θ is the Bragg angle, λ is the wavelength (1.5418 Å), and K is the so-called shape factor. Authors differ on the proper value for K, but values are usually in the range 0.9-1.0. In accordance with the recommendation of Klug and Alexander, a value of K = 0.9 was used; hence the calculated value of L_{002} to be discussed must be noted as being a lower limit for the average crystallite dimension of the Instron

strand. The use of the Scherrer equation is based on the assumption that a high degree of order exists within the crystallites.

Another important source of line broadening are lattice distortions of the second kind, as described in the Hosemann theory of paracrystals.[96] When such distortions are present, there is, strickly speaking, no discrete plane spacing since small errors in position tend to accumulate. Buchanan and Miller have demonstrated a method for separating crystal size effects from distortion effects.[97] This involves a Fourier analysis of at least three orders of the same (hkℓ) reflection and has not been used in the present instances because of intensity limitations and because the (004) and (006) reflections cannot be obtained with the available radiation. Although no estimate has been made for the effect of distortion, it was possible to obtain a lower bound on the value of $L_{hk\ell}$. That is, the Scherrer equation was used to calculate an apparent value for $L_{hk\ell}$ assuming that only crystallite size broadening was present. If distortion broadening were also present, the crystallite size broadening will have been overestimated, and thus the actual crystallite size will have been underestimated.

The experimental line profile for the (002) reflection was fitted to a Gaussian curve (see Figure 29). Cauchy functions were also tried but did not provide an adequate fit for the data. Corrections were applied (see Appendix III) for instrumental broadening, including the splitting of the

$\alpha_1 - \alpha_2$ doublet. L_{002} calculated with these corrections was found to be 285 Å. Specifically, this value represented the dimension of the average crystallite which has been found to be aligned in a direction $2^{o}58'$ from the capillary flow axis. A value of 220 Å was also measured in a similar manner from the (110) reflection obtained on the strand. In addition to these wide angle determinations of the crystallite dimensions, a low angle x-ray spacing of 230 $\pm$20 Å along the strand length has been determined. Note that the L_{002} value reflected only the dimension of the crystallites, while the low angle value represented the combined amorphous and crystalline spacing.

Electron Diffraction

Selected area electron diffraction using a Phillips EM 200 electron microscope equipped with a tilting stage has been carried out on samples obtained from the strands. In Figure 30, a carbon replica of the structure from the inner core was obtained on which several of the ultimate fibers (200-250 Å diameter) had adhered. These fibers were exposed to an electron beam which covered the area denoted in Figure 30 by a square. Spot diffraction patterns were obtained from this and other such target areas; the observed reciprocal lattice points were graphed (see Figure 31). The (ooℓ) reflections were observed, indicating that the polyethylene chains in the crystal lattice were oriented parallel to the length of the fibers. The presence of additional reflections as well as those from the (ooℓ) planes indicated that a continuous crystalline

order persisted in the fibers over the distance of the beam aperture (approximately 5000 Å). Furthermore, the electron diffraction patterns of the fibrous structure of the outer sheath showed only a few arcs, rather than sharp spots, indicative of a significantly less ordered structure than that of the inner core. More detailed information concerning the electron diffraction experiments has been presented in a previous report.[90]

Discussion

The electron diffraction data has supported the electron microscopy in delineating two different types of structures, one dominating the inner core and the other found in the outer sheath. On the basis of the electron diffraction (see Figure 31), the 200-250 Å diameter fibers of the inner core appeared to be composed of an extended chain crystal structure. Schematic diagrams of two extended chain crystal models were considered (see Figure 32-a and 32-b). The model for crystallization under high pressure was proposed for a structure that has been extensively discussed by Wunderlich.[91,98] In order to obtain such a perfect degree of crystalline order in which lamellae of same thickness as would result from completely extended chains were produced, static pressures of at least 3000 atm. must be used in conjunction with lengthy annealing times measured in hours. These conditions did not exist for the crystallization procedure in the Instron Rheometer where the pressure was limited to less than 2000 atm. and the crystallization time was usually measured in seconds. The extended chain crystals produced in the

rheometer under the combined orientation and pressure effects had, in all probability, a structure in which the polyethylene had not undergone molecular weight fractionation (as in the most perfect of the high pressure lamellae[98]), but had instead fitted into a crystalline lattice similar to that in Figure 32-b. Random defects, believed to be due primarily to chain ends, were intersperced throughout each of the 200-250 Å diameter fibers from the inner core. Neither of the models proposed in Figure 32-c and 32-d were justified for the inner core structure in view of the confirmed high degree of order over at least 5000 Å, the dimension of the electron beam resulting in sharp diffraction spots. Essentially, the multi-lamellae structure of the latter two models could not have resulted in a coherent diffraction for the observed non-(ooℓ) reflections. Note that the (ooℓ) reflections could be explained by any of the four models since the chains in the crystal lattice are all aligned parallel to the strand axis, as required by the measured orientation function.

Either of the models in Figures 32-c and 32-d can be used to explain the structure of the outer sheath. The x-ray L_{002} value of 285 Å for the crystallite size and the low angle spacing of 230 Å are believed to have been the result of diffraction only from this portion of the strand. A cross texture, resembling epitaxial lamellar growth, has been observed in the electron microscope for the outer sheath. Such an oriented lamellar structure would indeed give rise to both a low angle

spacing and sharp wide angle reflections. Thus the 3000 Å diameter fibers of the outer sheath are believed to be basically composed of lamellae. Such a structure is adequately described by either of the models in Figure 32-c and 32-d. Using that of Figure 32-c, the lamellae were held together by tie molecules that extended between adjacent lamellae. Such a structure has been proposed by Peterlin[92] for drawn polyethylene. The model in Figure 32-d was developed by Keller and Machin[99] for crystallization under stress. An extended chain backbone has nucleated chain folded lamellar growth in planes perpendicular to the fiber axis. Note that the Keller and Machin model, based on extended chain backbones, and the Peterlin model, with its tie molecules, were consistent with the measured degree of crystallite orientation and the high modulus values.[87]

Additional studies are presently being considered in order to evaluate the validity of the models for the structure in the outer sheath. However, the most interesting result so far obtained has been the formation of an extended chain crystal structure (the inner core of the strand) directly from the bulk state under pressures less than 2000 atm. and with relatively short crystallization times. The use of both orientation and pressure have resulted in a unique structure with a high degree of uniaxial coherence. The Instron procedure was also utilized to crystallize polypropylene, and the results are summarized in Appendix IV. In addition, Appendix V outlines suggested areas for future research.

REFERENCES

86. J. H. Southern and R. S. Porter (Chapter I), accepted for publication in J. Macromol. Sci. (Phys.) (1970).

87. J. H. Southern and R. S. Porter (Chapter II), accepted for publication in J. Appl. Polymer Sci. (1970).

88. C. R. Desper, J. H. Southern, R. D. Ulrich, and R. S. Porter (Chapter III), submitted to J. of Appl. Phys. (1970).

89. J. H. Southern and R. S. Porter (Chapter IV), to be submitted (1970).

90. R. G. Crystal and J. H. Southern (Chapter V), to be submitted to J. Polymer Sci. (1970).

91. B. Wunderlich and T. Arakawa, J. Polymer Sci., Pt. A, 2, 3697 (1964).

92. A. Peterlin, Kolloid-Z u. Z. Polymere, 216, 129 (1967).

93. P. Scherrer, Gottingen Nachrechten, 2, 98 (1918).

94. H. P. Klug and L. E. Alexander, X-ray Diffraction Procedures (New York: Wiley), Cpt. 9 (1954).

95. L. E. Alexander, X-ray Diffraction in Polymer Science (New York: Wiley), Cpt. 7 (1969).

96. R. Hosemann, Z. Physik, 128, 464 (1950).

97. D. R. Buchanan and R. L. Miller, J. Appl. Phys., 37, 4003 (1966).

98. F. R. Anderson, J. Polymer Sci., Pt. C, 3, 123 (1963).

99. A. Keller and M. J. Machin, J. Macromol. Sci. (Phys.), B1, 41 (1967).

LEGEND FOR ATTACHED FIGURES

INTENSITY DISTRIBUTION OF (002) REFLECTION FITTED WITH GAUSSIAN FUNCTIONS. DATA CORRECTED FOR BACKGROUND.

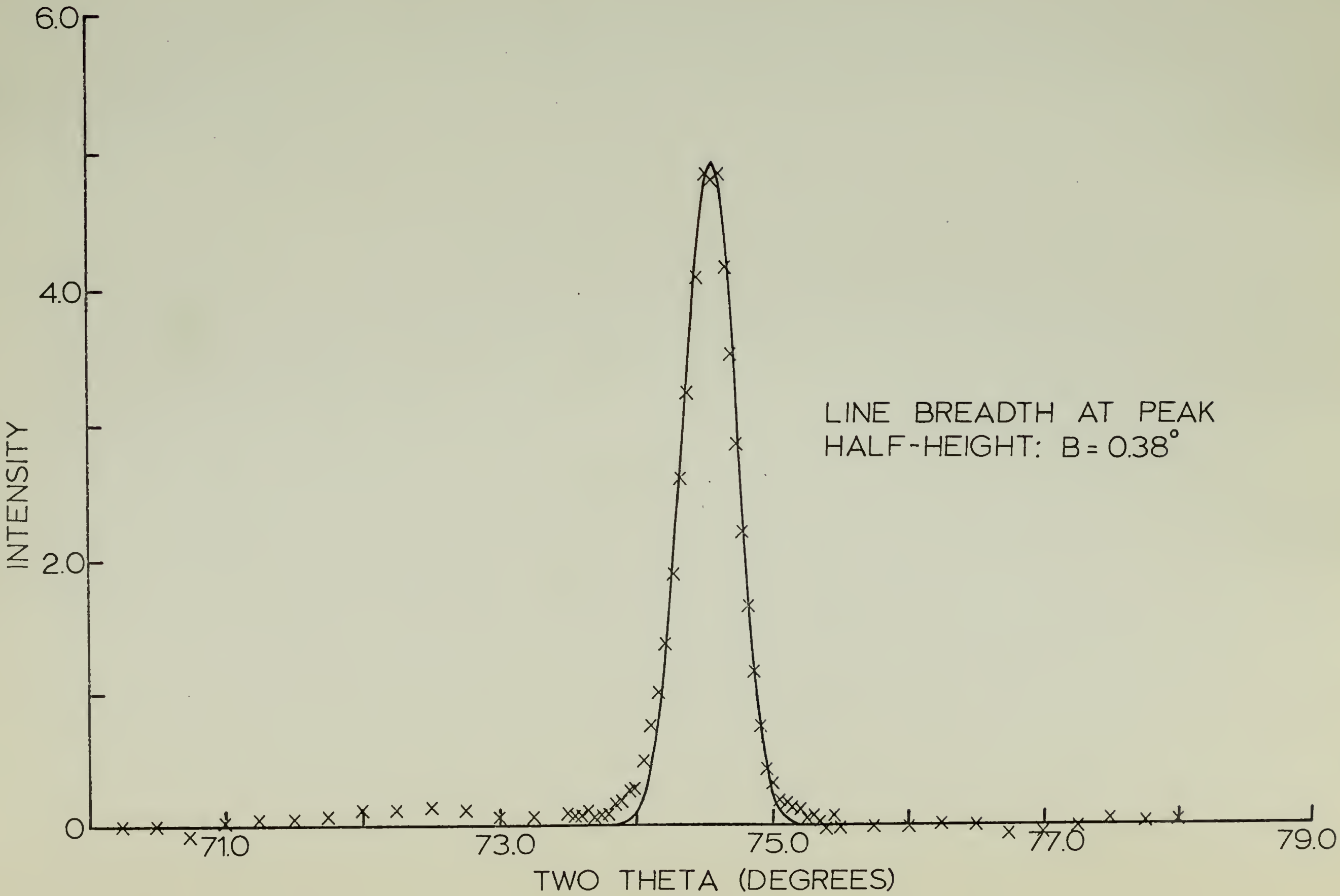

RECIPROCAL LATTICE DIAGRAM OF INNER CORE MATERIAL

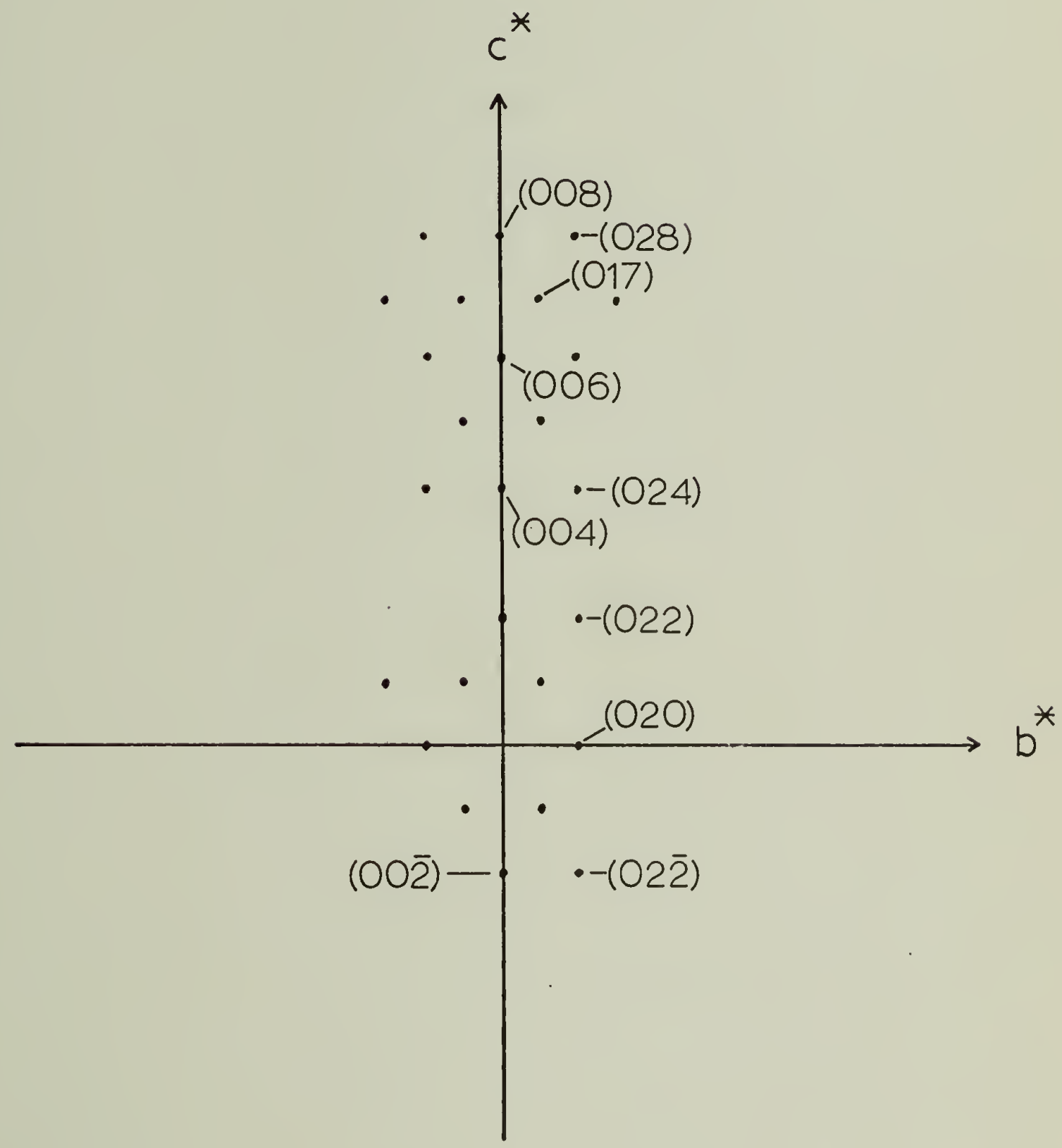

STRUCTURAL MODELS FOR POLYETHYLENE CRYSTALLIZED UNDER VARIOUS CONDITION

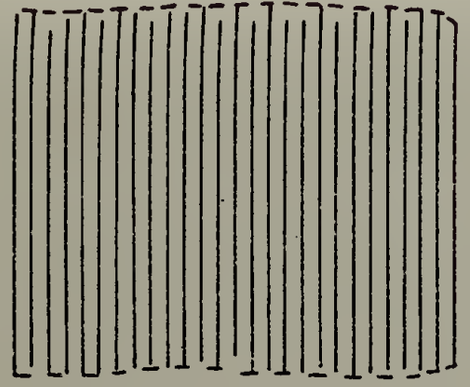

a. Extended Chain Model For Crystallization Under High Pressure

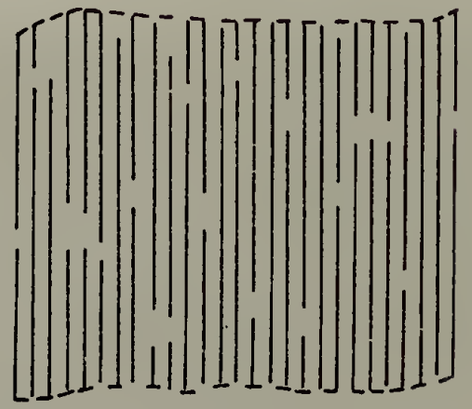

b. Extended Chain Model For The Inner Core Of The Instron Strands

STRAND AXIS

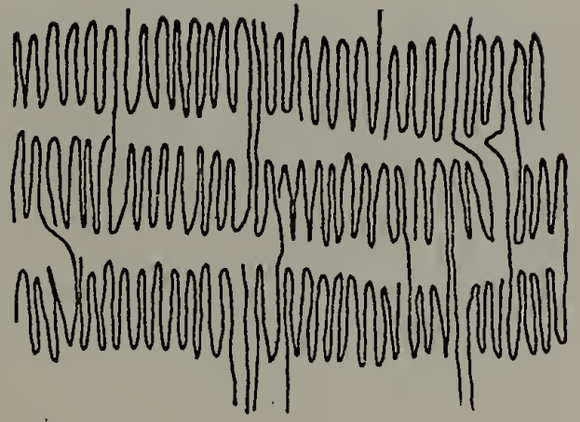

c. Chain Folded Model For Drawn Polyethylene

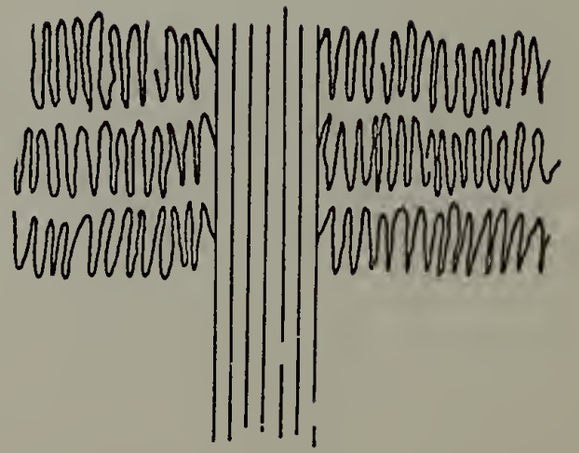

d. Composite Model For Crystallization Under Stress

(MODELS ARE NOT TO SCALE)

APPENDIX I.
OSCILLATING FLOW BEHAVIOR BELOW 150°C

Data is provided for the high density polyethylene in the region of oscillatory shear behavior (often referred to as the land melt fracture region). This region has been discussed in detail for temperatures greater than 150°C in research reported previously.[100-107] The purpose of this section is first to define the relationship of the irregular pressure oscillations that sometimes accompany crystallization to the regular oscillations indicative of land melt fracture[100] and second to discuss the oscillating pressure traces accompanying land melt fracture for temperatures below 150°C.

Figure 33 shows the flow curves for both Phillips Marlex 6009 and the lower viscosity Dupont Alathon 7050. At a temperature of 145°C, the Alathon 7050 showed regular stress oscillations (shaded area) at a nominal shear rate at the capillary wall of 923 sec^{-1}, oscillations which did not result in crystallization. In fact, the oscillations disappeared for the higher shear rate of 1845 sec^{-1} and 4614 sec^{-1}. For Marlex 6009, the regular-type stress oscillations between 1.60 and 2.00 x 10^6 dynes/cm.^{2} were found in the region including 185 sec^{-1} and 461 sec^{-1}. At a higher plunger velocity of 1.0 cm/min. corresponding to a nominal shear rate of 923 sec^{-1}, melt flow of the Marlex extrudate ceased; that is, massive crystallization occurred. However, at this plunger velocity irregular oscillations that accompanied crystallization did not start until a shear stress of 5.0 x 10^6 dynes/cm.^{2} was attained. Note that these observed

stress oscillations are analogous to the pressure oscillations of Figure 1, since the shear stress was computed only from the capillary geometry and the pressure drop. It is also relevant to note that the value of the lowest irregular oscillation (5.0×10^6 dynes/cm.^{2}) is more than a factor of two greater than the values stated above for the regular oscillations of the land melt fracture region. No attempt has been made to graphically plot the shear values accompanying crystallization; in fact, the terms shear stress and shear rate are used with caution in referring to the flow of a partially crystalline melt because the basic assumption of incompressibility is no longer valid.[108]

In view of the divergency between the pressure oscillations accompanying crystallization and those associated with melt fracture (both in shape and magnitude), it is reasonable to state that the two types of oscillations are not due to the same cause. At the present time, no evidence has been obtained that would result in an interrelationship of melt fracture with crystallization.

In the exploratory studies concerning a possible correlation of melt fracture and the crystallization process, a number of interesting points were observed in the land melt fracture process at temperatures below 150°C. On the basis of data obtained at temperatures greater than 170°C, Myerholtz[102] found that the upper critical shear stress increased by 2×10^4 dynes/cm.^{2}-°C (see Figure 33 for the definition of an upper critical shear stress, τ_u). Data obtained in these laboratories

shows an upper critical shear stress for Marlex 6009 of 2.9×10^6 dynes/cm.^{2} at 190°C and 2.0×10^6 dynes/cm.^{2} at 145°C (see Figure 33 for latter value). This drop in the upper critical shear stress of 0.9×10^6 dynes/cm.^{2} over a 45°C range is in agreement with the coefficient established by Myerholtz. Thus the upper critical shear stress is predicted accurately by the Myerholtz coefficient, even at temperatures as low as 145°C.

Also of interest to the topic of melt fracture is the effect of capillary entrance angle observed at a temperature of 148°C. From data obtained at 190°C, Metzger found that the capillary entrance angle had no significant effect on the initial shear rate at which the load oscillates.[107] Myerholtz, using an Instron Rheometer augmented with a variable speed drive mechanism, found a slight effect of the entrance angle at 190°C; the critical shear rate for the onset of oscillating flow (γ_c in Figure 33) decreased by approximately 10% on going from a 60° to a 180° entrance angle.[102] At a temperature of 148°C, an entirely different result was obtained; the critical shear rate increased on going from a 60° to a 180° entrance angle. Using stainless steel capillaries of 0.0508 cm diameter and 2.54 cm length, the 60° entrance angle capillary resulted in regular stress oscillations ($1.50 - 1.71 \times 10^6$ dynes/cm.^{2}) at a plunger velocity of 0.2 cm/min. corresponding to a nominal shear rate of 185 sec^{-1}. However, the 180° entrance angle capillary under the same plunger velocity resulted in an equilibrium (rather than oscillating) pressure trace corresponding

to a shear stress of 1.95 dynes/cm.^{2} (accompanied by gross extrudate swelling). Thus temperatures below 150°C may result in anomalous effects in melt fracture studies.

It is of interest to note that transparent strands have been produced at 136°C in capillaries having entrance angle geometries varying from 90° - 180°. The external appearance of strands produced with the Instron procedure did not vary in any consistent manner. No systematic study of orientation functions and melting points was conducted as a function of entrance angle.

REFERENCES

100. M. Shida and L. V. Cancio, ACS Preprints, Div. of Polymer Chem., 10, 144 (1969).

101. J. M. Lupton and J. W. Regester, Polymer Engineering and Sci., 5, 235 (1965).

102. R. W. Myerholtz, J. Appl. Polymer Sci., 11, 687 (1967).

103. J. P. Tordella, J. Polymer Sci., Pt. C, 15, 495 (1966).

104. J. P. Tordella, J. Appl. Polymer Sci., 7, 215 (1963).

105. J. P. Tordella, Trans. Soc. Rheol., 1, 203 (1957).

106. A. P. Metzger and C. W. Hamilton, SPE Trans., 4, 107 (1964).

107. A. P. Metzger, C. W. Hamilton, and E. H. Merz, SPE Trans., 3, 21 (1963).

108. S. Middleman, The Flow of High Polymers (New York: Interscience), 14 (1968).

109. B. Wunderlich and T. Arakawa, J. Polymer Sci., Pt. A, 2, 3697 (1964).

110. A. K. van der $V_e$gt and P. P. A. Smit, Advances in Polymer Science, Society of Chemical Industry, London, Monograph 26, 313 (1967).

LEGEND FOR ATTACHED FIGURE

Page 135. Figure 33.

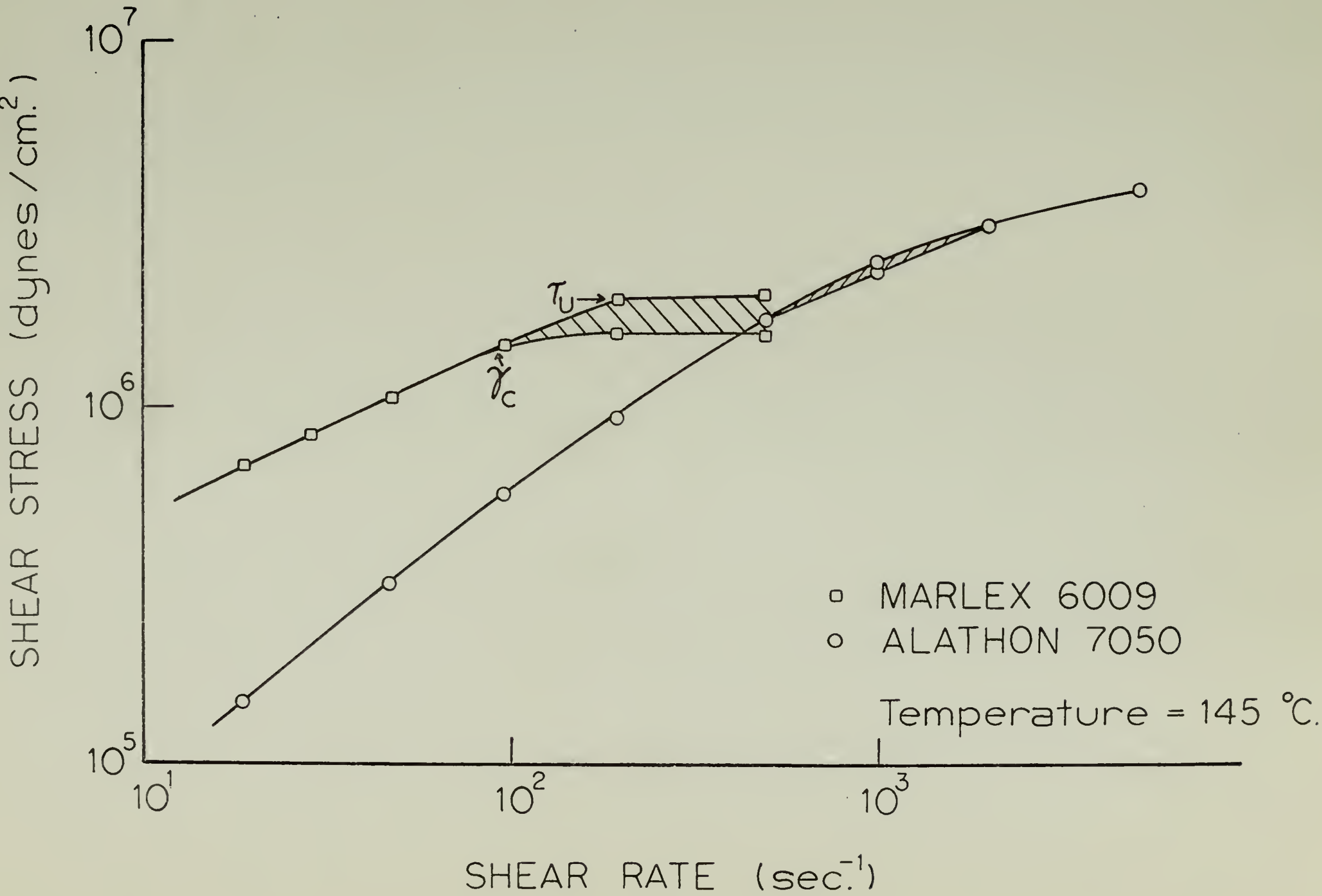
SHEAR STRESS (dynes/cm.²)
10⁷
10⁶
10⁵
10¹
10²
10³
SHEAR RATE (sec.⁻¹)
τU
γ̇C
MARLEX 6009
ALATHON 7050
Temperature = 145 °C.

APPENDIX II

INSTRUMENTAL CONDITIONS FOR THE X-RAY DIFFRACTION MEASUREMENTS

Quantitative intensity determinations were obtained using the Picker FACS-1 automated x-ray diffraction system. This unit includes an incident beam monochromator of the Furnas perpendicular-bounce design; using a highly oriented graphite crystal, a four-circle goniometer, a scintillation detector, and an on-line PDP-8S computer for automatic control. The FACS-1 unit was originally designed for single crystal structure determinations, but has since been adopted for studies of polycrystalline samples.

When speaking of the resolution of this system we must distinguish between Bragg angle (2θ) resolution and orientation angle (χ) resolution. In practice, we could attain high resolution in one angle only by sacrificing resolution in the other. Figure 34 illustrates the geometric principles involved. The x-ray source may be replaced by an apparent source of width w_s and height h_s located behind the monochromator crystal. The dimensions of the receiving aperture, w_r and h_r, may be conveniently varied without moving the location of the center of the aperture. Assuming a tiny sample, the error in 2θ is given by:

$$\delta(2\theta) = \frac{w_s}{L_s} + \frac{w_r}{L_r} \qquad (11)$$

while the error in χ is given by:

$$\delta(\chi) = \frac{h_s}{L_s} + \frac{h_r}{L_r} \qquad (12)$$

In the present work, broadening due to the finite size of the sample may be neglected.

As shown in Equation 12, the χ resolution depends upon h_s, L_s, h_r, and L_r. The height of the x-ray source h_s is a property of the x-ray tube and could not be conveniently adjusted. Similarly, no significant adjustment was possible with the distances L_s and L_r which are limited by the diffractometer design. The receiving slit height h_r was reduced to as small a value as was practical. The conditions used for high χ resolution were: h_s = 1.5 mm, L_s = 230 mm, h_r = 0.5 mm, L_r = 250 mm, resulting in $\delta(\chi)$ value of 0.5°. In other words, the intensity measured at any experimental χ value represents the total over a range of true χ values having a width 0.5°. This value of $\delta(\chi)$ is small enough, in comparison with the breadth of the azimuthal intensity curves, so that the effect of slit smearing on the χ intensity curves may be neglected.

The background correction is an important consideration in obtaining accurate orientation functions. In this context, the term background was used to denote all contributions to experimental intensity other than (hkℓ) diffraction; thus background includes diffuse coherent scattering, Compton scattering, air and slit scattering, and electronic noise. In the present work, no attempt was made to estimate or measure the different contributions due to background. Instead, it was assumed that all intensity observed at a χ value

sufficiently removed from the diffraction maximum may be attributed to background rather than to diffraction. Examination of the raw data showed that the intensity leveled off to a fairly constant low value at a point within 10° of the maximum in the χ distribution.

For the (002) peak, data points were obtained at 0.25° intervals from $\chi = 0^{\circ}$ to $\chi = 90^{\circ}$. The data obtained between $\chi = 0^{\circ}$ and $\chi = 80^{\circ}$, amounting to 321 data points, was averaged to give a single background value, which was subtracted from the remaining data points between $\chi = 80.25^{\circ}$ and $\chi = 90^{\circ}$. For the spherical integrations the data from $\chi = 0^{\circ}$ to $\chi = 80^{\circ}$ was set identically equal to zero, on the presumption that the fluctuations of intensity in this range were not significant compared to the counting error.

The same procedure was used for the (110), (200), and (020) peaks, except that data was taken over a 30° range in χ rather than the full 90°. Thus the background for each of these peaks represented the average of 81 data points instead of 321.

LEGEND FOR ATTACHED FIGURE

Page 139. Figure 34.

X-RAY DIFFRACTOMETER GEOMETRY

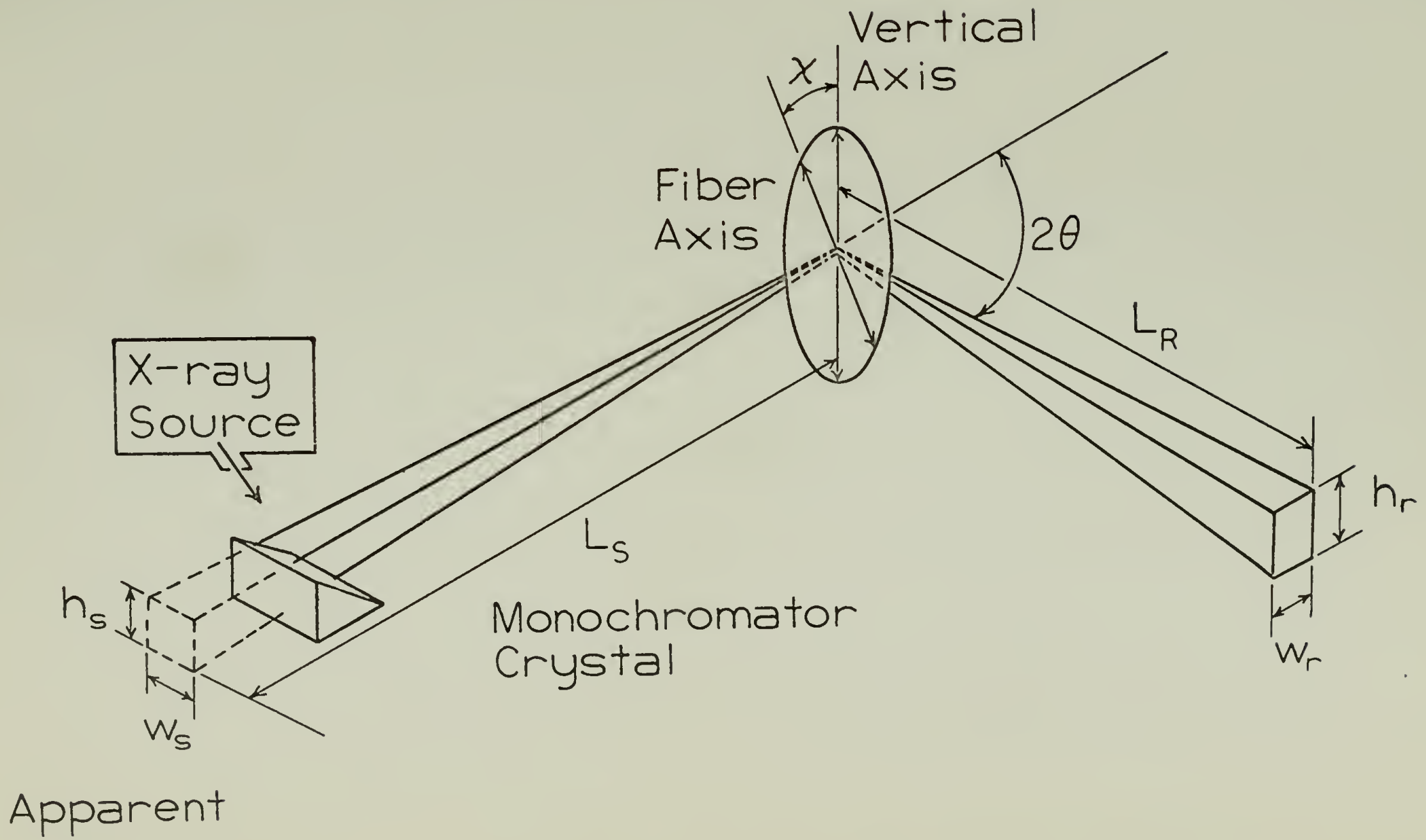

APPENDIX III

CRYSTAL SIZE CALCULATIONS

The procedure for extracting the intrinsic line broadening β from the experimental data was taken from the standard reference book of H. P. Klug and L. E. Alexander.[94]

The (002) peak was step-scanned at high 2θ resolution (see Figure 35) and the resulting data was fitted to a Gaussian curve of line breadth $B_o = 0.44^o$, where B_o is the peak width at half the maximum height. This peak is a composite of Cu K α_1 and Cu K α_2 diffraction peaks, so a correction was applied to account for the 0.25^o separation between α_1 and α_2. The resulting line breadth was $B = 0.31^o$. The equation

$$\beta = \sqrt{B^2 - b^2} \qquad (12)$$

was then used to correct for the breadth of the primary beam, where b is the line breadth at $2\theta = 0^o$ without the sample. The value obtained for β was substituted into Equation (11) in order to determine the crystallite size.

LEGEND FOR ATTACHED FIGURE

Page 140a. Figure 35.

INTENSITY DISTRIBUTION OF (002) REFLECTION FITTED TO A GAUSSIAN CURVE. DATA CORRECTED FOR BACKGROUND.

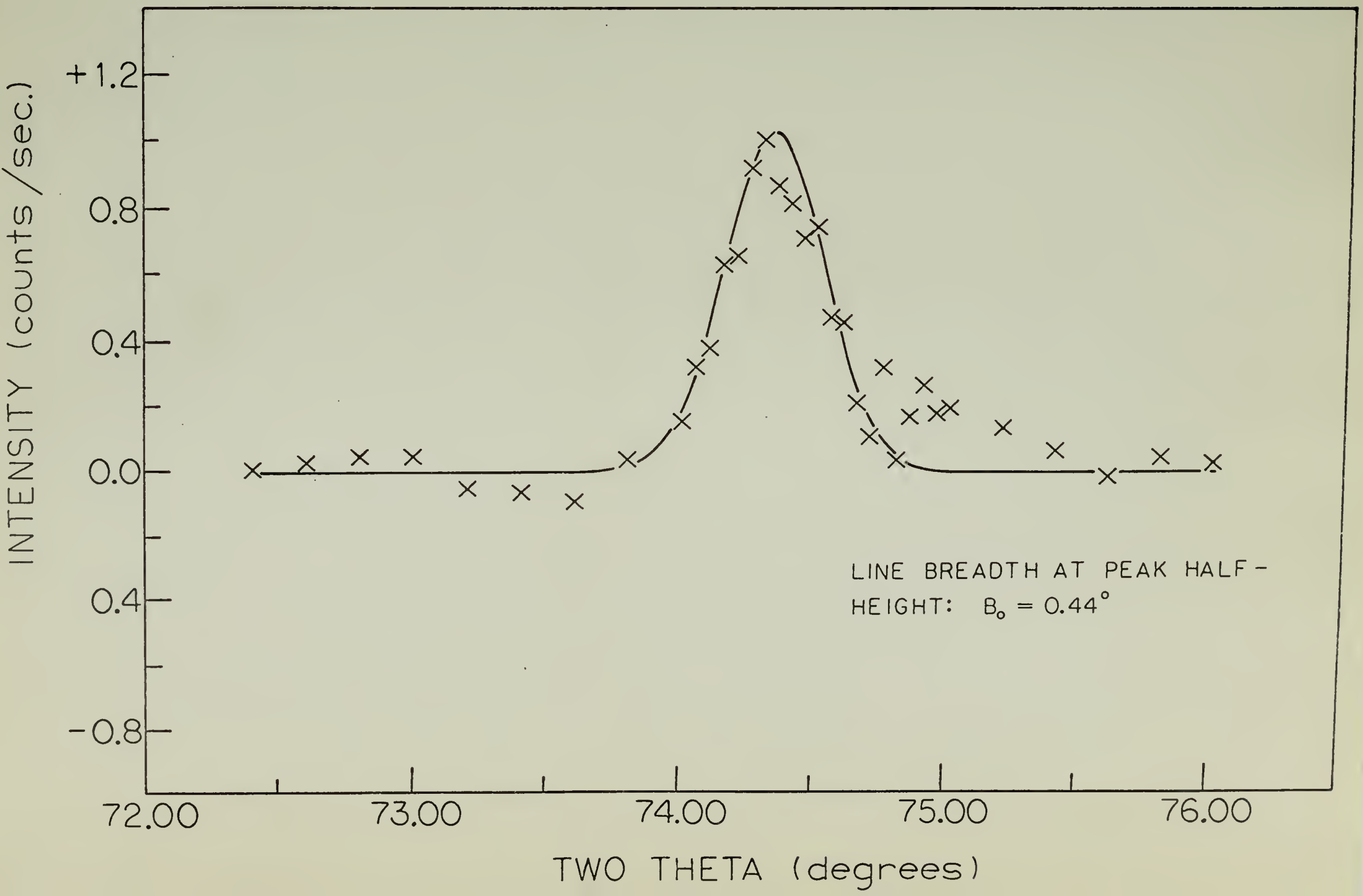

APPENDIX IV

POLYPROPYLENE CRYSTALLIZED UNDER THE ORIENTATION AND PRESSURE EFFECTS OF A PRESSURE CAPILLARY VISCOMETER

Evidence has been presented indicating that high density polyethylene can be crystallized into a transparent structure under the orientation and pressure effects available in the Instron Capillary Rheometer.[111-114] Furthermore, the structure so formed under these combined effects has an unusually high degree of crystallite orientation and perfection. With the exception of its excellent light transmission qualities, the properties of the structure are similar to those of a quenched high density polyethylene sample that is uniaxially oriented by cold drawing and then annealed for a period of many hours.[115] It is important to note that the structure crystallized in the Instron can be fully formed in a matter of seconds or less, certainly a significant distinction for possible commercial purposes. It is necessary to evaluate with polymers other than high density polyethylene the generality of the concept of an orientation-pressure induced crystallization procedure in order to obtain a morphology having an unusual combination of physical properties. Isotactic polypropylene is a reasonable choice in order to test the general applicability of the Instron crystallization procedure. Polypropylene is known to have greatly reduced rates of crystallization relative to those of high density polyethylene.[116] The primary purpose of this section will be to compare the effects of the Instron procedure on

polypropylene relative to those previously noted for high density polyethylene. In conjuction with this comparison, x-ray photographs and thermal data are presented in order to illustrate the specific effects of the orientation forces on the resulting polypropylene structure.

Sample Formation

The polypropylenes used for a detailed examination include Avisun 1010, Avisun 1014, and Shell 5520. Except where noted, similar effects were observed on all of the samples. Figure 36 shows the apparent viscosity as a function of shear rate for these polypropylenes. It is observed that the Avisun 1010 has a significantly higher viscosity and thus a higher molecular weight average than do the other two samples. The appearance of prominent shear thinning (reversible reduction of viscosity with increasing shear rate) is indicative of the molecular orientation effect that is utilized in producing the morphology of the polypropylene. The viscosity data presented in Figure 36 is uncorrected for pressure losses in the barrel, entrance effects, and the deviation in the apparent and true shear rates for a non-Newtonian material. Note, however, that end effects are minimized by using a capillary having the relatively large length-to-diameter ratio of 40.

In order to induce crystallization in the polypropylene, the velocity of the plunger in the rheometer barrel is increased (in fixed increments) until the pressure required to move the plunger has increased sufficiently to result in crystallization.

The formation of crystallites in the melt is evidenced by an abrupt increase in the pressure required to drive the plunger at the selected rate and by extreme extrudate swelling. The latter effect is attributed to the increased elastic energy absorption resulting from the crystallites in the flowing mass. Figure 37 shows the effect of crystallization on the pressure trace. The pressure simply rises to the maximum value attainable in the rheometer (1920 atm.) on initiating a plunger velocity at the relatively low speed of 0.1 cm/min. Note also that the higher viscosity Alathon 1010 has a more rapid rise in the pressure trace than that of Alathon 1014, indicating that crystallization occurred more rapidly for the higher viscosity polypropylene.

By choosing a rheometer temperature in the vicinity of the atmospheric melt transition of polypropylene, it is possible to supercool the flowing melt by increasing the applied pressure. The melting point of polypropylene goes up with increasing pressure, approximately $0.04^{\circ}C$/atm. for Avisun 1014,[117] and crystallization occurs when the polypropylene is sufficiently below its equilibrium melt transition. In addition to the supercooling effect of the pressure, the velocity gradients existing in the capillary entrance region likely have an effect on the degree of supercooling. As the melt is oriented due to these velocity gradients, its entropy is decreased so that the total change in entropy on going from the melt to the crystalline state is also decreased. The orientation effect would result

in an additional elevation of the melt transition, placing the flowing melt in a more supercooled state than that which would occur as the result of pressure alone. It is because of this orientation effect that it was previously postulated[112] that initial crystallization occurs in the upper portion of the capillary and in the capillary entrance region. Unfortunately, no method has as yet been devised to separate and evaluate the specific magnitudes of the orientation and pressure effects in the Instron Capillary Rheometer. In any case, the polypropylene crystallizes in the rheometer while significantly below its melt transition, as is the usual case for crystallization during commercial processes; the distinctly unusual factor is the orientation effect existing in the capillary entrance region before, during, and after the initial crystallites form. As is the case for polyethylene,[114] the final transparent polypropylene strands extracted from the capillary of the rheometer appear to be primarily the result of the forced extrusion of a semi-crystalline mass formed in the rheometer reservoir adjacent to the capillary entrance region. This is a process analogous to cold-drawing, with the specification that the material is being drawn near the melt transition, and the heat of fusion may actually increase during the process, implying an increase in the crystalline content during drawing.

Results

A comparison of the polypropylene structure resulting from the Instron procedure with that of thermally crystallized polypropylene can be made from the wide-angle x-ray photographs

shown in Figure 38. Refer to Sample 1. of Table IX for the details of the Instron procedure used to crystallize the sample for Figure 38-a. An examination of the (110) and (130) reflections of the oriented strand in Figure 38-a. reveals that the structure contains a mixture of a' - and c-axis crystallites, aligned parallel to the strand length; in fact, the crystal structure produced with the Instron procedure is similar to melt-extruded polypropylene and to polypropylene that is cold-drawn and then annealed.[118] An analogous procedure for polyethylene results in a high degree of c-axis orientation only, as would occur for cold-drawn polyethylene. However, a mixture of a'- and c-axis oriented polypropylene crystallites results from the Instron procedure even at extrusion temperatures as low as 130°C.

It is relevant to note that the polypropylene structure is held in the capillary at the crystallization temperature for approximately three minutes before the strand could be removed. A hypothesis that annealing might have occurred during this period with the resulting formation of a'-axis crystallites is evaluated in the following experiment. The polypropylene was crystallized at 130°C in a short capillary. The polypropylene crystallized in the capillary and then exited as a solid strand (implies the existence of plug flow in at least the lower portion of the capillary). This extruded strand was rapidly removed from the relatively hot rheometer surroundings and plunged into cold water, thereby minimizing post-crystallization annealing.

Even with this procedure, x-ray photographs revealed a mixture of a'-and c-axis oriented crystallites. It may be concluded that the Instron procedure in the vicinity of the melt transition consistently produces polypropylene samples that are dissimilar in crystalline orientation to purely cold-drawn (but not annealed) material. Hence crystallization of a flowing polypropylene melt and subsequent drawing in the capillary entrance region do not result in a high degree of uniaxial crystallite orientation (c-axis aligned parallel to the capillary axis of flow) under the conditions described in this report, as is, in fact, observed using an analogous procedure for polyethylene crystallization.

The effect of the orientation forces during the crystallization procedure have also been evaluated for polypropylene. The x-ray photographs in Figure 39 show the influence of the velocity gradient during crystallization. The photograph for the segment near the capillary entrance indicates a much lower degree of orientation than that for the segment obtained near the middle of the 7.62 cm long strand. Here degree of orientation refers to the sharpness of the crystallite distributions about the c- and a'-axes, rather than to the crystallite distribution about the c-axis alone. Specifically, an examination of the (110) reflections for the photographs shown in Figure 39, obtained under identical exposure and development times, reveals the differences between the crystallite orientation of the two structures. The lower degree of orientation of the upper segment is defined by the ring that can be observed for the (110) reflection at any azimuthal angle; thus, there is such a broad

scattering of crystallite orientation that a number of crystallites can be regarded as being neither c- nor a'-axis oriented, but rather randomly oriented. The random orientation for the middle segment of the strand is negligible (no appearance of a concentric ring for the (110) reflection). The particular conditions for formation of these segments were such that the top segment was formed under an orientation effect resulting from the acceleration of the polypropylene in the capillary entrance region from essentially zero velocity in the barrel to approximately 0.05 cm/min. in the capillary. In contrast, the middle segment was formed under a significantly larger longitudinal velocity gradient resulting from the acceleration of the material 5 to 780 cm/min. over the same entrance region, assuming that the extrusion rate at the instant of initial crystallization was determined only by the geometry of the system and the plunger velocity. The conditions for sample formation are listed in Table I, Sample 3. After crystallization occurred, the pressure was held at 1900 atm. for thirty minutes and slow extrusion continued at the rate of 0.05 cm/min. It was under this greatly reduced velocity that the top segment was crystallized, while the middle segment can be reasonably assumed to be the result of crystallization under a much greater orientation force due to the acceleration to a velocity of 780 cm/min. over the same entrance region. Hence, the different degree of orientation in the crystal structure is very probably the direct result of the different velocity gradients.

Relevant to the above conclusions, annealing may have a significant effect on crystallite orientation, and it is of interest to evaluate the effects of annealing in the samples examined in Figure 40. Thus polypropylene was crystallized under identical conditions except that the pressure was removed immediately after crystallization was induced in the capillary. This procedure resulted in a decrease in total orientation, as evidenced by the x-ray photographs of Figure 40. One sample was annealed for thirty minutes and the other was removed from the capillary immediately after formation. As both samples were formed under identical pressure conditions and in the same capillary, it is assumed that the orientation effects due to the velocity gradients are identical. The original crystallites cause the diffraction observed in the x-ray of the unannealed sample. Randomly oriented crystallites apparently formed during annealing, as indicated by the appearance of scattering for all azimuthal angles of the (110) reflections for the annealed sample. The randomly oriented material is mainly attributed to the formation of new crystallites rather than the reorganization of the initially crystallized polypropylene, as indicated by a 7% rise in the heat of fusion (measured by the Perkin-Elmer Differential Scanning Calorimeter Model 1-B (DSC)). Note that an annealing effect cannot be used to explain the previous observations concerning Figures 39 because the most oriented sample was also the most subject to annealing (samples prior to annealing for Figure 39 were crystallized in the same manner as Sample 3 of Table IX).

It was found that the combined orientation-pressure effects on the crystallization process in the rheometer produced a relatively low melting point structure. Table X shows values of the melting point as a function of length from the capillary entrance for a strand crystallized according to Table IX, Sample 3. A second strand reported in Table X shows the effect of annealing without pressure for 30 minutes. The initially formed crystal structure must be relatively imperfect in order for such a large annealing effect to occur; compare the segments of the two strands at equivalent distances from the capillary entrance. The dual peak at 165.3 and 173.8°C of the annealed segment (59.3-63.1 min.) is a typical result for the melting of annealed polypropylene in which as many as twelve different peaks have been recorded as the result of twelve different annealing[119] temperatures. For the annealed samples in this experiment, two different degrees of supercooling were used (150°C at 1900 atm. and 150°C at 1 atm.) in order to obtain two distinct annealing effects that resulted in the dual peak fusion curve. It is of interest to note that Sieglaff[120] has attached a different significance to dual DSC peaks obtained from the crystallization of polypropylene in the Instron Rheometer. Specifically, he has suggested that the higher melting point is due to the melting of the crystal structure formed under the orientation effects existing in the capillary entrance region, i.e. the shear-induced crystal structure.

It is also relevant to note that an increase in the melting point cannot be consistently related to an increase in the orientation of the structure crystallized in the rheometer; in fact, it was generally found that the highest melting point segments, located near the capillary exit, had the least amount of orientation. This too is contrary to the results of Sieglaff, who reported that the greatest content of high melting point material occurred in the segment of the strand adjacent to the capillary entrance region in which, he asserted, the maximum crystallite orientation occurred.[120]

Previous research indicates that high density polyethylene behaves in exactly the opposite manner[111-114] relative to the data presented herein for polypropylene, and this is the primary conclusion of this appendix. An Instron crystallized polyethylene sample with a c-axis orientation function of +0.9 had a DSC melting point of 140°C, while a sample having an orientation function of +0.6 had a melting point of only 139°C.[112] No correlation of melting point and orientation was found for polypropylene. For polyethylene, the high melting point accompanied by a high degree of orientation can be explained in terms of an extended chain component in the crystal structure. The melting point of the perfect polyethylene crystal is 142±1°C. Noting that the melting point of the perfect polypropylene crystal is 220°C,[121] the observed polypropylene melting points in the vicinity of 170°C are not sufficiently high to constitute evidence that is consistent with the presence of an extended

chain component, thus emphasizing the distinct differences that the Instron crystallization procedure has on polyethylene and polypropylene. In opposition to these assertions, Sieglaff has reported melting points for Instron crystallized polypropylene as high as 225°C,[121] and the small amount of material that melted at this temperature may indeed be an extended chain crystal structure.

REFERENCES

111. J. H. Southern and R. S. Porter (Chapter I), accepted for publication in J. Macromol. Sci. (1970).

112. J. H. Southern and R. S. Porter (Chapter II), accepted for publication in J. Appl. Polymer Sci. (1970).

113. C. R. Desper, J. H. Southern, R. D. Ulrich, and R. S. Porter (Chapter III), submitted to J. Appl. Phys. (1970).

114. R. G. Crystal and J. H. Southern (Chapter V), to be submitted to J. Polymer Sci. (1970).

115. M. Takayanagi et al., J. Polymer Sci., Pt.C, No. 15, 263 (1966).

116. F. Price, private conversation (1970).

117. J. R. Knox, private communication (1970).

118. R. J. Samuels, The Science and Technology of Polymer Films, O. J. Sweeting, ed. (New York: Interscience), vol. I, 256 (1968).

119. K. D. Pae and J. A. Sauer, J. Appl. Polymer Sci., 12, 1901 (1968).

120. C. L. Sieglaff and K. J. O'Leary, ACS Polymer Preprints, 10, 57 (1969).

121. W. W. Cox and A. A. Duswalt, Polymer Eng. and Sci., 7, 1 (1967).

TABLE IX

SPECIFICATIONS FOR CRYSTALLIZATION
IN THE INSTRON RHEOMETER

Identification	Plunger Velocity (cm/min.)	Rheometer Temperature (^{o}C)	Capillary Dimensions(cm.)** Length	Diameter
Sample 1.	5.0	170	7.62	0.0762
Sample 2.	5.0	130	0.62	0.0508
Sample 3.	5.0	150	7.62	0.0762

*All experiments were done with Shell 5520 unless noted otherwise.

**All capillaries used in these experiments had a 90^{o} entrance angle and were constructed from tungsten carbide.

TABLE X

MELTING POINTS OF SEGMENTS OF A SHELL 5520 POLYPROPYLENE STRAND OBTAINED FROM THE INSTRON PROCEDURE

Distance from Capillary Entrance (mm)	In from Peak of DSC Fusion Curve at 10°C/min. Heating Rate (°C)
SAMPLE* CRYSTALLIZED AND REMOVED IMMEDIATELY FROM THE CAPILLARY	
0.0-3.8	166.2
11.8-15.8	165.2
15.8-19.8	166.0
19.8-23.8	166.2
23.8-29.3	166.2
29.8-33.8	166.6
33.8-39.8	166.8
39.8-44.1	168.7
44.1-48.3	169.0
54.5-58.3	170.7
58.3-62.9	171.3
62.9-66.5	171.5
66.5-70.5	171.6
SAMPLE* CRYSTALLIZED AND ANNEALED FOR 30 MIN. AT 150°C	
0.0-4.0	169.6
34.0-37.3	174.5
59.3-63.1	165.3, 173.8

*See Table IX, Sample 3 for details of the Instron procedure.

LEGEND FOR ATTACHED FIGURES

VISCOSITY CHANGE WITH SHEAR RATE AT 190°C

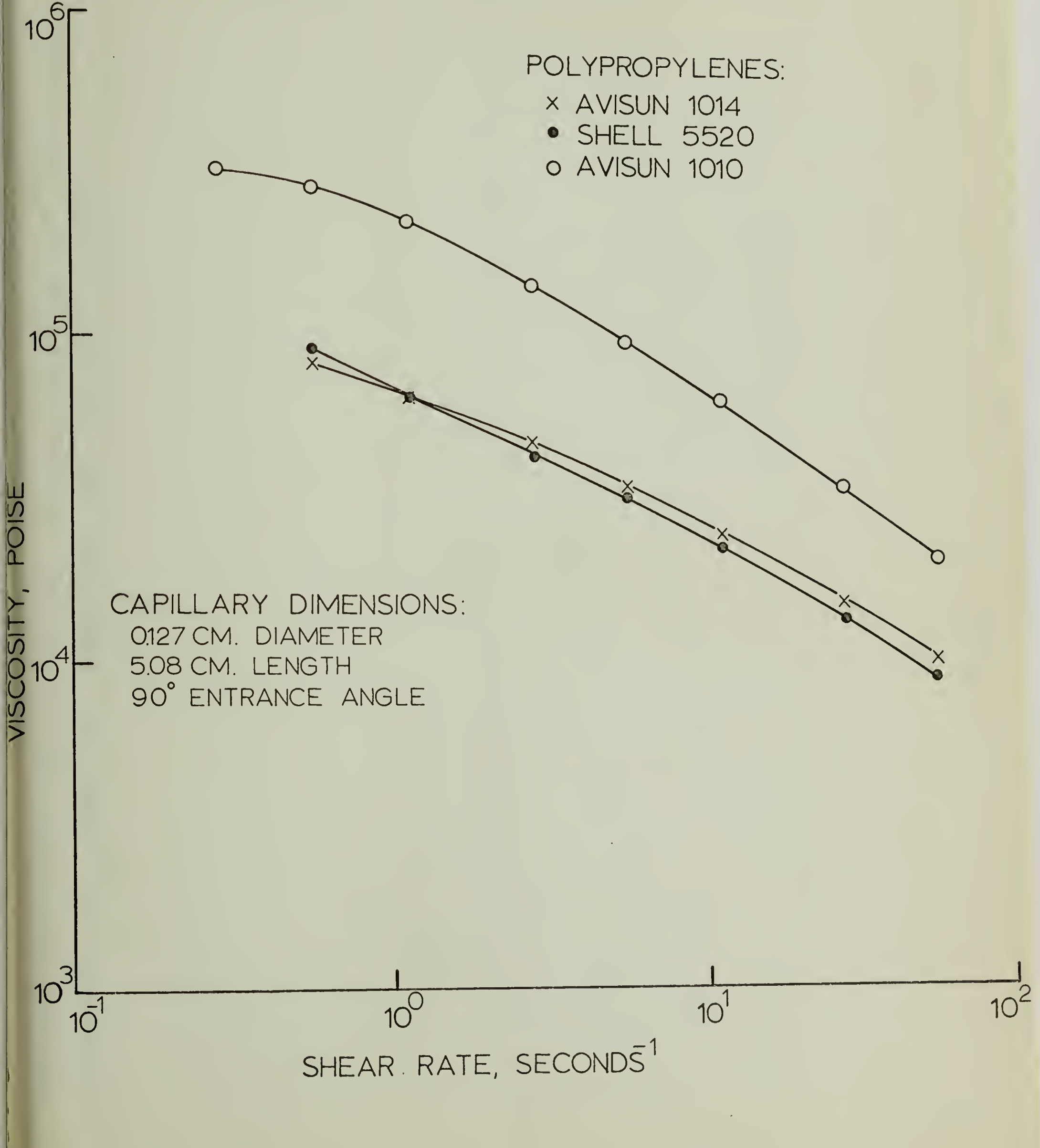

INSTRON PRESSURE TRACES DURING CRYSTALLIZATION AT 170°C USING A CAPILLARY OF 0.0508 CM. DIAMETER AND 5.08 CM. LENGTH

FIGURE 38. X-RAY OF POLYPROPYLENE

Thermally Crystallized.

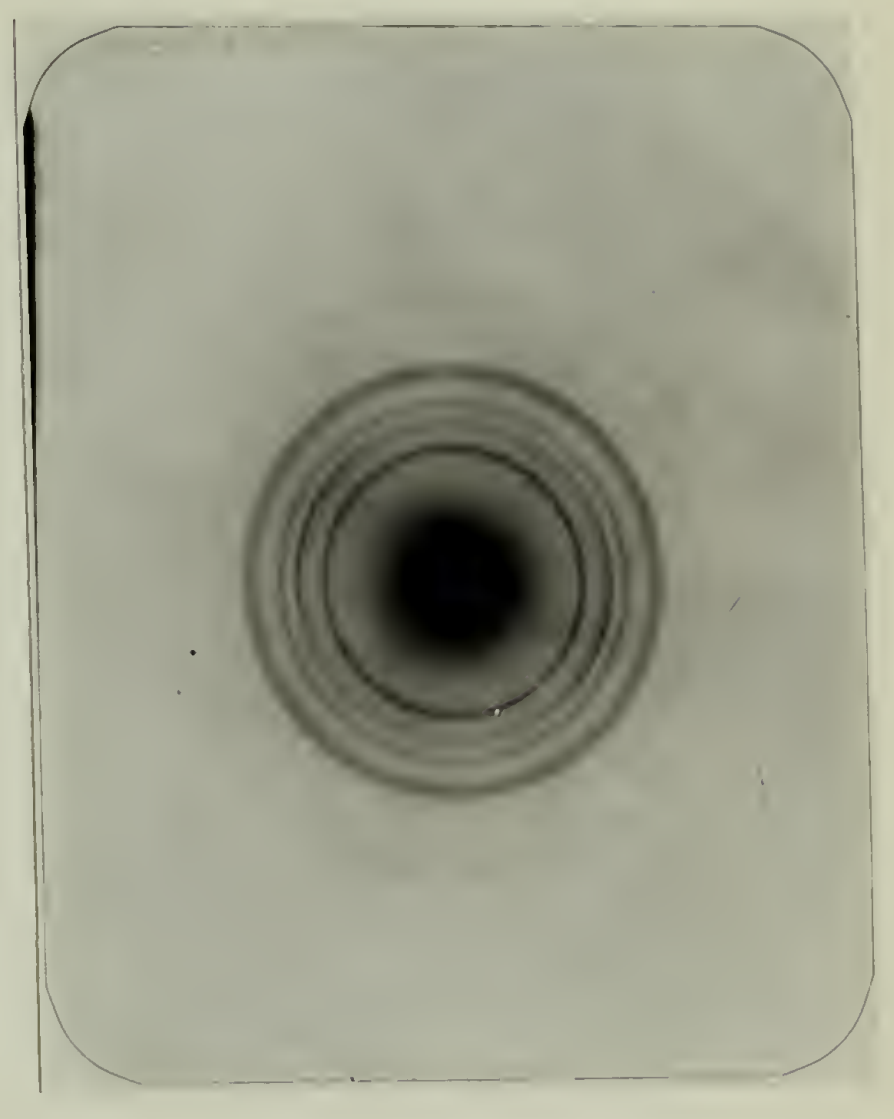

Crystallized at 170°C
Under the Combined Effects
of Orientation and Pressure.

FIGURE 39. EFFECT OF VELOCITY GRADIENT ON THE CRYSTALLITE ORIENTATION

Middle Segment.

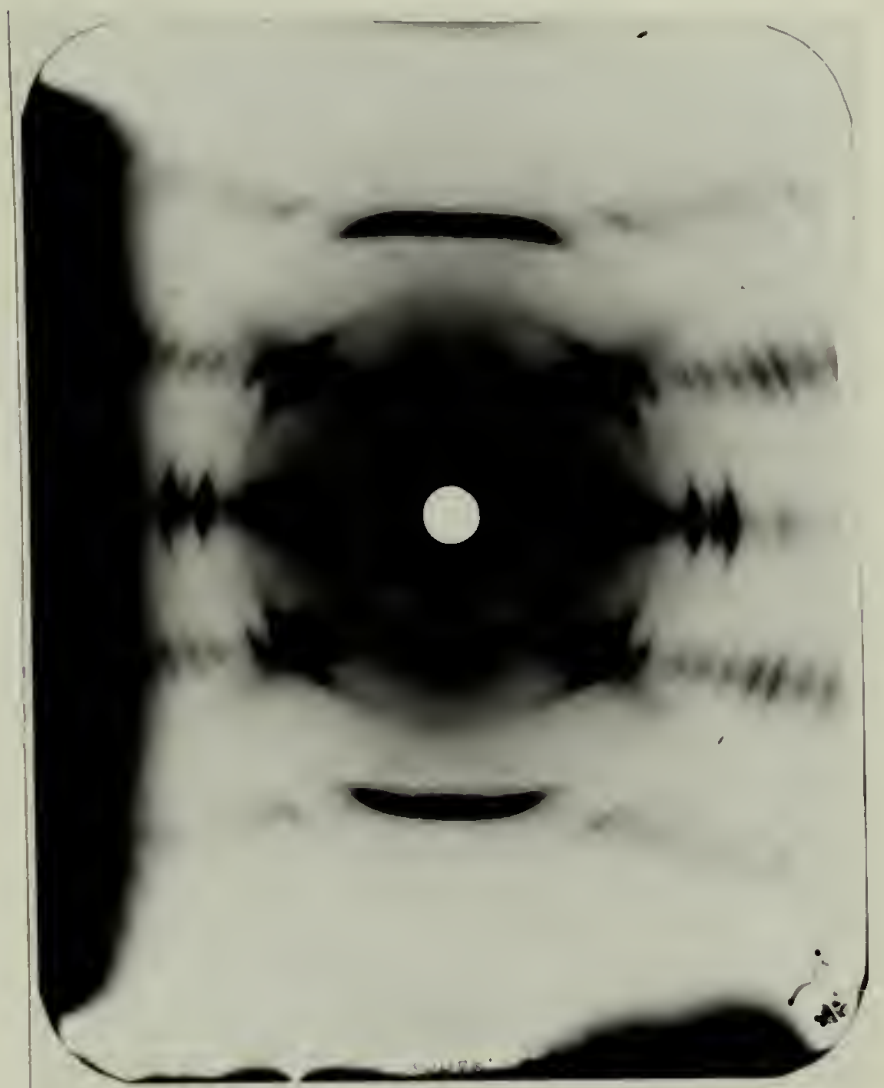

Top Segment.

FIGURE 40. EFFECT OF ANNEALING
ON CRYSTAL ORIENTATION

No Annealing.

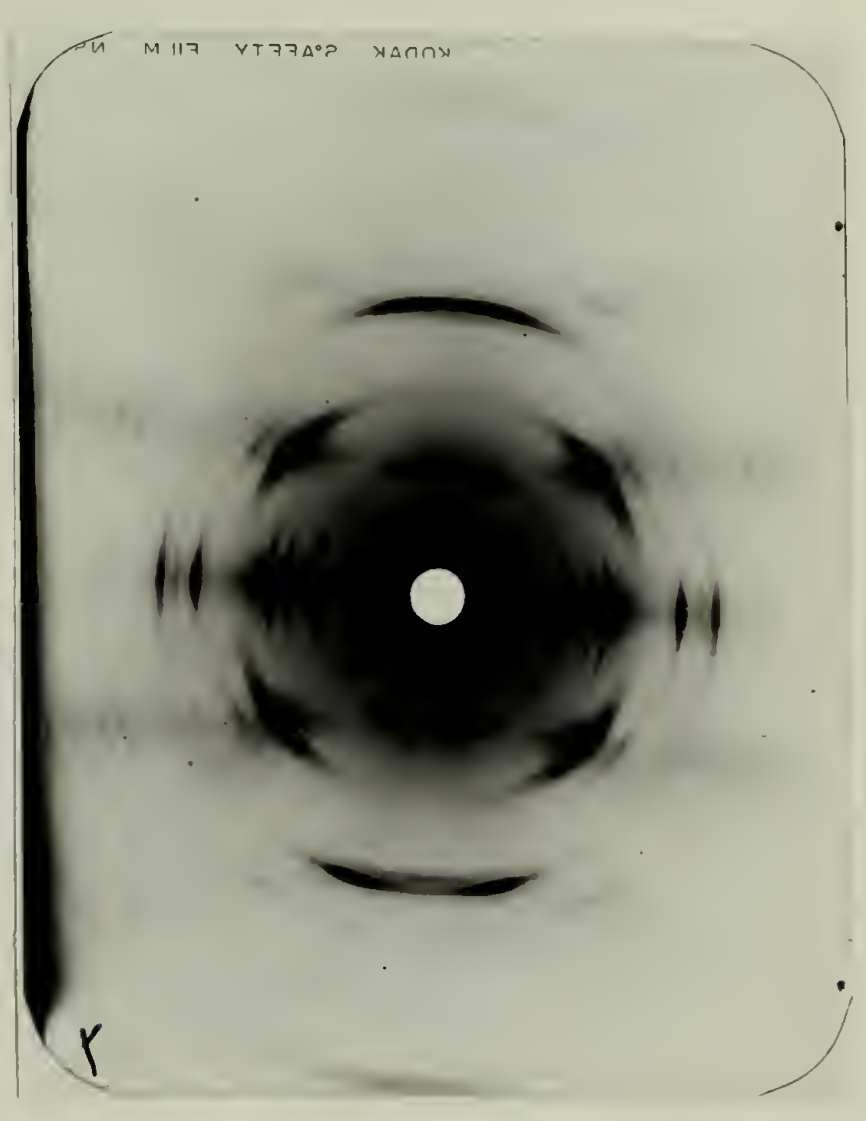

Annealed for
30 Minutes at 150°C.

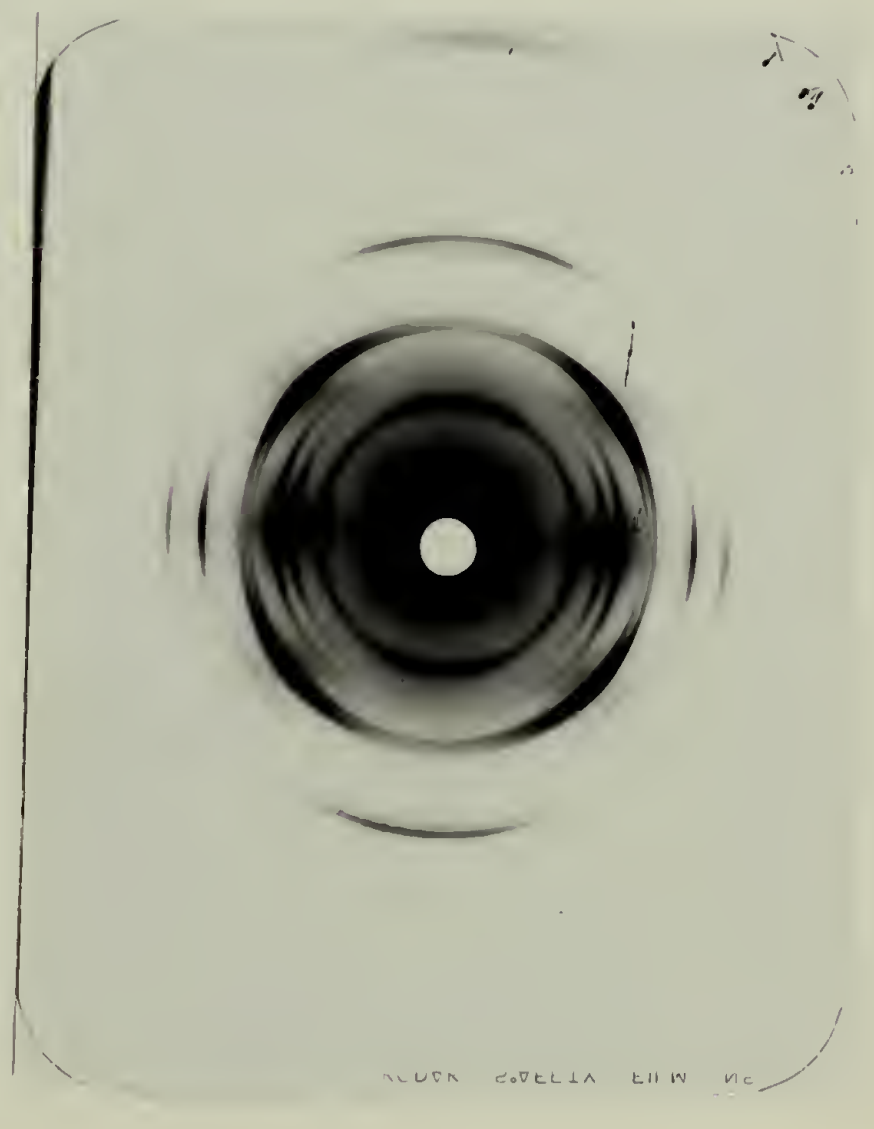

APPENDIX V

SUGGESTED AREAS FOR FUTURE STUDY

A number of experiments for future research are suggested from the procedures used in this thesis. Among these are the use of different types of equipment, other than the Instron Capillary Rheometer, to induce crystallization under the effect of orientation. Light scattering and crystallization kinetics data should also be obtained in further defining the Instron crystallization procedure and the structure so formed.

It is suggested that useful information concerning crystallization induced from an oriented melt can be obtained from the Weissenberg Rheogoniometer as well as the Instron Rheometer. The Weissenberg may be especially useful in separating the orientation effect from the pressure effect. Kawai[122] has used a third type of geometry, that of the concentric cylinder viscometer, to induce crystallization from the dilute solution at shear rates up to 629 sec^{-1}. As a high shear concentric cylinder viscometer is now available, it is of interest to carry out further studies under the greater orientation effects that result from high shear rates applied to the undiluted melts. Experiments using the concentric cylinder viscometer are of commercial interest as a possible means of studying the formation of transparent films of high density polyethylene that have been produced on calendering equipment (adjacent cylinders rotating at different rates) that was specially adapted for use at relatively high shear rates.[123] The continuous films

so produced are fibrillar and may in fact have a structure identical to that resulting from the Instron Rheometer studies detailed in the thesis.

It is also of interest to define the nucleation and growth kinetics as a function of temperature and orientation forces applied to the melt in order to develop a more complete understanding of the crystallization processes occurring within the Instron Rheometer. Specifically, a transparent shearing hot plate can be used in conjunction with a high speed camera in order to detect the effect of a velocity gradient on the crystallization kinetics. This is a thermostated concentric disc viscometer in which the discs are constructed from glass and are placed between crossed polarizers. Driving the upper disc produces a shear field in the polymer sample located between the discs. While the upper disc rotates at a fixed rate, the number of spherulites as well as their size is recorded on the film as a function of time. The crystal structure so produced can be compared with that of the strands produced in the Instron Rheometer. A shearing hot plate capable of shear rates on the order of 100 sec^{-1} and thermostated to $\pm 0.1^{o}C$ is presently available in our laboratories.

A concentric cylinder viscometric dilatometer can also be used for the study of crystallization kinetics. This instrument relies on a relationship between the volume change of the mercury level in a capillary attached to the reservoir of the concentric cylinders and the volume change due to crystallization of the polymer between the concentric cylinders. The data

is interpreted in terms of the Avrami equation:[124]

$$x = e^{-\frac{4\dot{n}\pi g^3 t^3}{3v}}$$

where x = volume fraction remaining in the melt

$\dot{n}$ = nucleation rate

v = volume of entire system

g = growth rate

t = time

Both the concentric cylinder and disk instruments can provide a rather interesting and original set of data on the crystallization of polyethylene under shearing conditions. It is, as yet, uncertain whether the data from these instruments can also be extrapolated to the conditions existing in the Instron Rheometer; however, preliminary studies with the Weissenberg Rheogoniometer suggest that the structures crystallized under high shear in the various equipment will at least be similar to that obtained from the Instron.

An additional area for future study is that of the light scattering of the Instron samples. A light scattering study confirmed the presence of an oriented, fiber structure in the Instron strands, and it is of interest to pursue this study in further explaining the transparency of the structure, previously attributed to the high crystal orientation and crystal content (see Chapter III). These factors minimize the orientation and density fluctuations responsible for light scattering. It has been specifically postulated that the orientation fluctuations

have a correlation distance much greater than the wavelength of light. In order to evaluate this hypothesis, a transparent film can be crystallized from a slit die* and used as a subject of a quantitative light scattering study. The I_{VV} pattern (polarizer and analyzer aligned vertical to the plane defined by the incident and scattered beam) is known to be a combination of both the density and orientation fluctuations, while the I_{HV} pattern is the result of orientation fluctuations alone. It is proposed that the individual correlation distances for density and orientation fluctuations can be defined from these two patterns.

In conclusion, this thesis has been primarily concerned with high density polyethylene. It is suggested that the Instron crystallization procedure be applied to other polymers, such as nylon and trans-1,4-polybutadiene. Furthermore, several projects that were discontinued prior to completion during this thesis should be given additional study. In particular, the dynamic tensile modulus as a function of temperature (Vibron) and the nitric acid studies merit further research. In the latter project, 0.0508 cm diameter strands produced at 136°C with the Instron procedure were placed in fuming nitric acid for varying times (0.5 g polyethylene/ 100 ml HNO_3 at 80°C). These strands were significantly more resistant to the nitric acid than the typical melt-crystallized polyethylene segments which became brittle after only four hours in acid. The Instron-produced,

* Dr. C. R. Desper found that the transparent film so produced in a slit die of dimensions 0.1246 x 0.0055 - 0.0056 x 1.00" is biaxially oriented; however, no systematic orientation or melting point studies of the films were conducted in this thesis project.

transparent segments remained relatively tenacious even after 24 hours exposure. The fibrillar structure of the treated Instron strands was readily apparent when viewed with an optical microscope using reflected light. In addition, some broadening of the DSC fusion curves of the acid treated strands was observed. Qualitative thermal studies were not attempted since it was not feasible to remove the products of the acid treatment from the polyethylene itself.

REFERENCES

122. T. Kawai, T. Matsumoto, M. Kato, and H. Maeda, Kolloid-Z. u. Z. Polymere, 222, 1 (1968).

123. T. Wang, H. Chen, and T. Kwei, accepted for publication in ACS Polymer Preprints (1970).

124. P. Meares, Polymers: Structure and Bulk Properties (London: van Nostrand), Cpt. 5 (1965).